Space-time coded cooperation in Wireless Networks

Samir Sakr

A Thesis
In the Department
of
Electrical and Computer Engineering
Presented in Partial Fulfillment of the Requirements
for the Degree of Master of Applied Sciences at
Concordia University
Montreal, Quebec, Canada
March 2014

© Samir Sakr, 2014

CONCORDIA UNIVERSITY
SCHOOL OF GRADUATE STUDIES

This is to certify that the thesis prepared

By: Samir Sakr

Entitled: "Space-time Coded Cooperation in Wireless Networks"

and submitted in partial fulfillment of the requirements for the degree of

Master of Applied Science

Complies with the regulations of this University and meets the accepted standards with respect to originality and quality.

Signed by the final examining committee:

_____ Chair
Dr. M. Z. Kabir

_____ Examiner, External
Dr. A. Ramamurthy (BCEE) To the Program

_____ Examiner
Dr. Y. R. Shayan

_____ Supervisor
Dr. M. R. Soleymani

Approved by: _____
Dr. W. E. Lynch, Chair
Department of Electrical and Computer Engineering

_____20_____

_____
Dr. C. W. Trueman
Interim Dean, Faculty of Engineering
and Computer Science

ABSTRACT

Space-time coded cooperation in Wireless Networks

Samir Sakr

Nowadays, the concept of spatial diversity and cooperative networks attract a lot of interest because they improve the reliability of transmission in wireless networks. Spatial diversity is achieved when multiple antennas are at the transmitter. With great growth and demand for high speed high data rate wireless communication, more and more antennas are required. In order to achieve maximum diversity, these antennas should be well separated so that the fading on each link is uncorrelated. This condition makes it difficult to have more than two antennas on a mobile terminal. The relay's cooperation helps increase the diversity order without extra hardware cost. However, its main inconvenience is the use of multiple time slots compared to the direct link transmission.

In this thesis, we develop a cooperation model which is composed of three terminals: source, relay and destination. The transmitters (source and relay) are composed of 2 antennas at the transmitter and the receivers (relay and destination) have 4 antennas. In the first proposed model, transmitters and decoders are composed of an Alamouti encoder and decoder respectively. In the second model, we also add a turbo encoder at transmitters and iterative decoding takes place at receivers. In both cases, the transmission cycle is composed of two time slots and the decode and forward (DF) protocol is applied. Multiple scenarios are considered by changing the environment of the

transmission, such as line of sight (LOS) or non line of sight (NLOS) or by modifying the location of the relay between the source and destination. We also simulate an uplink and a downlink communication. All the scenarios show a coding gain with the turbo coded space-time cooperation.

.

ACKNOWLEDGMENTS

I am sincerely thankful to everyone who gave me the opportunity to complete this thesis. First and foremost, I would like to express my deepest gratitude to Professor Dr. M. Reza Soleymani for his continuous support, time, effort, and knowledge sharing throughout my research work. Without his supervision and guidance it would have been very difficult to submit this thesis. I would like to extend my gratitude to my colleagues in the wireless and satellite communications lab.

I am always grateful to my parents Pierre and Viviane for their unconditional support.

Table of contents

List of Figures

List of Tables

List of Acronyms and Symbols

List of Acronyms

Acronym	Explanation
AF	Amplify and Forward
AWGN	Additive White Gaussian Noise
BCJR	Bahl, Cocke, Jelinek and Raviv
BER	Bit Error Rate
BPSK	Binary Phase Shift Keying
BS	Base Station
CRC	Cyclic Redundancy Check
CSI	Channel State Information
DF	Decode and Forward
EGC	Equal Gain Combining
FEC	Forward Error Correcting codes
FER	Frame Error Rate
GF	Generator Forward
GR	Generator Backward
LLR	Log Likelihood Ratio
LOS	line of sight
MAP	Maximum A Posteriori
MIMO	Multiple Input Multiple Output
MISO	Multiple Input Single Output
ML	Maximum Likelihood
MRC	Maximum Ratio Combining
MS	Mobile Station
NC	Network Coding
NLOS	non line of sight

PCCC	Parallel Concatenated Convolutional Codes
QPSK	Quadrature Phase Shift Keying
R-D	Relay-Destination
RSC	Recursive Systematic Convolutional Codes
SC	Selection Combining
S-D	Source-Destination
SIMO	Single Input Multiple Output
SISO	Soft Input Soft Output
SNR	Signal to Noise Ratio
S-R	Source-Relay
STBC	Space Time Block Code
STC	Space Time Code
STTC	Space Time Trellis Code

List of Symbols

Symbols	Explanation
A_i	Amplitude of the received signal
$a_i(t)$	Fading amplitude in time
α_i	Weighting factor in combining methods
$\alpha_k(s')$	Forward recursion in MAP algorithm
B_d	Doppler spread
β	Path loss coefficient
$\beta_{k-1}(s')$	Backward recursion in MAP algorithm
C_{AWGN}	Capacity channel of AWGN
C_h	InstantaneousCapacity channel of fading channe
d	Distance
DG	Diversity gain
$(\Delta t)_c$	Coherence time
E_b	Bit energy
$erfc$	Complementary error function
$h_{i,j}$	Fading coefficient on the link from i to j
$L(u)$	Log-likelihood ratio of information bits
$L^i(\hat{u})$	A Posteriori LLR value at decoder i
L_c	Channel reliability
L_e	Extrinsic information
$n_{i,j}$	Noise componoent on the link from i to j
N_0	Noise spectral density
n_R	Number of receivers
n_T	Number of transmitters
σ^2	Noise variance

P_b	Probability of error for a bit
PL	Path loss in dB
P_{outage}	Outage probability
P_r	Received power at receiver
P_t	Transmitted power at transmitter
ϕ_i	Phase of the received signal
π	Interleaver
Q	Q function
R	Turbo code rate
$\tau_i(t)$	Propagation delay in time
W	Signal bandwitdth
x	Transmitted signal
y	Received signal
y_{1p}	Received Parity 1 bits
y_{2p}	Received Parity 2 bits
y_{1s}	Received Systematic bits
$\gamma_{i,j}$	Instantaneous received SNR on the link from i tc
$\gamma_k(s', s)$	Branch metric in MAP algorithm

Chapter 1: Introduction

In wireless communications, fading is the channel variation in space, frequency and time. These variations can cause poor performance in a communication system because they can result in a loss of signal power at the receiver without reducing the power of the noise. Another issue is the large distance between the source and destination. The received power at destination decreases proportionally with some power of distance between the transmitter and the receiver.

From that perspective, the relay cooperation is key to improve the quality of the received sequence at the destination. In this thesis, we consider a relaying process in space-time coded cooperation as well as turbo-coded space-time code cooperation.

1.1 Motivation

In mobile technology, portable electronic devices establish a communication between each other and/or the base station through a wireless channel, which is often affected by fading. Fading is modeled as a random process and results mainly from two obstacles: multipath propagation and shadowing. Multipath fading, also referred to as multipath induced fading is a non-coherent combination of signals arriving at the receiver and shadowing, also known as shadow fading, and is due to obstacles affecting the wave propagation. These fades may occur at a particular point in space, in time or in frequency and can result in a degradation of the quality of signals at the receiving antenna, which makes it impossible to detect and decode the data correctly. These imperfections create important demands and needs for reliable, high data rate and low power communication

over wireless channels. These fades are combated by diversity schemes; two or more communication channels with different characteristics are used in order to improve the reliability of the signal.

Spatial diversity employs multiple antennas at both transmitter and receiver that have the same characteristics and separated physically from one another in order to minimize correlation between the resulting channels [1]. Also, in an urban environment, it is easy to find many mobile devices which can cooperate with each other in order to transmit and/or receive their information: it is called cooperative diversity [2]. Previous studies have shown that cooperative diversity can provide a diversity gain equal to that of multiple antenna system [2][3][4][7].

1.2 Contributions

In the case of space-time code cooperation, the transmission cycle consists of two phases: in the first phase, the source broadcasts the message to both relay and destination. Then if the relay is able to decode the message, it transmits another version of the same message with another channel state information and the source remains silent during phase 2. Else, both the source and the relay remain silent during phase 2. One way to enhance the model is to extend the evaluation to space-time coding at the transmitter as well as maximal-ratio combining at the receiver when the relay cooperates, which improves the overall bit error rate performance of the system. The performance is compared to the direct link transmission in different scenarios: LOS, NLOS, varying the location of the relay, uplink and downlink environments. We also considered different

power allocation strategies. The simulation shows an improvement of 4 dBs in the case of a downlink transmission compared to a direct link transmission.

Then, the same model is extended to Turbo space-time coded cooperation with a different transmission cycle. During the first phase, the source sends half the systematic and parity bits to the relay and destination. And if the relay decodes successfully the information bits, it sends to the destination the second half of the information and parity bits. Else, the source has to send those bits. At the destination, the received frames during phase 1 and 2 are multiplexed in order to obtain the full systematic and parity sequences before the iterative decoding. The turbo coded space-time cooperation model provides a gain of 7.8 dBs in the case of uplink communication compared to a space-time coded cooperation.

1.3 Thesis Outline

The remainder of this thesis is organized as follows. We present some background knowledge on the wireless communication in fading environments, including diversity techniques, MIMO channels and equalization schemes as well as space-time codes.

In Chapter 3 we present a space-time code cooperation system model and the proposed protocol: the results of the simulations are illustrated and show the advantage of having a relay cooperation versus a direct link transmission. Chapter 4 consists of a Turbo coded space-time code cooperation model and contains details of the simulations parameters and we present the encoder/decoder scheme used from source to relay. Compared to the system presented in chapter 3, we observe the gain obtained by adding turbo coding.

In Chapter 5 we conclude the results obtained during the thesis and recommend future research work.

Chapter 2: Literature Review and Background

In this Chapter we present literature and background of wireless communication in fading environments: both types of fading (slow versus fast) are discussed. Then we explain multiple diversity techniques in order to minimize the fading effects on the performance of wireless channels. In the third place, we cover different MIMO and equalization schemes followed by a discussion of space-time codes. Finally we summarize the existing literature on cooperative diversity that could be seen as an efficient type of spatial diversity for wireless networks.

Our proposed models in Chapters three and four combine both spatial and cooperative diversity.

2.1 Wireless Channels and Fading

A key characteristic of the wireless channel is the variation of its characteristics over time and over frequency. The notion of fading can be divided into two main groups based on the position of the receiver relative to the transmitter.

- Large-scale fading is due to the path loss of signal and occurs for channel propagation over long distances. It is a result of distance and shadowing by large scale objects, such as buildings, trees or hills; it is independent of the frequency.
- Small-scale fading results from effects that are found near to the receiver antenna. It is a product of the constructive and destructive interference of the multiple

signal paths between the transmitter and receiver; unlike large-scale fading, it is frequency dependent.

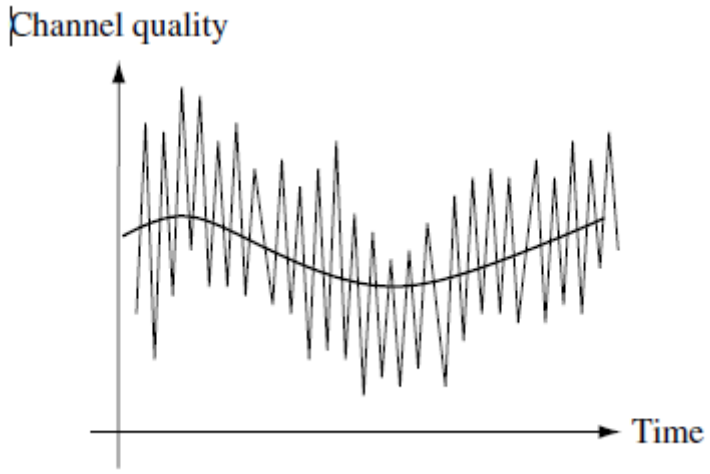

Figure 2.1 Channel variation in time: large-scale fading versus small-scale fading

As shown in the Figure above, there are different models available for large and small scale fading. The use of log-normal distributions for large scale and Rayleigh distribution for small scale fading is very common. We follow this model in this thesis. The destructive effects of small-scale fading are less predictable and more severe than large-scale fading; we will mainly focus on the latter. But before doing so, we will first explain the general path loss in large-scale fading.

2.1.1 Path Loss In Large-Scale Fading

Path loss, also known as path attenuation, is the reduction in power density (or attenuation) of an electromagnetic wave as it propagates through space. It normally includes propagation losses due to the natural expansion of the radio wave in free space, absorption losses when the signal passes through medium that is not transparent to electromagnetic waves, and diffraction losses when the wave is obstructed by an opaque obstacle. All these interfering waves result in a Rayleigh fading scenario that varies quickly as a function of space: it is known as small-scale fading. As defined in the section above, small-scale fading refers to rapid changes in radio signal amplitude in a short period of time.

Path loss can be represented by the path loss exponent, and its value is typically in the range 2 to 6 where 2 is for free space propagation and 4 is for relatively lossy environments. In buildings, stadiums and other high construction environments, the path loss exponent exceeds 4 and can reach till 6. Table 2.1 shows some typical path loss exponents measured in different environments.

Environment	**Path loss exponent, β**
Free space	2
Urban area	2.7 *to* 3.5
Shadowed urban area	3 *to* 5
In building line of sight	1.6 *to* 1.8
Obstructed building	4 *to* 6

Table 2.1 Path Loss Exponent for Different Environments [8]

The path loss is inversely proportional to a certain power of the distance between the transmitter and the receiver and can be written as:

$$\overline{P}_r = \frac{c}{d^{\beta}} P_t, \tag{2.1}$$

where c is a constant and d is the distance between the transmitter and the receiver, and β is defined as the path loss exponent of the channel [6]. As noted in the table above, β varies from and environment to another. Accurate network planning is critical for large wireless networks: path loss considerations at a certain distance d from the transmitter can be defined relatively to a known measured value of path loss at a distance d_0. The path loss (PL) at a particular location d is:

$$PL(d) = PL(d_0) - 10\beta \log(\frac{d}{d_0}) + X_{\sigma} \tag{2.2}$$

where $PL(d_0)$ is the measured value of path loss at distance d_0 from the transmitter. X_{σ} is a Gaussian random variable with standard deviation σ ; it is added in (2.2) to account for environmental influences at the transmitter and receiver [8].

2.1.2 Small-Scale Fading

Small-scale fading is a characteristic of radio propagation resulting from the presence of reflectors and scatterers that cause multiple versions of the transmitted signal to arrive at the receiver, each distorted in amplitude, phase, and angle of arrival. Thus, the many replicas of the signal arrive at the receiver with a different time varying amplitude,

phase shift and delay and these different multipath copies of the signal may add up in a destructive or constructive manner, which causes random fluctuations in the received signal amplitude and phase. We can model the received signal $y(t)$ as

$$y(t) = \sum_{i}^{L} a_i(t)x(t - \tau_i(t)) + n(t) \tag{2.3}$$

In the above formula, $a_i(t)$ is the amplitude in time and $\tau_i(t)$ is the propagation delay of the i^{th} component of the multipath received signal, $n(t)$ is the additive white Gaussian noise (AWGN), and L is the total number of multipath components.

The *delay spread*, also known as the *multipath spread* is the time between the reception of the first version of the signal and the last one and is defined by the difference between the minimum and the maximum value of $\tau_i(t)$. It is also noted as T_m. If the delay spread of the channel is very small compared to the signal duration, it is assumed that all multipath components of the received signal have arrived almost at the same time and the shape of the transmitted symbol is intact. While the delay spread is a natural phenomenon, we can define the *coherence bandwidth* B_C as a statistical measure of the range of frequencies over which the channel can be considered as flat.

$$B_C \approx \frac{1}{T_m} \tag{2.4}$$

If the bandwidth of the transmitted signal is smaller than the coherence bandwidth of the channel, the channel is *flat fading* and passes all the spectral components of the multipath signal with approximately equal gain and phase. Else, the channel is considered as

frequency selective fading and certain frequencies are cancelled at the receiver. For flat fading channels, Equation (2.3) becomes

$$y(t) = x(t)\sum_{i}^{L} a_i(t) + n(t) \tag{2.5}$$

$$y(t) = h(t)x(t) + n(t) \tag{2.6}$$

In Equation (2.6) the fading coefficients are noted as $h(t) = \sum_{i}^{L} a_i(t)$

The delay spread and the coherence bandwidth of the channel describe the nature of the channel in a local area; however, they offer no information about the relative motion of the transmitting and the receiving mobile terminals, which causes time variation of the received amplitudes. This information is offered by two parameters: *Doppler spread* B_d and *coherence time* $(\Delta t)_c$. Doppler spread is the range of frequencies for which the Doppler power spectrum in non-zero. The coherence time is the inverse of the Doppler spread and is the average time over which the channel fading coefficient is constant.

$$(\Delta t)_c \approx \frac{1}{B_d} \tag{2.7}$$

When the coherence time of the channel is large relative to the delay constraint of the channel, *slow fading* occurs and amplitude and phase change imposed by the channel can be considered roughly constant over the period of use. Otherwise, the channel is *fast fading* and a symbol can undergo several different attenuations.

In the existing literature, there are three main types of fading: Rayleigh, Rician and Nakagami-m fading. Assuming that L, the number of the multipath signals received in flat fading is large; we can apply the central limit theorem and approximate the distribution of the channel impulse response by a Gaussian process. Consider that there is

no line of sight (LOS) between the transmitter and receiver, the Gaussian process will be zero-mean and thus the channel gain at any time will be a Rayleigh random variable and its phase is uniformly distributed over the interval $(0,2\pi)$. In this case, the channel is a Rayleigh flat fading channel. In case of LOS between source and destination, the Gaussian process has a non-zero mean and the channel can be modeled following a Rician distribution: it is called a Rician fading channel. The Nakagami-m fading occurs for multipath scattering with relatively large delay-time spreads, with different clusters of reflected waves; this model matches empirical observations for channel fading. A detailed explanation of these models is presented in [8] and [9]. Rayleigh fading constitutes a convenient choice in the absence of LOS and we will consider slow Rayleigh fading throughout this thesis.

A simple comparison between Rayleigh fading and AWGN is analyzed in the following paragraph in order to emphasize its severe effects on wireless communications. If we consider the case of a binary phase-shift keying (BPSK) modulation with averages received signal-to-noise ratio $SNR = \frac{E_b}{N_0}$, we can define the received signal as

$$y = hx + n \tag{2.8}$$

In the above equation h is the channel coefficient, x the transmitted signal with values $\pm\sqrt{E_b}$ and n is the AWGN that follows a Gaussian distribution such that $N(0,\frac{N_0}{2})$. The theoretical bit error rate of the channel for any given value of h is

$$P_b(h) = Q(\sqrt{2|h|^2 \frac{E_b}{N_0}}) \tag{2.9}$$

$|h|$ Follows a Rayleigh distribution and the probability density function (pdf) is defined by the following equation:

$$p_{|h|}(u) = \frac{2u}{\Omega} e^{\frac{-u^2}{\Omega}} \qquad u \geq 0 \tag{2.10}$$

Where $\Omega = E(h^2)$ and is the average fading power. If we assume $\gamma = h^2 E_b / N_0$, Equation (2.10) has the form of a chi-square probability distribution with two degrees of freedom

$$p(\gamma) = \frac{1}{\bar{\gamma}} \exp(-\frac{\gamma}{\bar{\gamma}}) \tag{2.11}$$

And $\bar{\gamma}$ is the average of γ. By combining equations (2.11) and (2.9), we can average the condition bit error rate

$$P_b = \int_0^\infty P_b(\gamma) p(\gamma) d\gamma \tag{2.12}$$

Considering average fading power is equal to one ($\Omega = 1$), we can simplify Equation (2.12)

$$P_{b,rayleigh} = \frac{1}{2}(1 - \sqrt{\frac{\bar{\gamma}}{1+\bar{\gamma}}}) \tag{2.13}$$

Which becomes for large $\bar{\gamma}$ values

$$P_{b,Rayleigh} \approx \frac{1}{4\bar{\gamma}} \tag{2.14}$$

We know that bit error rate for BPSK in AWGN channel can be calculated and upper bounded by

$$P_{b,AWGN} = Q(2\frac{E_b}{N_0}) \le \frac{1}{2}\exp(-\frac{E_b}{N_0}) \qquad (2.15)$$

By comparing equations (2.14) and (2.15) it can be easily shown that the bit error rate decreases exponentially with SNR in AWGN channel while it only declines linearly with the inverse of SNR in Rayleigh fading, as shown in Figure (2.2)

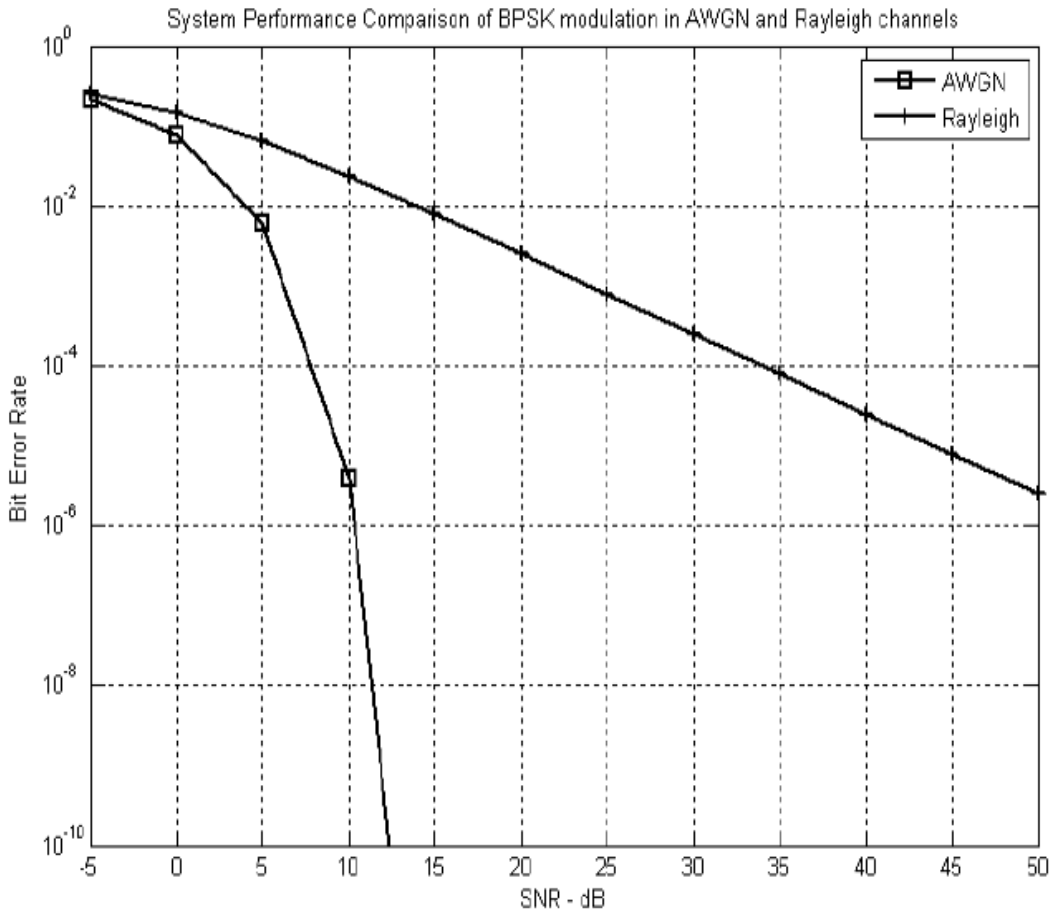

Figure 2.2 Bit error rates of BPSK modulation over AWGN and Rayleigh fading channels

Equation (2.13) was used to obtain the curve of the theoretical bit error rate for Rayleigh fading channels, which means that we have to transmit an infinite number of bits. Given the impracticability of this scenario, we can use the *frame error rate* (FER) as a new

reference. A successful transmission is achieved when its FER is above a certain threshold which varies with the SNR which in turn fluctuates with the fading coefficients. If we know the probability distribution of the fading coefficients, we can then determine the probability of the event when the instantaneous SNR falls below the defined threshold and thus, know if a transmission is successful. This is called the *outage probability*.

In the case of the thesis, for slow flat Rayleigh fading channel, fading coefficients remain constant during the transmission of a fixed length frame of data. Let's assume $\gamma_{\min}$ is the threshold SNR to achieve frame error rate, the outage probability can be defined as

$$P_{outage} = P\left[\gamma \le \bar{\gamma}_{\min}\right] = \int_0^{\gamma_{\min}} p(\gamma)d\gamma = \int_0^{\gamma_{\min}} \frac{1}{\bar{\gamma}} e^{\frac{-\gamma}{\bar{\gamma}}} d\gamma \qquad (2.16)$$

For high SNR, the above can be approximated by

$$P_{outage} \approx \frac{\gamma_{\min}}{\bar{\gamma}} \qquad (2.17)$$

The outage probability only decays inversely with the signal to noise ratio which is a poor performance in wireless communications. For slow fading, outage probability has two main characteristics: transmission rate and instantaneous channel capacity. The capacity of a channel is the maximum amount of information that can be transmitted reliably through a channel. The Shannon limit or Shannon capacity of a communications channel is the theoretical maximum information transmission rate of the channel, for a particular noise level: it is impossible to decode the received message with an arbitrary small probability of error [10]. The capacity of a channel is a function of the channel

condition and is defined in bits per channel use. Obviously, this value is not the same for AWGN and Rayleigh fading:

$$C_{AWGN} = W\log(1+\frac{S}{N}) = W\log(1+\frac{E_b R}{N_0 W}) \tag{2.18}$$

$$C_h = \log(1+|h|^2\frac{E_b}{N_0}) \tag{2.19}$$

As shown in equations (2.19) and (2.20), the channel capacity is constant in AWGN channel for a given SNR while it varies in the case of Rayleigh fading because of the fading coefficients. According to [10], when the instantaneous channel capacity C_h becomes smaller than the information transmission rate R, it is impossible to decode the received message without error. Thus, we can define an outage probability as:

$$P_{outage} = P[C_h < R] \tag{2.20}$$

The maximum transmission rate that can be achieved has a probability of $1-P_{outage}$ and is called *outage capacity*. In quasi-static fading channels, the outage probability can be considered as the lower bound to the frame error rate and is useful to evaluate the performance of a coded system.

2.2 Diversity Techniques

In the previous section, we explained the undesirable effects of fading on the performance of a communication system. In wireless mobile communications, *diversity techniques* are often used to combat the effects of multipath fading and to improve the reliability of transmission without increasing the transmitted power or sacrificing the bandwidth [8][11]. Multiple replicas of the transmitted signals are required at the

receiver, all carrying the same information on different channels. If two or more independent samples of a signal are taken, their fading is uncorrelated and some will be less severely attenuated than others, which means that the probabilities of all the samples signal to noise ratio being below a certain threshold γ is lower than having one signal's signal to noise below that level. It can be proven. Let's assume we have L replicas of the signal at the receiver and an outage occurs when the received signal to noise ratio is below the required threshold with probability $P_{outage,i} = p$. Given the number of replicas is L and that the fading channels are independent, the probability that the L replicas fall below a certain level is $P_{outage,L} = p^L$. Given that $p < 1$, $p^L < p$, $P_{outage,L} < P_{outage,i}$. Therefore, if L independent channels are available, the outage probability defined in the previous section will decrease inversely with the L^{th} power of the average SNR : the system provides a diversity of order L. More generally, if we define P_e the error rate of the system, we can determine the diversity order by

$$Diversity \quad Gain = -\lim_{SNR \to \infty} \frac{\log(P_e)}{\log(SNR)} \tag{2.21}$$

Thus, a good combination of the various samples could help greatly reduce the severity of the fading, and correspondingly, improve the reliability of the communication. Three main types of diversity exist: time, frequency and space diversity.

One way to achieve diversity is to transmit identical messages in different time slots, which results in uncorrelated fading signals at the receiver. However the signals need to be separated by at least the coherence time of the channel. The replicas are provided to the receiver in the form of redundancy in the time domain introduced by error control coding [12]. The time separation between the replicas is provided by time

interleaving in order to obtain independent fades, and the interleaving time creates delays. This technique is effective for fast fading channels where the coherence time is small. However, for slow fading channels, a large interleaver can cause significant delays. One of the inconvenient of this method is the loss of bandwidth efficiency due to the redundancy introduced by the time interleaving. By transmitting the same information L times, this can be considered a repetition code with rate $1/L$.

Another way to achieve diversity is to transmit the same message on many different frequencies. For the frequencies to ensure independent fading, they must be separated by at least the coherence bandwidth. However, if the coherence bandwidth is smaller than the spreading bandwidth of the signal, the multipath delay will be small compared to the symbol period and we cannot obtain frequency diversity. This scheme has the same drawback as time diversity; it induces a loss in bandwidth efficiency due to redundancy introduced in the frequency domain. The achieved order of diversity can be approximated by $L = W/B_C$ where W is the bandwidth of the transmitted signal.

Space diversity, also known as antenna diversity, uses multiple antennas or antenna arrays arranged together at the transmitting and receiving end. In order to avoid correlation between transmissions, the antennas must be physically separated by a certain distance, depending on the physical characteristic of the antenna itself, propagation environment and frequency. In space diversity, the replicas of the signals observe a redundancy in the space domain. This scheme is preferred over time and frequency diversity in high data rate wireless communications because it does not include bandwidth loss. We can have multiple antennas used for transmission or reception, and the respective models are divided into two categories: receive diversity or transmit

diversity [13]. In the case of receive diversity, the spatial separation between the receive antennas must be more than half of the wavelength for the fading to be modeled as independent [5]. Assume we have one transmit antenna and L receive antennas, this results in L different channels, and we can achieve a diversity of order L.

Since bandwidth is one of the main characteristics of a communication channel, it is critical to avoid major losses. This is a main reason why we will focus on spatial diversity for the rest of the thesis. Spatial diversity can be achieved if we have at least two antennas at the receiver and/or transmitter, given that these antennas are spatially separated to obtain independent fading. A briefing of the different types of spatial diversity is shown in below:

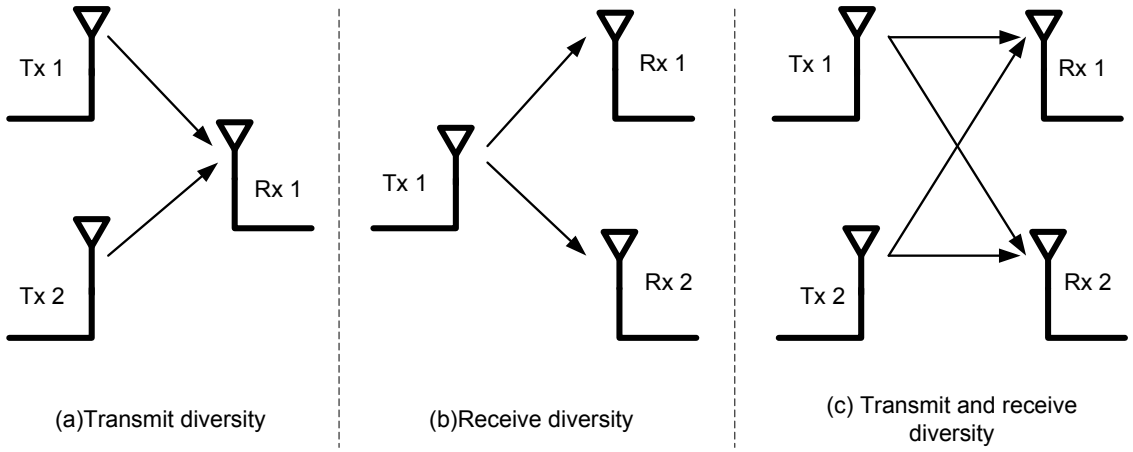

Figure 2.3 Different types of spatial diversity

The next section will mainly focus on diversity combining methods.

2.2.1 Diversity combining methods

In the previous section, we classified diversity techniques according to the domain where diversity is applied: time, frequency and space. We will now discuss the diversity combining schemes at the receiver and present four main techniques: selection combining, switched combining, equal-gain combining (EGC) and maximal ratio combining (MRC) [11][8]. For the rest of section 2.2.1 let's assume that we have one transmit antenna and L receive antennas.

In selection combining (SC), we select the signal with the highest instantaneous signal-to-noise ratio (SNR). In reality, it is rather difficult to measure the SNR of a signal, so the sum of signal and noise power $(S+N)$ is calculated for each signal and the signal with the highest value is selected.

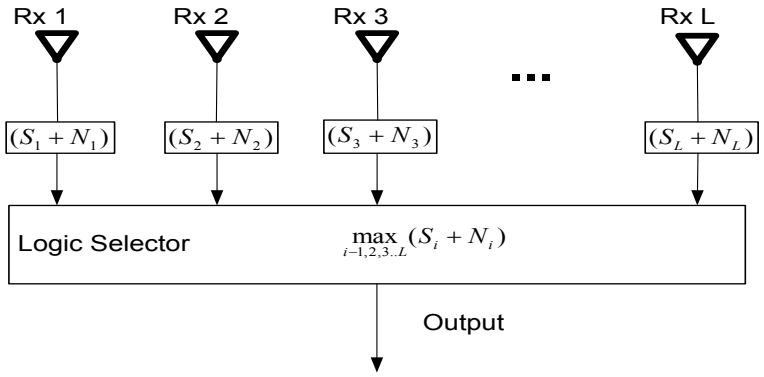

Figure 2.4 Selection combining scheme

Switched combining diversity is a simple diversity combining method. The receiver scans the L branches and selects a branch whose SNR is above a certain threshold, and the

particular signal is selected as the output until its SNR drops below that threshold. In this case, the receiver starts scanning again and switches to another branch. This scheme has a weaker performance than selection combining in the sense that, it does not continually pick up the best SNR.

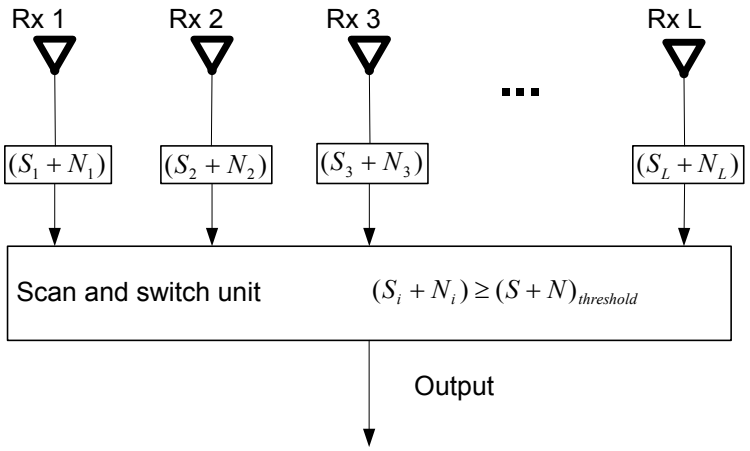

Figure 2.5 Switched combining scheme

However, both selection and switched combining present a major drawback as the output is equal to only one of all the L signals. The next two models proposed combine all the signals received.

Equal gain combining is a suboptimal linear method. It does not use estimation of the fading amplitude for the branch and the received signals are co-phased and then summed together with equal gain. It offers a better performance than selection and switched combining. In fact, the weighting factor for all the signals is set to unity.

$$\alpha_i = e^{-j\phi_i} \tag{2.22}$$

Unlike equal gain combining, various signal inputs are individually weighted and added together to obtain an optimal output signal in maximal ratio combining [8], as shown in Equation (2.26). The weighting factor is chosen to be in proportion to the signal-to-noise ratio of each receive antenna. If we assume that the receive antennas all have the same average noise power, the weighting factor can be defined as

$$\alpha_i = A_i e^{-j\phi_i} \tag{2.23}$$

Where A_i and ϕ_i are respectively the amplitude and phase of the received signal.

The Figure below is a scheme of equal gain and maximal ratio combining.

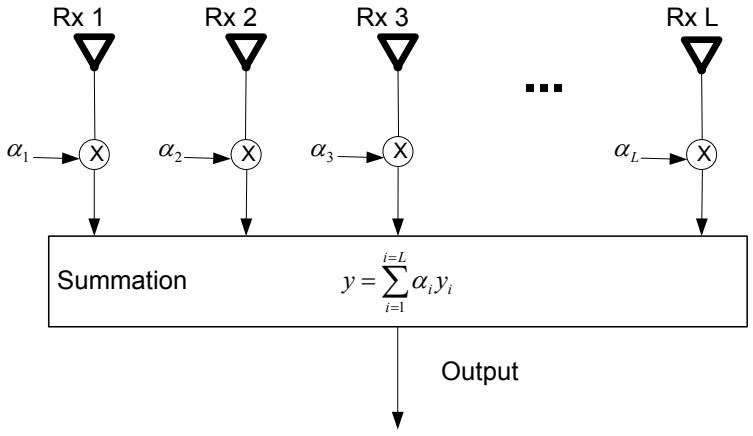

Figure 2.6 Equal-Gain combining and Maximal ratio combining scheme

It is an optimum combining, as it can maximize the output SNR by adding up the instantaneous SNRs of the individual signals [8]. Each signal is co-phased, weighted with the corresponding amplitude and summed. Channel state information is required for this model. Compared to other combining models, MRC offers the best performance despite its complex implementation. If we assume that the received signal from each branch is given by Equation (2.24)

$$y_i = h_i x + n_i \tag{2.24}$$

where n_i a zero-mean Gaussian noise with variance $N_0/2$.

Then the output of the combiner can be written as

$$y = \left(\sum_{i=1}^{L} |h_i|^2 \right) x + \left(\sum_{i=1}^{L} h_i n_i \right) \tag{2.25}$$

Finally, the effective signal to noise ratio of the combined signal at the output is:

$$\gamma_{MRC,eff} = \frac{\left(\sum_{i=1}^{L} |h_i|^2 \right)^2 E_b}{N_0 \sum_{i=1}^{L} |h_i|^2} = \sum_{i=1}^{L} |h_i|^2 \frac{E_b}{N_0} = \sum_{i=1}^{L} \gamma_i \tag{2.26}$$

2.3 Multiple Input Multiple Output (MIMO)

The use of multiple antennas at both transmitter and receiver is called a Multiple-input multiple output system. This technology is important in wireless communication as it offers a significant increase of the data throughput: it has been shown that the transmission rate can reach $\min\{n_{T,} n_R\}$ symbol per channel use [14][15]. It has also been shown by Telatar [14] as well as Foschini and Gans [15] that the spectral efficiency of MIMO channels grows approximately linearly with the number of antennas when all fading channels are mutually independent. MIMO technology offers three main gains that are explained below: array gain – spatial diversity gain – spatial multiplexing gain.

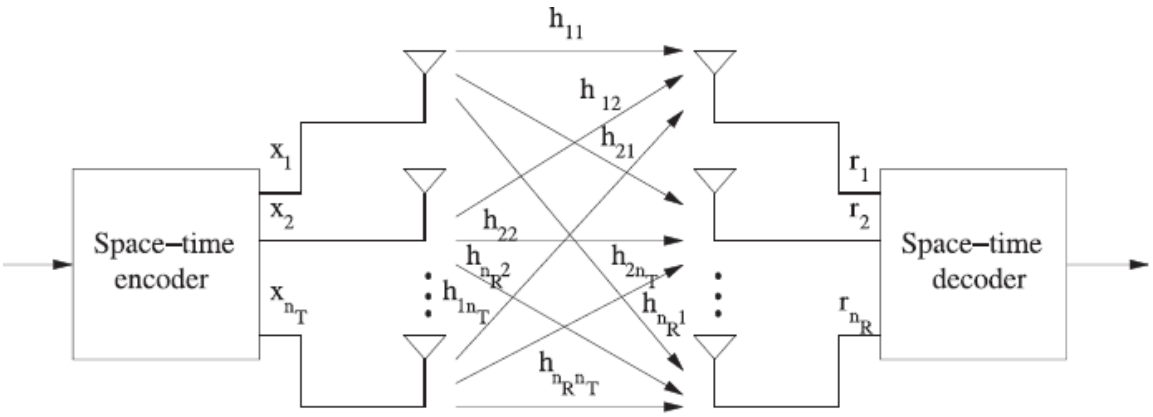

Figure 2.7 MIMO communication channel model [53]

The array gain is the improvement in the receive signal-to-noise ratio (SNR) that results from a coherent combining of the information signals. This can be achieved by doing spatial processing at the receive antenna array and/or spatial pre-coding at the transmit array. It is the horizontal shift of the bit error rate versus transmitted or received power due to the gain in SNR.

Spatial diversity gain represents the improvement in link reliability which is obtained by receiving more than one version of the data through different fading links. By doing so, we increase the probability that at least one of the signals received is not experiencing a deep fade and this improves the quality and reliability of the reception. A MIMO system composed of n_T transmit and n_R received antennas offers $n_T * n_R$ independently fading links and thus a spatial diversity of order $n_T * n_R$ [16].

Contrary to the array and diversity gains that also exist in single input multiple output (SIMO) and multiple input single output (MISO) models, the multiplexing gain is a unique characteristic of MIMO channels. It consists of transmitting multiple, independent data streams within the bandwidth of operation. In spatial multiplexing, a high rate signal

is split into multiple lower rate streams and each stream is transmitted from a different transmit antenna in the same frequency channel. That way, the receiver can separate the data streams and each stream will have at least the same channel quality as in SISO system, which enhances the capacity by a multiplicative factor equal to the number of substreams. The number of substreams that can be reliably supported by a MIMO system is the minimum of the number of transmit antennas n_T and the number of the receive antennas n_R.

However, there is a trade-off to be done between multiplexing gain and diversity gain. According to L. Zheng and D. Tse, if we suppose a multiplexing gain $l = 0,1,..., \min\{n_T, n_R\}$, the maximum achievable diversity gain is [17] :

$$DG(l) = (n_R - l)(n_T - l) \tag{2.27}$$

2.4 Space-Time Codes

Space-time codes (STC) are employed to improve the reliability of data transmission in MIMO wireless communication. This method is based on transmitting antennas and may be split into two main categories: Space-time trellis codes (STTC) distribute a trellis code over multiple transmitting antennas and multiple time slots [18] and Space-time block codes (STBC) that transmit per block of data [19][20]. We will mainly focus in this section on STBC codes by presenting the Alamouti code in the section below.

2.4.1 Alamouti STBC code

Alamouti space-time block coding is a transmit diversity scheme where the information is sent across multiple antennas at the transmitter, which helps improve the reliability of data-transfer [19]. For instance, if we consider a $2x1$ system, there will be two antennas transmitting and thus, two different fading coefficients which imply that some of the received copies of the data will be better than others. This redundancy improves the chances of correctly decoding the received signal. In Alamouti's code, all the signals received are combined in an optimal way that helps extract the most information from each of them.

Assume we have a transmission sequence of: $[x_1 \quad x_2 \quad x_3 \quad ...]$

In normal transmission, we will be sending x_1 in the first time slot, x_2 in the second time slot, and so on.

In Alamouti scheme, we will be sending in the first time slot x_1 and x_2, and in the second time slot $-x_2^*$ and, respectively from antenna 1 and antenna 2.

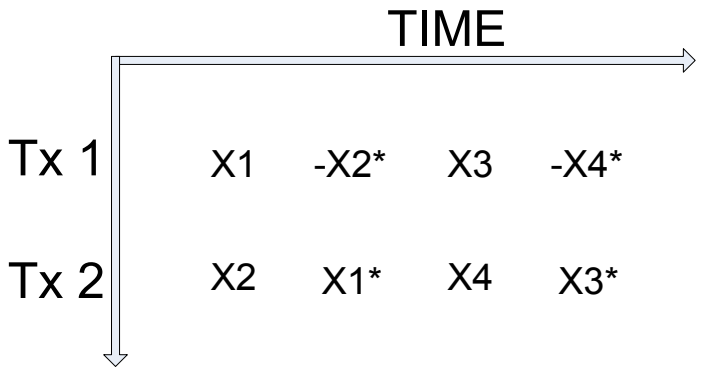

Figure 2.8 Alamouti code transmission

In the first and second time slots, the received signals are defined as:

$$y_1 = [h1 \quad h2] * \begin{bmatrix} x_1 \\ x_2 \end{bmatrix} + n_1$$
$$y_2 = [h1 \quad h2] * \begin{bmatrix} -x_2^* \\ x_1^* \end{bmatrix} + n_2 \tag{2.28}$$

By simplifying the above equation we obtain:

$$\begin{bmatrix} y_1 \\ y_2 \end{bmatrix} = \begin{bmatrix} h1 & h2 \\ h1 & h2 \end{bmatrix} \begin{bmatrix} x_1 & -x_2^* \\ x_2 & x_1^* \end{bmatrix} + \begin{bmatrix} n_1 \\ n_2 \end{bmatrix} \tag{2.29}$$

$$\begin{bmatrix} y_1 \\ y_2^* \end{bmatrix} = \begin{bmatrix} h1 & h2 \\ h2^* & -h1^* \end{bmatrix} \begin{bmatrix} x_1 \\ x_2 \end{bmatrix} + \begin{bmatrix} n_1 \\ n_2^* \end{bmatrix} = H * \begin{bmatrix} x_1 \\ x_2 \end{bmatrix} + \begin{bmatrix} n_1 \\ n_2^* \end{bmatrix},$$
$$H = \begin{bmatrix} h1 & h2 \\ h2^* & -h1^* \end{bmatrix} \tag{2.30}$$

Thus the estimated values of the transmitted bits:

$$\begin{bmatrix} \hat{x}_1 \\ \hat{x}_2 \end{bmatrix} = (H^H H)^{-1} H^H \begin{bmatrix} y_1 \\ y^*{}_2 \end{bmatrix} = \begin{bmatrix} x_1 \\ x_2 \end{bmatrix} + (H^H H)^{-1} H^H \begin{bmatrix} n_1 \\ n_2^* \end{bmatrix} \tag{2.31}$$

2.4.2 Space-time codes

Space-Time Codes (STC) were first introduced by Tarokh et al. from AT&T research labs [18] in 1998 as a transmitting diversity method for the multiple-antenna fading channel. There are two main types of such codes: space-time trellis codes (STTC) as well as space-time block codes (STBC).

STTCs produce a vector composed of the symbol of each antenna. It operates on one input symbol at a time. On the other hand, STBCs operate on a block of input symbols

and produce a $n \times m$ matrix, where each row represents a time slot and each column represents one antenna's transmissions over time.

STTCs provide both diversity and coding gain while STBCs provide only diversity gain and could produce coding gain if concatenated with an outer code, such as Turbo codes. The Alamouti code presented in the previous subsection is the only standard orthogonal STBC that achieves a full rate (rate 1). In this thesis, we will focus on the STBC codes and more specifically, Alamouti code.

2.5 Cooperative diversity

The rise of resource-demanding services and applications as well as the increasing number of users require a higher link data rate than the one that can be achieved in current wireless networks [21]. The design of wireless cellular networks takes into consideration limited radio resources such as transmit power and bandwidth, and they should be respectively minimized and maximized [22]. The MIMO technique, as explained in the previous section, offers better system capacity and helps increase the robustness of a link as well as its data rate. Unfortunately, implementing multiple antennas in modern mobile devices is a challenge due to their small sizes [23]. Cooperative diversity or relay-assisted communication has then been introduced as an alternative solution: several nodes cooperate to transmit/receive information.

2.5.1 Cooperative Communication

The method of relaying was first introduced by Van der Meulen in 1971 [24] in which he presents a wireless communication model composed of three terminals. Cover and El Gamal [25] later studied the model from an information theoretical point of view and showed that the capacity of such relaying scheme exceeds that of a direct link. Since then, many studies covered cooperative diversity. In [26], the authors propose a very simple and effective user cooperation protocol. Assume a mobile station (MS) broadcasts its data frame to the base station (BS) and to an adjacent MS, which in turn retransmits the frame to the BS. Given that the channels from both MSs to BS are uncorrelated, we obtain a higher degree of diversity.

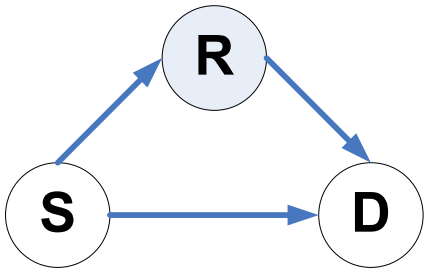

Figure 2.9 The relay channel, source (S), relay (R), and destination (D)

The cooperative communication, which was introduced in [27] is based on the scheme in Figure 2.9 but with the relay terminal being another source. Both sources send their own information as well as their partner's data. In the study, it was assumed that both sources are transmitting in full duplex mode: they transmit their own data and receive a noisy version of their partner's. This model achieves the ergodic capacity

In general, it is considered that the relay node works in full-duplex mode: it receives and sends data at the same time. This problem can be solved by assuming that the frequency

on which the main-link (S-D) transmission occurs is different than the one that the relaying link uses. However, in reality the terminals transmit in half-duplex mode and it impacts the spectral efficiency of the model: in the first phase, the relay listens and it transmits in the second phase. Even though multiplexing gains are not possible in half-duplex relaying, there can be significant capacity gains [28][29].

2.5.2 Overview of relay protocols

In [30][31], the authors define three half-duplex relaying protocols as shown in Figure 2.10.

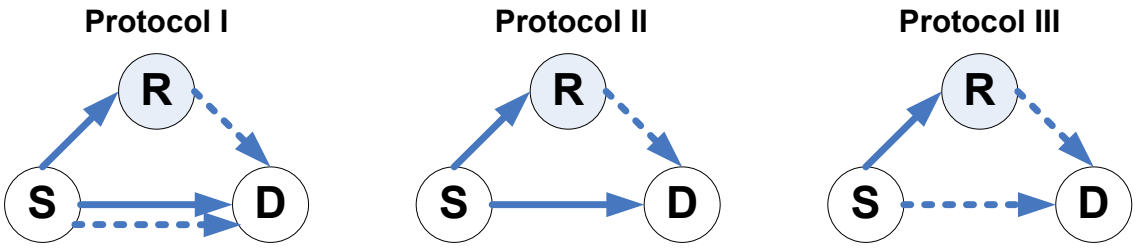

Figure 2.10 Half-Duplex forwarding and relaying protocols. Solid lines represent the relay-receive phase and dashed lines are for relay-transmit phase.

In protocol I, the source communicates with both relay and destination in the first time slot (solid lines) and in the second time slot, both source and relay transmit to the destination (dashed lines). In protocol II, the source broadcasts to both relay and destination in the first time slot while only the relay transmits in the second time slot. Finally, in protocol III, the source transmits uniquely to the relay in the first time slot and both the source and the relay send the information to destination in the second time slot.

2.5.2 Strategies of relay-assisted transmission

The strategies of the relay-assisted transmission have to consider the decoding at the destination, resource allocation as well as the cooperation protocols which are, fixed, selection and incremental relaying. Two principal relaying schemes are discussed in this section: amplify-and-forward (AF) and decode-and-forward (DF).

In fixed relaying, the relay transmits constantly independently of the channel state information (CSI). In amplify-and-forward, the relay amplifies the received signal from the source and transmits it to the destination. The main inconvenient of this strategy is the amplification of the noise at the receiver of the relay. Despite that, fixed-relaying and AF achieve order 2 diversity as two different antennas are transmitting. In the proposed decode-and-forward scheme [21], the relay decodes the received symbols from the source before deciding to forward the information to the destination. The relay declares an error if the message is not decoded successfully and does not transmit to the destination. In this case, the model only achieves a diversity of order 1. The fixed-relaying can be a waste of bandwidth especially if the source-destination has a good CSI.

In selection relaying, the nodes have access to channel state information and make use of this information to improve its cooperation strategy. The source constantly monitors the source-relay gain. When this gain drops below a certain threshold, it transmits another version of information to the destination in the second phase. Unlike the fixed-relaying, this technique achieves full diversity for both AF and DF [6].

In incremental relaying technique, the destination sends a one bit feedback to the relay at the end of the first phase and asks for cooperation only when needed; the relay does not transmit unnecessary information to the destination and this increases the

spectral efficiency of the communication system. The authors in [6] show that this scheme achieves full diversity with better spectral efficiency than both fixed-relaying and selection-relaying.

AF and DF strategies both present a main drawback in a multiple relay model: there is a huge waste of bandwidth. For the different node channels to avoid interference with each other, the relays have to transmit in different time slots or frequency channels, thus transmitting in time-division multiple access or frequency-division multiple access. Distributed space-time codes were introduced [9] to combat this problem.

The transmission rate depends heavily on the geometrical position of the relay node; when the relay is closer to the source, the transmission rate in the source-relay link can be higher (phase 1) and when the relay is closer to the destination, the transmission rate in the relay-destination link can be higher (phase 2) [31]. This means that the transmit diversity protocol has a better performance when the relay is closer to the source and when the relay is closer to the destination, the receiver diversity protocol has a better performance. Both source and relay transmit in the second phase using STC while the source remains silent and the relay uses a regular channel code to transmit data to the destination. Other protocols have been proposed as well, including multi-hopping relaying, where only one node transmits at a time and the receiver uses only this information to decode. Multi-hopping does not achieve full diversity.

2.6 Turbo codes

Turbo codes are a high performance class of Forward Error Correcting codes (FEC) and are widely used in a variety of wireless applications, including mobile,

satellite and wireless systems [37], [43]. Initially introduced by Berrou, Glavieux and Thitimajshim [32], [33] in 1993, they achieved a bit error rate (BER) of 10^{-5} at 0.7 dB in an AWGN channel using Binary Phase Shift Keying (BPSK) modulation at a transmission rate of $1/2$. Further researches and papers adjusted different settings of Turbo codes depending on their needs, such as the rate, the interleaver, or the memory size [34], [35], [36]. New class types of Turbo codes were developed as well, such as Block and Non-Binary Turbo codes [38][39][40][41][42].

The main components of Turbo codes are an encoder and a decoder. The encoder is formed by the parallel concatenation of two recursive systematic convolutional component (RSC) codes which are separated by an interleaver while the Turbo Decoder is composed of two iterative Soft Input Soft Output (SISO) decoders that utilize the Maximum a posteriori (MAP) algorithm to decode the data. Then they exchange their output data to reach an accurate decision on the received stream.

2.6.1 Turbo Encoder

A Turbo Encoder, as shown in Figure.2.11 is composed of two systematic convolutional encoders that can be either recursive or non-recursive. It has been shown in [44][45] that the BER performance of Turbo codes using recursive encoders improves as the size of the interleaver increases. The use of recursive encoders is necessary to obtain an interleaving gain. An information sequence of length N is input to the first systematic encoder and the output of this encoder is the parity sequence as well as the information sequence: the rate of the first encoder is $1/2$. Then the interleaved information sequence

is input to the second convolutional encoder and at the output consists of the parity check sequence only so the rate of the second encoder is also $1/2$. The overall rate of the Turbo Encoder is $1/3$ and the output is composed of the information bits, as well as the parity sequence of the first and second encoder respectively. At the end of the information bits, the two encoders are terminated with tail bits that reset the encoders to the zero state.

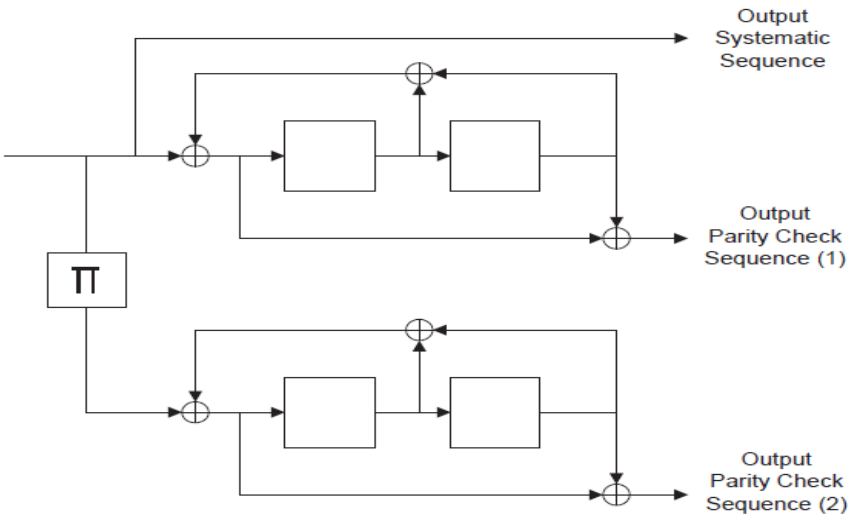

Figure 2.11 Turbo Encoder diagram

A convolutional encoder is described by its generator vectors for its feedforward and feedback connections. If we note GF1 and GR1 respectively the feedforward and feedback generators of the encoder 1 and GF2, GR2 the generators for encoder 2, then the overall Turbo Encoder is denoted as: PCCC(1,GF1/GR1,GF2/GR2). In the case of the above example, it is a symmetric Turbo Encoder and GF1=GF2=[101]=5_8 and GR1 = GR2 = [111] = 7_8. The Turbo Encoder in Figure 2.11 follows the notation PCCC $(1,5/7,5/7)_8$.

The 4-state diagram of the Turbo Encoder described in this section is presented below:

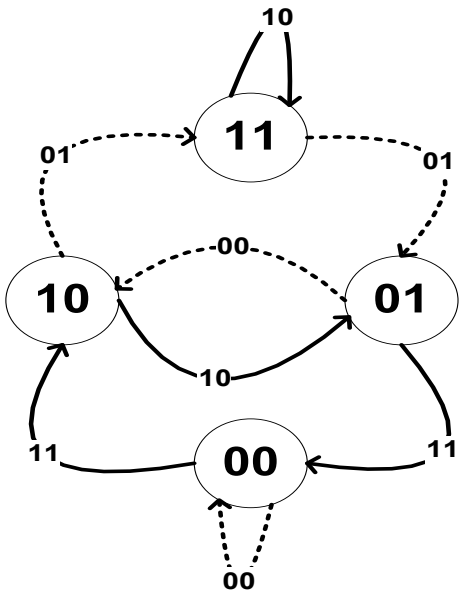

Figure 2.12 Turbo Encoder state diagram

Figure 2.12 shows the state diagram of the convolutional encoder used in (1,5/7,5/7) Turbo Encoder. It is a 4-state diagram and a dashed line corresponds to a "1" as an input while the solid line represents an input equal to "0".

2.6.2 Turbo Decoder

Like the Turbo Encoder, a Turbo Decoder is composed of two component decoders that are connected in series via an interleaver that is identical to the one used at the encoder, and its de-interleaver.

The two SISO decoders cooperate together to estimate the transmitted information sequence in an iterative manner. The binary sequence of information is $y_{1s} = [y_{1s}(1) \quad y_{1s}(2) \quad y_{1s}(3) \quad ... \quad y_{1s}(N)]$ is input to a Turbo Encoder and its interleaved version is input to Turbo Encoder 2. The resulting encoder bits are respectively $y_{1p} = [y_{1p}(1) \quad y_{1p}(2) \quad y_{1p}(3) \quad ... \quad y_{1p}(N)]$ and $y_{1p} = [y_{2p}(1) \quad y_{2p}(2) \quad y_{2p}(3) \quad ... \quad y_{2p}(N)]$. The transmitted bits form a vector $x = [y_{1s} \quad y_{1p} \quad y_{2p}]$ that is composed of the systematic, parity 1 and parity 2 bits respectively and has a length of $3 \times N$. Valenti summarized the equations of iterative Turbo decoding in [37]:

$$L^1(\hat{u}) = \log \frac{P\left[m_i = 1 \middle| y_{1s}, y_{1p}, L_e^{2'}\right]}{P\left[m_i = 0 \middle| y_{1s}, y_{1p}, L_e^{2'}\right]} \tag{2.31}$$

$$L^2(\hat{u}) = \log \frac{P\left[\tilde{m}_i = 1 \middle| y_{1s}^{'}, y_{2p}, L_e^{1'}\right]}{P\left[\tilde{m}_i = 0 \middle| y_{1s}^{'}, y_{2p}, L_e^{1'}\right]} \tag{2.32}$$

Where y_{1s} is the Log Likelihood ratio of the systematic bits and $y_{1s}^{'}$ its interleaved version, and y_{1p} and y_{2p} are respectively the LLR values for the parity bits from the first and second encoder. The a posteriori LLR computed at decoder 1 is noted $L^1(\hat{u})$ and $L^2(\hat{u})$ is computed at decoder 2, while the extrinsic value of each decoder is defined by L_e

$$L_e^1 = L^1(\hat{u}) - y_{1s} - L_e^{2'} \tag{2.33}$$

$$L_e^2 = L^2(\hat{u}) - y_{1s}^{'} - L_e^{1'} \tag{2.34}$$

The SISO decoder 2 uses the extrinsic information calculated from decoder 1 in order to define its own extrinsic information that decoder 1 will use. The two decoders keep exchanging their soft information between each other for a predefined number of

iterations. As the iterative process continues, the a posteriori probability of the information bit is refined and this results in an improvement in the bit error rate performance of the decoded bits. At the final iteration, a hard decision on the decoded bits is made as such:

$$m_i = \begin{cases} 1 & if \quad L^{2"}(u) > 0 \\ 0 & else \end{cases} \tag{2.35}$$

Where $L^{2"}(u)$ is the de-interleaved vector of $L^2(u)$.

The iterative process of Turbo decoding is summarized in the below diagram

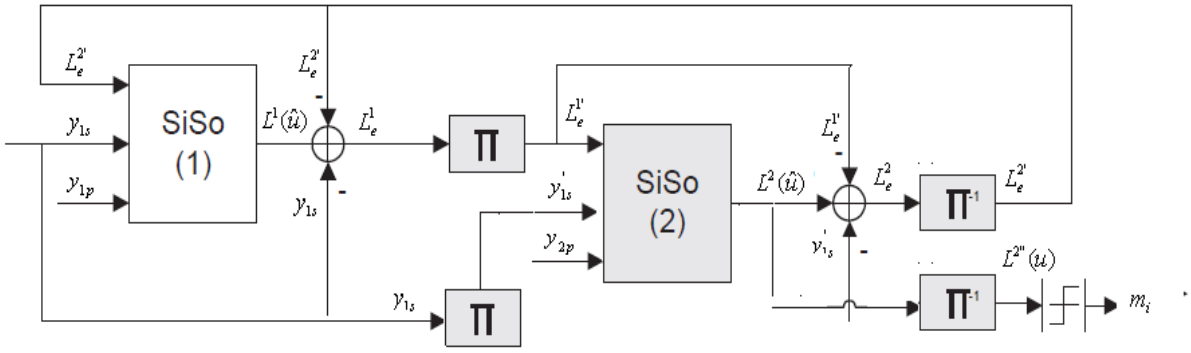

Figure 2.13 Turbo Decoder

2.6.3 Principle of iterative decoding

Each of the decoders that compose the Turbo Decoder has soft input and soft output

Figure 2.14 "Soft Input, Soft Output" decoder

The log likelihood ratio (LLR) of the a priori probability of all information bits $L(u)$ and channel reliability measure L_c are the two soft inputs to the SISO decoder. The LLR value of information bits is defined as :

$$L(u) = \ln \frac{P(u_k = +1)}{P(u_k = -1)} \tag{2.36}$$

At the first iteration, given that we assume that we have equal probabilities for $u_k = \pm 1$ for the first SISO decoder, the LLR value is $L(u) = 0$.

The channel reliability is a function of the transmission rate, as well as the channel condition; it is defined as

$$L_c = 4RE_b / N_0 \tag{2.37}$$

Where R is the code rate and E_b / N_0 is the ratio of energy per transmitted bit over the noise density.

For systematic codes, the soft output of the information bits is the sum of three terms

$$L(\hat{u}) = L_c \cdot y + L(u) + L_e(\hat{u}) \tag{2.38}$$

Where L_e is the extrinsic value for all the information bits and is used as an estimate of the a priori LLR for the other decoder.

2.6.4 MAP algorithm

There are two main trellis based algorithms that are used in the SISO decoder and both use the state diagram presented in Figure 2.12: the Viterbi algorithm analyzed in [46] and the maximum a posteriori (MAP) algorithm [32]. The Viterbi algorithm is optimal for ML decoding, but it only provides a sequence of decoded bits without reliability values in the form of likelihood. However, this is an important information for the information exchange between both SISO decoders. In [32] Berrou et Al have computed a MAP method based on the BCJR algorithm which was proposed in 1974 by Bahl, Cocke, Jelinek and Raviv [47]. In the next paragraph we give a short summary of the BCJR algorithm, as used by each individual component SISO decoder of a Turbo code.

The maximum a posteriori algorithm, based on BCJR, computes the most probable state $\hat{s}_i$ at any instant i considering the received sequence y .

$$\hat{s}_i = \arg\left\{ \max_{s_i} P\left[s_i | y \right] \right\} \tag{2.39}$$

The BCJR algorithm is based on backward and forward recursions and provides for each information bit u_k a probability that it is sent as a $+1$ or a -1 given the received bit y_k

$$L(u) = \ln \frac{P(u_k = +1)}{P(u_k = -1)} = \ln \frac{\sum_{u=+1}^{(s',s)} P(s', s, y)}{\sum_{u=-1}^{(s',s)} P(s', s, y)} \tag{2.40}$$

Where s' is the initial state and s is the next state.

$$P(s', s, y) = P(s', y_{j<k}) \cdot P(s, y_k | s') \cdot P(y_{j>k} | s) \quad (2.41)$$

$$P(s', s, y) = \alpha_{k-1}(s') \cdot \gamma_k(s', s) \cdot \beta_k(s) \quad (2.42)$$

Where $\alpha_{k-1}(s')$ is the forward recursion value, $\beta_k(s)$ the backward recursion value and $\gamma_k(s', s)$ the branch metric. The forward and backward metrics, as well as the branch metrics are expressed in [48] as

$$\alpha_k(s') = \sum_{(s',s)} \gamma_k(s', s) \cdot \alpha_{k-1}(s') \quad (2.43)$$

$$\beta_{k-1}(s') = \sum_{(s',s)} \gamma_k(s', s) \cdot \beta_k(s') \quad (2.44)$$

$$\gamma_k(s', s) = A_k \cdot B_k \cdot \exp\left(\frac{1}{2}\left(L_c \cdot y_{k,1} \cdot u_k + \sum_{v=2}^{n} L_c \cdot y_{k,v} \cdot x_{k,v} + u_k \cdot L(u_k)\right)\right) \quad (2.45)$$

Regrouping equations (2.40) to (2.45) the LLR of each received bit can be written as

$$L(\hat{u}_k) = \ln \frac{\sum_{u=+1}^{(s',s)} \alpha_{k-1}(s') \cdot \gamma_k(s', s) \cdot \beta_k(s)}{\sum_{u=-1}^{(s',s)} \alpha_{k-1}(s') \cdot \gamma_k(s', s) \cdot \beta_k(s)} \quad (2.46)$$

2.6.5 Suboptimal algorithms

The computation of the parameters in the MAP algorithm is extremely complex, requiring the a posteriori LLR value for each decoded bit. Modifications were proposed to reduce its complexity while maintaining and other alternatives were proposed, such as Log Map and Max log Map algorithms [49]

In the logarithmic domain, the multiplication that is computed in the MAP algorithm becomes a simple addition and it reduces the complexity. Using the Jacobian algorithm, the addition in the log domain can be further simplified:

$$\begin{aligned} \ln(e^x + e^y) &= \max(x, y) + \ln(1 + \exp(-|y - x|)) \\ \ln(e^x + e^y) &= \max(x, y) + f_c(y - x) \end{aligned} \tag{2.47}$$

Where $f_c(y-x)$ is the correction function. If y and x are different, the correction function is close to zero, which implies that :

$$\ln(e^x + e^y) \approx \max(x, y) \tag{2.48}$$

The Log-Map algorithm computes its LLR values using Equation (2.47) while the Max-Log-Map algorithm uses Equation (2.48) to compute its LLR values.

The drastic reduction in computational complexity results in some degradation in the performance: it is why they are called suboptimal algorithms.

2.6.6 Turbo code performance

The performance of Turbo codes is a function of various variables such as the number of iterations, the decoding algorithm, the interleaver size, the generator vectors and the rate. Also, they do not have the same performance depending on the type of the channel; in this subsection, we will present its bit error rate performance for Turbo codes in the different environments.

2.6.6.1 Turbo code performance in AWGN channel

As mentioned above, the performance of the Turbo code changes a lot depending on different parameters. The bit error rate performance shown in Figure 2.15 has a Turbo

Encoder (1,5/7,5/7) and the decoding algorithm used is the Log-MAP algorithm for 8 iterations. The channel is an additive white Gaussian noise (AWGN) and the modulation is BPSK.

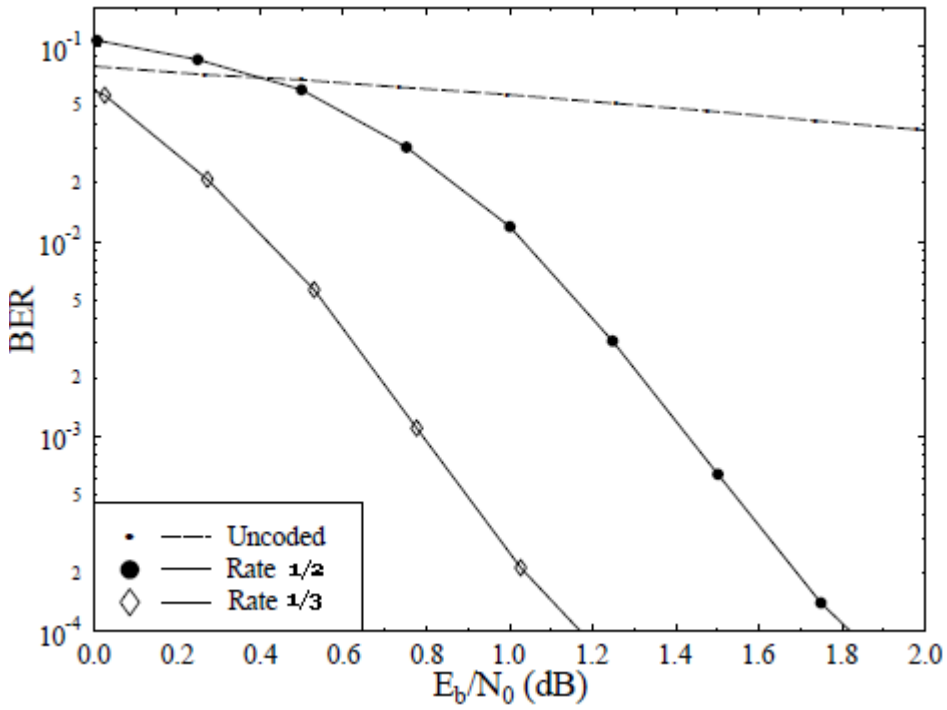

Figure 2.15 Bit error rate performance for Turbo code (1,5/7,5/7) in AWGN channel using different code rates [51]

As we can see, a code of rate $\frac{1}{3}$ achieves an improvement of approximately 6 dBs for a bit error rate of 10^{-4}. However, this comes at an expense of channel use. The code of rate $\frac{1}{2}$ has been punctured, all the information bits are sent and half of each parity bits are sent.

2.6.6.2 Turbo code performance in fast Rayleigh fading channel

Turbo code in fast Rayleigh fading has a much better performance than in slow Rayleigh fading. Assume the same Turbo code, with encoder $(1,5/7,5/7)$, a $1/3$ code rate achieves a bit error rate of 10^{-4} at $2.3\,\text{dB}$ while the punctured code achieves such a performance at $3.8\,\text{dB}$. A fast fading channel is equivalent to perfect interleaving, and the improvement in the bit error rate compared to slow fading is justified by the interleaving gain.

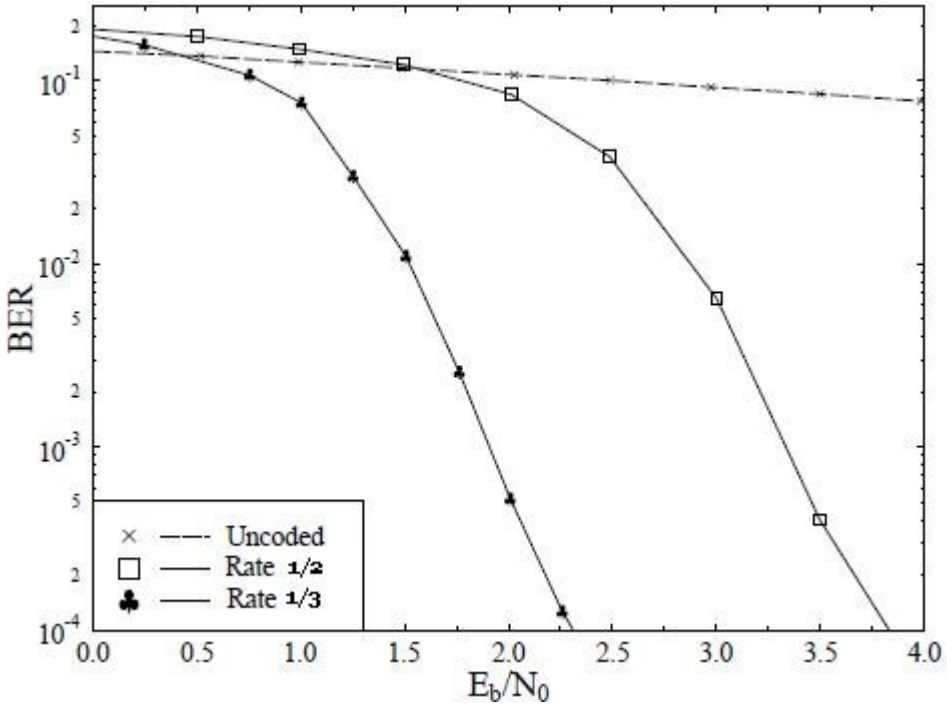

Figure 2.16 Bit error rate performance for Turbo code (1,5/7,5/7) in fast Rayleigh fading channel using different decoding algorithms [51]

2.7 Water-filling

The water-filling method is composed of two principal algorithms: the rate-adaptive which maximizes the transmission rate for a fixed energy and the margin-adaptive which in turn minimizes the energy for a fixed rate.

2.7.1 Rate-adaptive algorithm

This algorithm maximizes the number of bits per symbol subject to a fixed energy constraint and is characterized by both equations:

$$\begin{aligned} &\max_{\varepsilon_n} \quad b = \sum_{n=1}^{N} \frac{1}{2} \cdot \log_2 (1 + \frac{\varepsilon_n \cdot g_n}{\Gamma}) \\ &N \cdot \bar{\varepsilon}_x = \sum_{n=1}^{N} \varepsilon_n \end{aligned} \tag{2.49}$$

Where g_n is a function of the channel and is equal to $g_n = \frac{\left|H_n{}^2\right|}{\sigma_n^2}$, $\left|H_n{}^2\right|$ is the channel gain and Γ is the gap of the code. There are $N+1$ equations for $N+1$ unknowns which are the energies ε_n and the constant K.

$$\begin{aligned} &\varepsilon_1 + \Gamma / g_1 = K \\ &\varepsilon_2 + \Gamma / g_2 = K \\ &\bullet \\ &\bullet \\ &\varepsilon_N + \Gamma / g_N = K \\ &\sum_{n=1}^{N} \varepsilon_n = N \cdot \bar{\varepsilon}_x \end{aligned} \tag{2.50}$$

The negative solutions and energies are eliminated ad the corresponding ε_n is zeroed. The sets of equations are solved recursively until a solution with no negative energy occurs.

For the first iteration, the solution is:

$$K = \frac{1}{N}\left[N \cdot \bar{\varepsilon}_x + \Gamma \cdot \sum_{n=1}^{N} \frac{1}{g_n} \right]$$
$$\varepsilon_n = K - \frac{\Gamma}{g_n}, n = 1,2,.., N \tag{2.51}$$

And the capacity of each subchannel can be determined

$$b_n = \frac{1}{2} \cdot \log_2(1 + \varepsilon_n \cdot g_n) \tag{2.52}$$

The rate adaptive algorithm can be summarized by the diagram:

2.7.2 Margin-adaptive algorithm

The margin-adaptive algorithm minimizes the energy subject to a fixed bits/symbol rate

$$\min_{\varepsilon_n} \quad \varepsilon_x = \sum_{n=1}^{N} \varepsilon_n$$
$$b = \sum_{n=1}^{N} \frac{1}{2} \cdot \log_2(1 + \frac{\varepsilon_n \cdot g_n}{\Gamma}) \tag{2.53}$$

The minimized energy in the MA algorithm is defined below

$$\varepsilon_n = K_{ma} - \frac{\Gamma}{g_n} \tag{2.54}$$

Where K_{ma} is a constant defined for each subchannel

$$K_{ma} = \Gamma \cdot \left(\frac{2^{2b}}{\Pi_{n=1}^{N} g_n} \right)^{1/N} \tag{2.55}$$

Chapter 3: Space-time coded cooperation

In this Chapter, we consider a three terminals relay model: a source, a relay and a destination in a slow Rayleigh fading channel. We analyze the system performance in various scenarios while focusing on some key factors, such as the cooperation rate and the bit error rate of the overall system. Assume a source mobile user that has two transmit antennas, a relay mobile user that has four receive antenna and two transmit antennas and finally a base station that has four receive antennas. Alamouti and space-time coding are applied and transmission is done over QPSK modulation.

The system communication happens in two phases: in phase 1, the source broadcasts the message to both the relay and base station. If the message is received correctly at the relay, the relay transmits to the destination in phase 2 and maximal ratio combining is applied at the destination. Else, the relay remains silent in phase 2, as well as the source.

3.1 System model

Similar to [52], the communication system used in this Chapter is a cooperative MIMO space-time coded system with a single relay. Each link uses space-time block code over a slow Rayleigh channel.

The system has two transmission phases: at first, the source broadcasts a message to the destination and the relay using a 2x4 Alamouti code. Then if the relay has successfully decoded, it collaborates in the second phase and sends another copy of the frame that was sent by the source during phase 1.

So if the relay collaborates, the destination receives two versions of the same frame in different channel state conditions, and maximal ratio combining is applied as shown in [52]. Else, the destination receives only one copy of the frame and is decoded like any 2x4 Alamouti code.

We assume that the mobile terminals operate in half duplex mode; they can transmit or receive at the time, using the same frequency band.

In this Chapter, we will simulate many cases of power allocation. Static power allocation and dynamic power allocation will be compared.

3.1.1 Broadcast phase

In the broadcast phase, we have an Alamouti encoder of 2x4; the initial frame is encoded and broadcasted to the the relay and the destination. We note that the channel state information is different for both relay and destination.

3.1.2 Collaboration phase

The protocol adopted for our work is decode and forward. In order to optimize the protocol, we also use a CRC check at the relay to make sure that a correct frame it is sending correct information. The received frame at the relay is decoded using a maximum likelihood detector and then passes a CRC check. If the frame is correctly decoded, then the relay will cooperate. Else, it will remain idle.

Overall, we have two scenarios. The first, in which the destination receives two copies of the frame, one from the source during phase 1 and another one from the relay during

phase 2. And in the second scenario, if the relay cannot decode correctly the frame, the destination receives one copy of the frame from the source and the relay remains idle.

The scheme below resumes the model of Chapter 3.

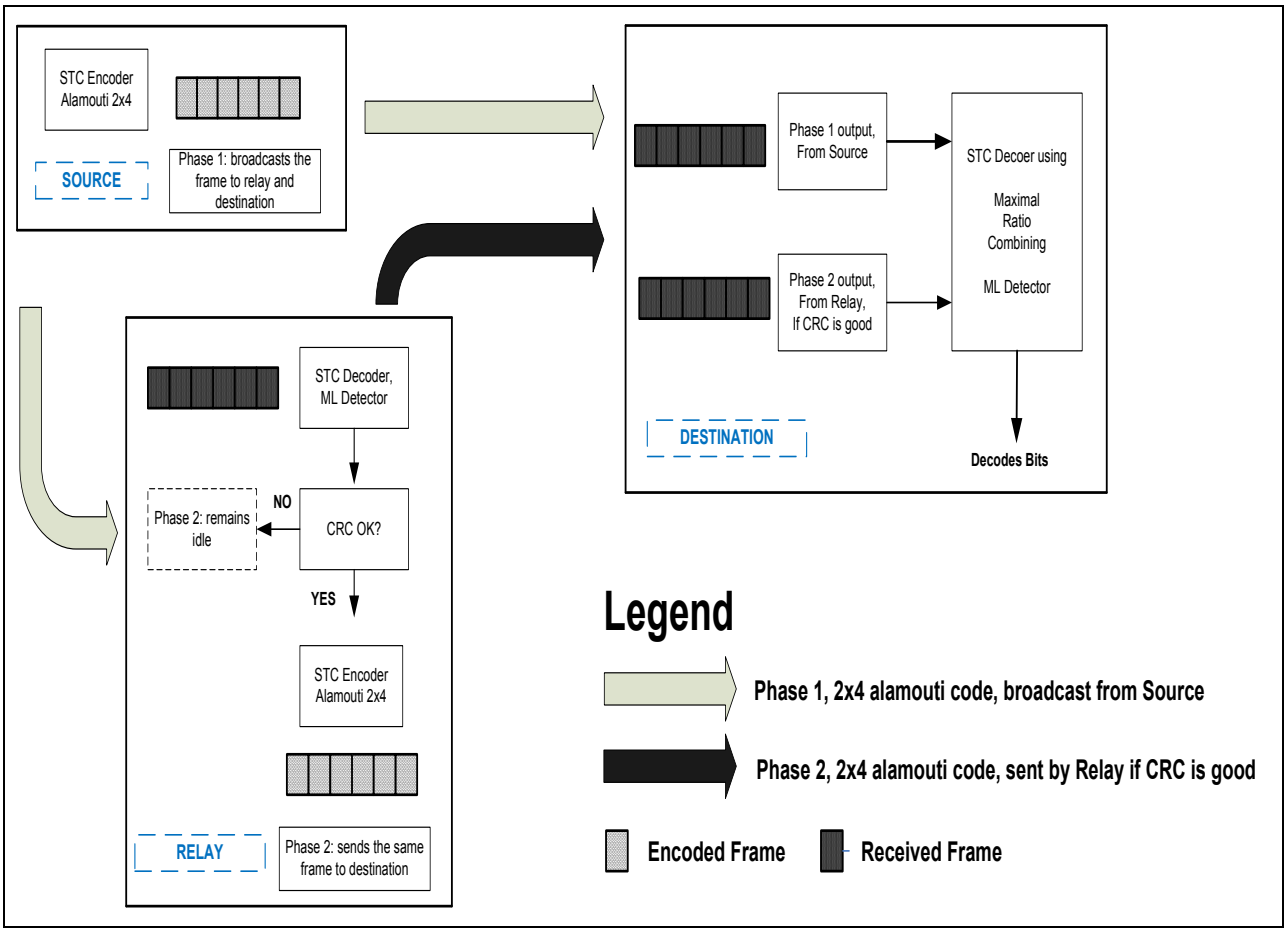

Figure 3.1 System Model

3.2 Example of Alamouti and space-time code simulations

In this section, we present analytical results as well as simulations for the bit error rate performance for some space-time codes in a slow Rayleigh fading channel.

3.2.1 2x1 Alamouti code

The Alamouti space-time code scheme was proposed in 1998 by Alamouti [19] for a system with two transmitting antennas and one receiving antenna. We assume a slow Rayleigh fading channel, so channel coefficients $h_{i,j}$ are constant across the transmission of a frame. The first antenna sends $[x_1 \quad -x_2^*]$ and the second antenna sends $[x_2 \quad x_1^*]$ so the first symbol period is $[x_1 \quad x_2]$ and the second $[-x_2^* \quad x_1^*]$ is where x_1^* is the complex conjugate of x_1.

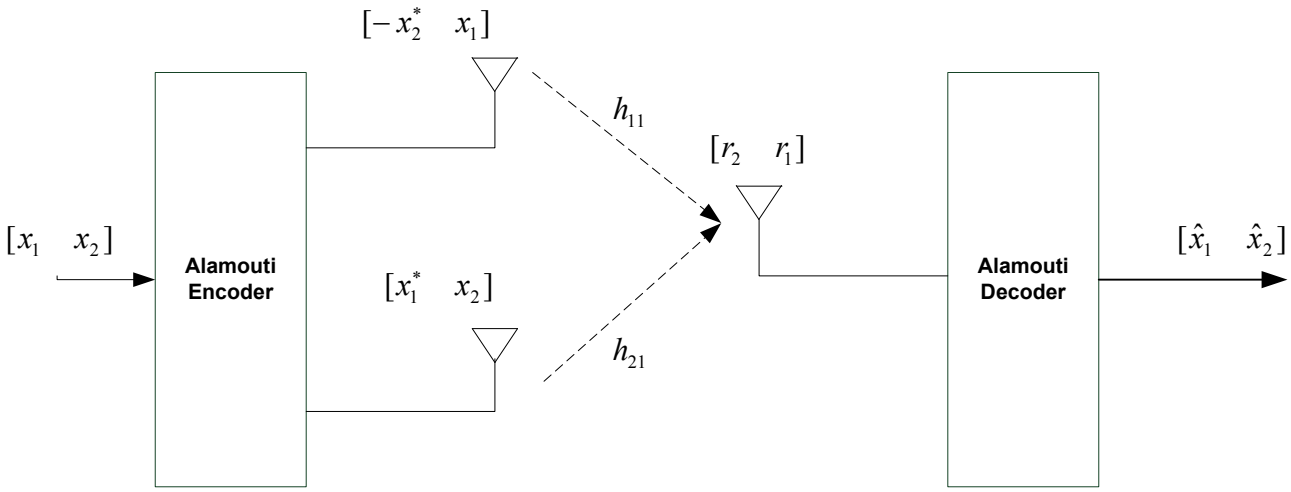

Figure 3.2 Alamouti 2×1 Scheme for slow Rayleigh fading channel

For the channel condition of slow Rayleigh fading, we note that channel coefficients are constant over the period of the frame transmission:

$$\begin{aligned} h_{11} &= h_{11}(t) \\ h_{21} &= h_{21}(t) \end{aligned} \tag{3.1}$$

And the received signals are defined as:

$$\begin{aligned} r_1 &= h_{11} \cdot x_1 + h_{21} \cdot x_2 + n_0 \\ r_2 &= -h_{11} \cdot x_2^* + h_{21} \cdot x_1^* + n_1 \end{aligned} \tag{3.2}$$

According to [20], the decoded signals at the receiver are:

$$\begin{aligned} \hat{x}_1 &= h_{11}^* \cdot r_1 + h_{21} \cdot r_2^* \\ \hat{x}_2 &= h_{21}^* \cdot r_1 - h_{11} \cdot r_2^* \end{aligned} \tag{3.3}$$

And finally a decision is made according to

$$x_i = \begin{cases} 1 & if\ \hat{x}_i \geq 0 \\ 0 & if\ \hat{x}_i < 0 \end{cases} \tag{3.4}$$

The bit error rate performance for a 2x1 Alamouti code considering a direct link transmission and a distance of 1, as well as a path loss factor of 1 is shown below.

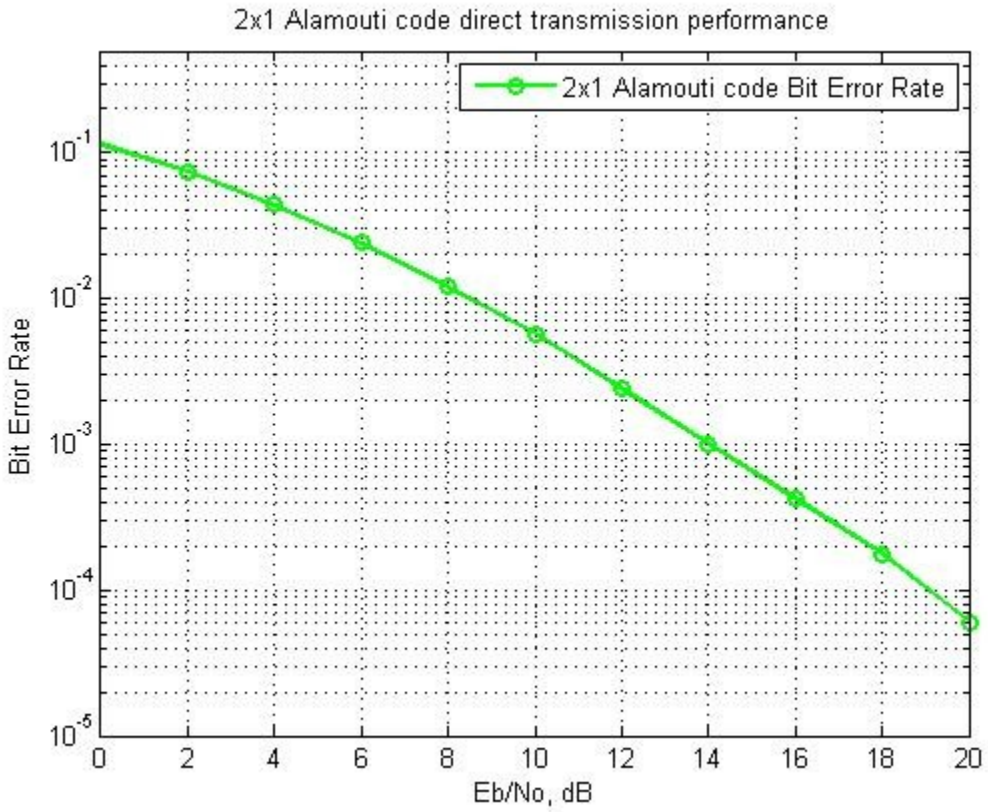

Figure 3.3 2x1 Alamouti code bit error rate

3.2.2 2x2 Alamouti code

In [19] Alamouti also extended the protocol to two receiving antennas as shown in the Figure below:

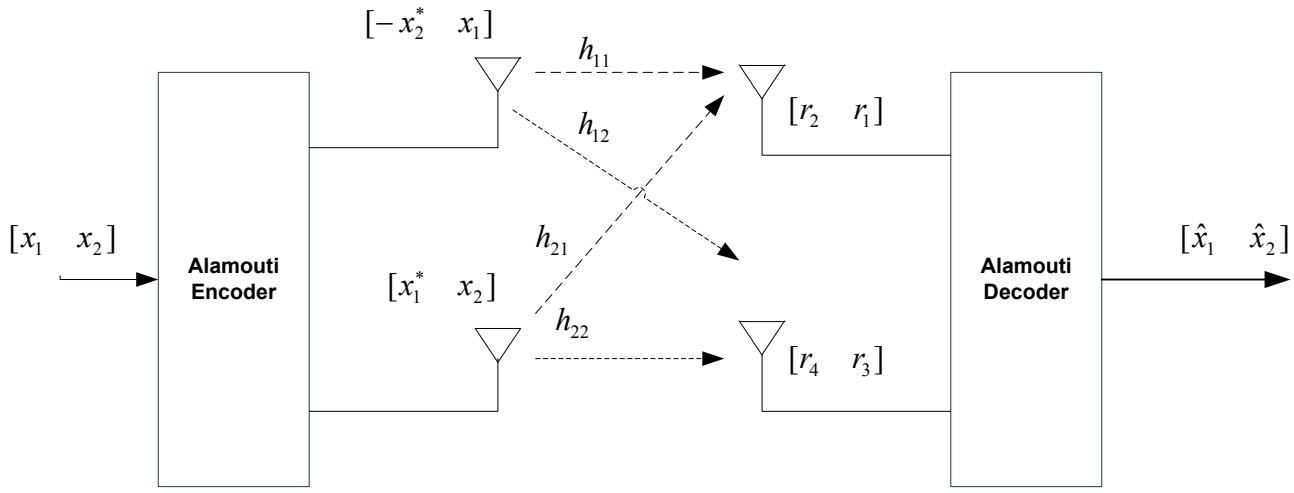

Figure 3.4 Alamouti 2×2 Scheme for slow Rayleigh fading channel

The received signals are defined as:

$$\begin{aligned} r_1 &= h_{11}\cdot x_1 + h_{21}\cdot x_2 + n_0 \\ r_2 &= -h_{11}\cdot x_2^* + h_{21}\cdot x_1^* + n_1 \\ r_3 &= h_{12}\cdot x_1 + h_{22}\cdot x_2 + n_0 \\ r_4 &= -h_{12}\cdot x_2^* + h_{22}\cdot x_1^* + n_1 \end{aligned} \tag{3.5}$$

Similarly to (3.3), the decoded bits at destination are:

$$\begin{aligned} \hat{x}_1 &= h_{11}^*\cdot r_1 + h_{21}\cdot r_2^* + h_{12}^*\cdot r_3 + h_{22}\cdot r_4^* \\ \hat{x}_2 &= h_{21}^*\cdot r_1 - h_{11}\cdot r_2^* + h_{22}^*\cdot r_3 - h_{12}\cdot r_4^* \end{aligned} \tag{3.6}$$

We apply the same equation as in (3.4) to decode the received bit.

With a second antenna at the receiver, we observe an improvement in the performance of the bit error rate. For a bit error rate of 10^{-3} we observe an improvement of approximately 4 dBs. This threshold is obtained at 10 dBs for a second antenna at the receiver while it is obtained for 14 dBs with a single

antenna.

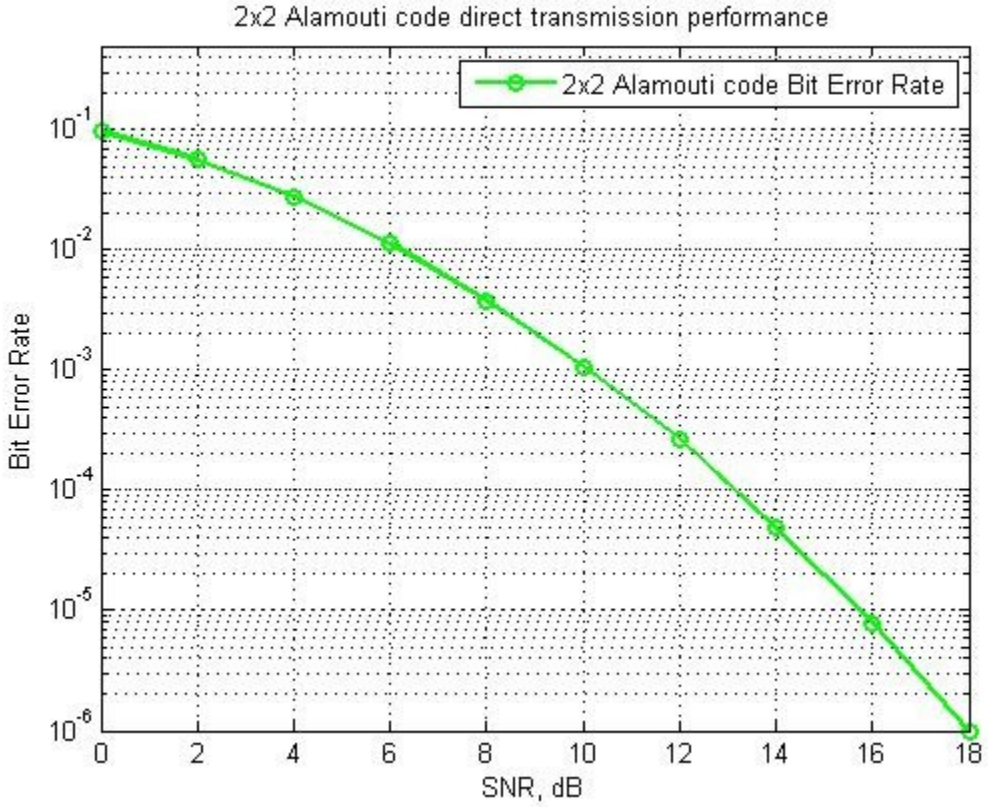

Figure 3.5 2x2 Alamouti code bit error rate

3.2.3 2x4 Alamouti code

The Alamouti code can also be extended to m receiving antennas. Assume $m = 4$.

At the destination, the received signals are

$$
\begin{aligned}
r_1 &= h_{11} \cdot x_1 + h_{21} \cdot x_2 + n_0 \\
r_2 &= -h_{11} \cdot x_2^* + h_{21} \cdot x_1^* + n_1 \\
r_3 &= h_{12} \cdot x_1 + h_{22} \cdot x_2 + n_2 \\
r_4 &= -h_{12} \cdot x_2^* + h_{22} \cdot x_1^* + n_3 \\
r_5 &= h_{13} \cdot x_1 + h_{23} \cdot x_2 + n_4 \\
r_6 &= -h_{13} \cdot x_2^* + h_{23} \cdot x_1^* + n_5 \\
r_7 &= h_{14} \cdot x_1 + h_{24} \cdot x_2 + n_6 \\
r_8 &= -h_{14} \cdot x_2^* + h_{24} \cdot x_1^* + n_7
\end{aligned}
\tag{3.7}
$$

Where h_{ij} is the Rayleigh fading channel on which antenna i is transmitting and antenna j is receiving.

The received signals similarly to a 2x1 and 2x2 Alamouti code, are computed the following way:

$$
\begin{aligned}
\hat{x}_1 &= h_{11}^* \cdot r_1 + h_{21} \cdot r_2^* + h_{12}^* \cdot r_2 + h_{22} \cdot r_2^* + h_{13}^* \cdot r_1 + h_{23} \cdot r_2^* + h_{14}^* \cdot r_1 + h_{24} \cdot r_2^* \\
\hat{x}_2 &= h_{21}^* \cdot r_1 - h_{11} \cdot r_2^* + h_{22}^* \cdot r_1 - h_{12} \cdot r_2^* + h_{23}^* \cdot r_1 - h_{13} \cdot r_2^* + h_{24}^* \cdot r_1 - h_{14} \cdot r_2^*
\end{aligned}
\tag{3.8}
$$

The threshold of bit error rate 10^{-3} is attained for less than $2.5\,\text{dBs}$, which is at least $7.5\,\text{dBs}$ better than a 2x2 model and $11.5\,\text{dBs}$ better than a 2x1 model.

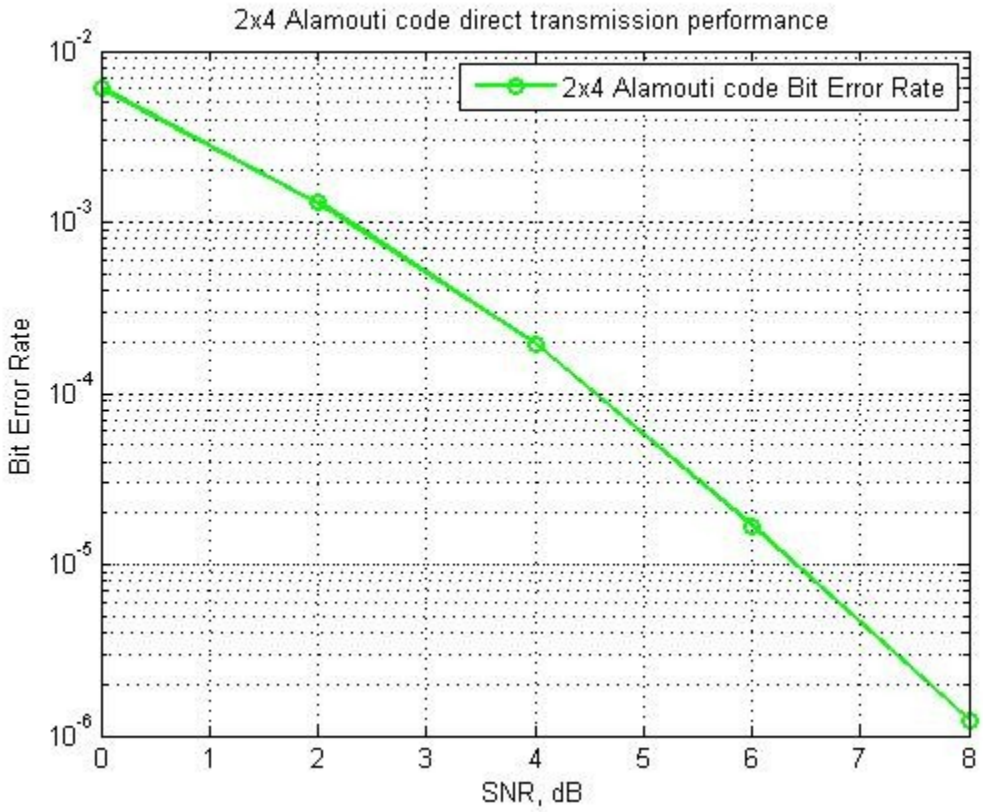

Figure 3.6 2x4 Alamouti code bit error rate

3.2.4 4x4 Space-time code

G. Ganesan and P. Stoica defined in [50] a space-time code in which 4 antennas transmit and another 4 antennas receive. The code has a rate of $\frac{3}{4}$ as three symbols are transmitted in four time slots.

$$C_{4,3/4} = \begin{bmatrix} x_1 & x_2 & x_3 & 0 \\ -x_2^* & x_1^* & 0 & x_3 \\ -x_3^* & 0 & x_1^* & -x_2 \\ 0 & -x_3^* & x_2^* & x_1 \end{bmatrix} \tag{3.9}$$

In this case, 16 signals are received during four time slots.

Time slot	**Receiver Antenna Rx1**	**Receiver Antenna Rx2**	**Receiver Antenna Rx3**	**Receiver Antenna Rx4**
$t_1 = t$	r_1	r_2	r_3	r_4
$t_2 = t + T$	r_5	r_6	r_7	r_8
$t_2 = t + 2 \cdot T$	r_9	r_{10}	r_{11}	r_{12}
$t_2 = t + 3 \cdot T$	r_{13}	r_{14}	r_{15}	r_{16}

Table 3.1 Space-time block code 4x4 transmission

The signals defined in the table above are computed as:

$$
\begin{aligned}
r_1 &= h_{11}\cdot x_1 + h_{21}\cdot x_2 + h_{31}\cdot x_3 + n_0\\
r_2 &= -h_{11}\cdot x_2^* + h_{21}\cdot x_1^* + h_{41}\cdot x_3 + n_1\\
r_3 &= -h_{11}\cdot x_3^* + h_{31}\cdot x_1^* - h_{41}\cdot x_2 + n_2\\
r_4 &= -h_{21}\cdot x_3^* + h_{31}\cdot x_2^* + h_{41}\cdot x_1 + n_3\\
r_5 &= h_{12}\cdot x_1 + h_{22}\cdot x_2 + h_{32}\cdot x_3 + n_4\\
r_6 &= -h_{12}\cdot x_2^* + h_{22}\cdot x_1^* + h_{42}\cdot x_3 + n_5\\
r_7 &= -h_{12}\cdot x_3^* + h_{32}\cdot x_1^* - h_{42}\cdot x_2 + n_6\\
r_8 &= -h_{22}\cdot x_3^* + h_{32}\cdot x_2^* + h_{42}\cdot x_1 + n_7\\
r_9 &= h_{13}\cdot x_1 + h_{23}\cdot x_2 + h_{33}\cdot x_3 + n_8\\
r_{10} &= -h_{13}\cdot x_2^* + h_{23}\cdot x_1^* + h_{43}\cdot x_3 + n_9\\
r_{11} &= -h_{13}\cdot x_3^* + h_{33}\cdot x_1^* - h_{43}\cdot x_2 + n_{10}\\
r_{12} &= -h_{23}\cdot x_3^* + h_{33}\cdot x_2^* + h_{43}\cdot x_1 + n_{11}\\
r_{13} &= h_{14}\cdot x_1 + h_{24}\cdot x_2 + h_{34}\cdot x_3 + n_{12}\\
r_{14} &= -h_{14}\cdot x_2^* + h_{24}\cdot x_1^* + h_{44}\cdot x_3 + n_{13}\\
r_{15} &= -h_{14}\cdot x_3^* + h_{34}\cdot x_1^* - h_{44}\cdot x_2 + n_{14}\\
r_{16} &= -h_{24}\cdot x_3^* + h_{34}\cdot x_2^* + h_{44}\cdot x_1 + n_{15}
\end{aligned}
\qquad (3.10)
$$

Where h_{ij} is the Rayleigh fading coefficient on which antenna i is transmitting and antenna j is receiving and n_k is a AWGN noise.

Given the orthogonality of the code, the decoded signals, $\begin{bmatrix}\hat{x}_1 & \hat{x}_2 & \hat{x}_3\end{bmatrix}$ are obtained by a simple computation by combining the received messages at different time slots.

$$
\begin{aligned}
\hat{x}_1 &= h_{11}^*\cdot r_1 + h_{21}\cdot r_2^* + h_{31}\cdot r_3^* + h_{41}^*\cdot r_4 + h_{12}^*\cdot r_5 + h_{22}\cdot r_6^* + h_{32}\cdot r_7^* + h_{42}^*\cdot r_8 +\\
&\quad h_{13}^*\cdot r_9 + h_{23}\cdot r_{10}^* + h_{33}\cdot r_{11}^* + h_{43}^*\cdot r_{12} + h_{14}^*\cdot r_{13} + h_{24}\cdot r_{14}^* + h_{34}\cdot r_{15}^* + h_{44}^*\cdot r_{16}
\end{aligned}
$$

$$
\begin{aligned}
\hat{x}_2 &= h_{21}^*\cdot r_1 - h_{11}\cdot r_2^* - h_{41}^*\cdot r_3 + h_{31}\cdot r_4^* + h_{22}^*\cdot r_5 - h_{12}\cdot r_6^* - h_{42}^*\cdot r_7 + h_{32}\cdot r_8^* +\\
&\quad h_{23}^*\cdot r_9 - h_{13}\cdot r_{10}^* - h_{43}^*\cdot r_{11} + h_{33}\cdot r_{12}^* + h_{24}^*\cdot r_{13} - h_{14}\cdot r_{14}^* - h_{44}^*\cdot r_{15} + h_{34}\cdot r_{16}^*
\end{aligned}
\qquad (3.11)
$$

$$
\begin{aligned}
\hat{x}_3 &= h_{31}^*\cdot r_1 + h_{41}^*\cdot r_2 - h_{11}\cdot r_3^* - h_{21}\cdot r_4^* + h_{32}^*\cdot r_5 + h_{42}^*\cdot r_6 - h_{12}\cdot r_7^* - h_{22}\cdot r_8^* +\\
&\quad h_{33}^*\cdot r_9 + h_{43}^*\cdot r_{10} - h_{13}\cdot r_{11}^* - h_{23}\cdot r_{12}^* + h_{34}^*\cdot r_{13} + h_{44}^*\cdot r_{14} - h_{14}\cdot r_{15}^* - h_{24}\cdot r_{16}^*
\end{aligned}
$$

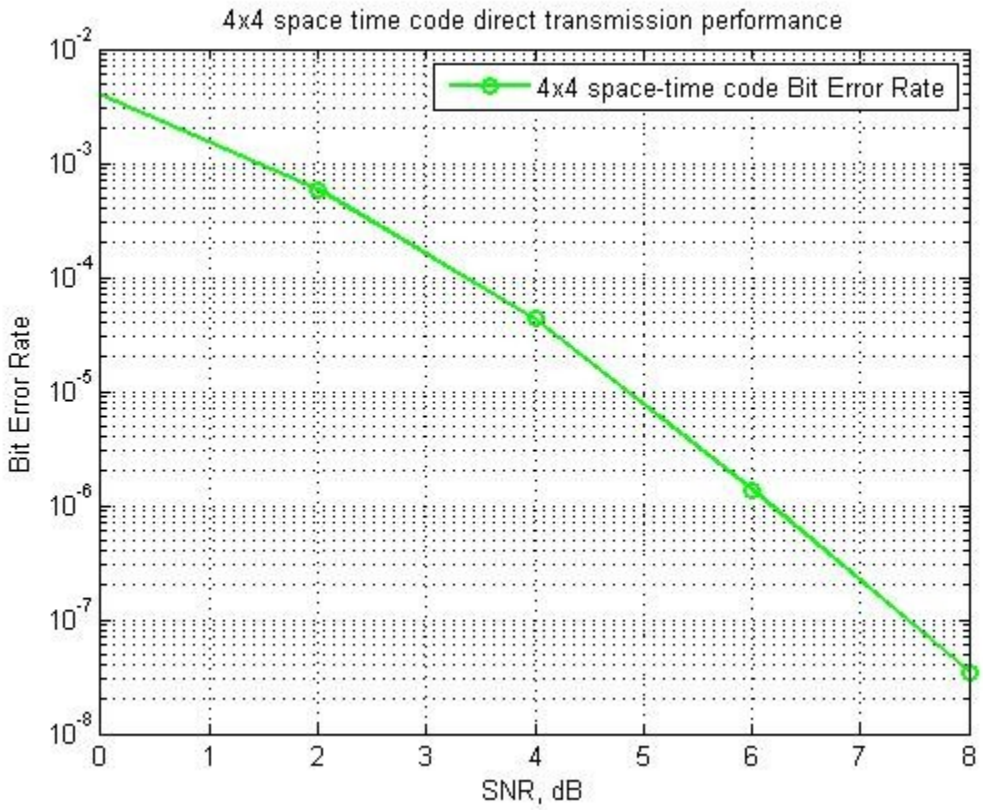

Figure 3.7 4x4 Space-time code bit error rate

3.3 Space-time coded cooperation performance

For this section, we consider a frame length of 1440 bits in a slow flat Rayleigh fading environment.

For the simulations, we assumed that the distance between the source and the destination is unitary $d_{sd} = 10$ and the position of the relay is between the source and the destination

such that $d_{sr} \in [0 \quad 10]$ and $d_{rd} = d_{sd} - d_{sr}$ where d_{rd} is the distance between the relay and the destination.

Also, we have compared a couple different power allocations, depending on the position of the relay.

For Chapters 3 and 4, the considered SNR is at the transmitter. We also consider that the transmitters (source and relay) do not have knowledge of the channel state information, unlike the destination. Given that both transmitters are composed of two antennas, we assume that the power is equally split between both for each terminal.

3.3.1 Case 1: Relay at equal distance between source and destination

3.3.1.1 LOS Environment

In this case, we consider the position of the relay at equal distance from the source and the destination and we consider that all the channels are in line-of-sight :

$$\begin{aligned} d_{sd} &= 10 \\ d_{sr} &= d_{rd} = d_{sd}/2 = 5 \\ \beta_{sd} &= \beta_{sr} = \beta_{rd} = 2 \end{aligned} \tag{3.12}$$

Also, four different scenarios were considered for the power allocation:

$$\begin{aligned} P_s &= 2 \times P_r \\ P_s &= P_r \\ P_s &= P_r / 2 \\ P_s &= \mu \times P_{tot}, P_r = (1-\mu) \times P_{tot} \qquad \mu \in [0 \quad 1] \end{aligned} \tag{3.13}$$

We define a coefficient μ that is dynamic and changes in function of the distance such that the power received at the relay is equal to the power received at the destination.

$$\mu = \frac{d_{sr}^{\beta_{sr}}}{(d_{sd} - d_{sr})^{\beta_{rd}}} \tag{3.14}$$

This value of μ is such that the received signal at the relay in phase 1 (from source) and the received signal at destination in phase 2 (from relay) have equal powers. For that condition to be respected, the power transmitted at both source and relay should be defined as

$$\frac{P_s}{d_{sr}^{\beta_{sr}}} = \frac{P_r}{d_{rd}^{\beta_{rdr}}}$$

$$P_s = \frac{d_{sr}^{\beta_{sr}}}{(d_{sd} - d_{sr})^{\beta_{rd}}} P_r \tag{3.15}$$

For the rest of the Chapter, we will define k such that

$$P_s = kP_r$$

$$k = \frac{d_{sr}^{\beta_{sr}}}{(d_{sd} - d_{sr})^{\beta_{rd}}} \tag{3.16}$$

We were able to identify the collaboration rate of the relay for the different power allocations. The highest rate is when we have more power at the source and $P_s = 2 \times P_r$ and the smallest rate is when we have less power at the source and $P_s = P_r / 2$. Also, we observe that the case $P_s = P_r$ and $P_s = kP_r$ are the same because in this particular scenario $\mu = 1/2$ and $k = 1$ and this is why the blue and purple curves are the same.

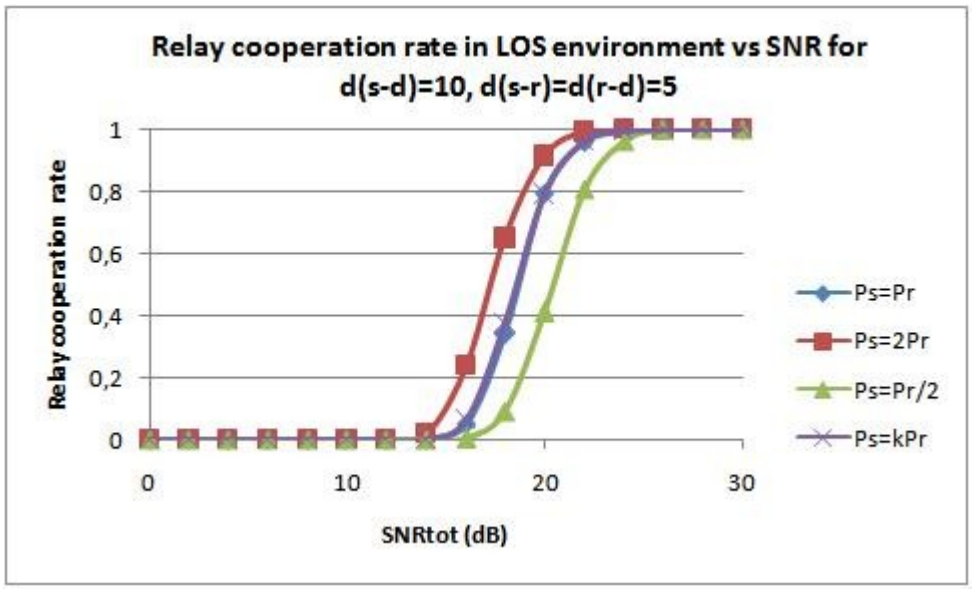

Figure 3.8 Relay cooperation vs total SNR in LOS environment

However, having the best collaboration at the relay does not necessarily imply that the end-to-end bit error rate is the best as there should be enough power to send the frame during the second phase at the relay. The best bit error rate performance is for $P_s = P_r$ as shown in the Figure below.

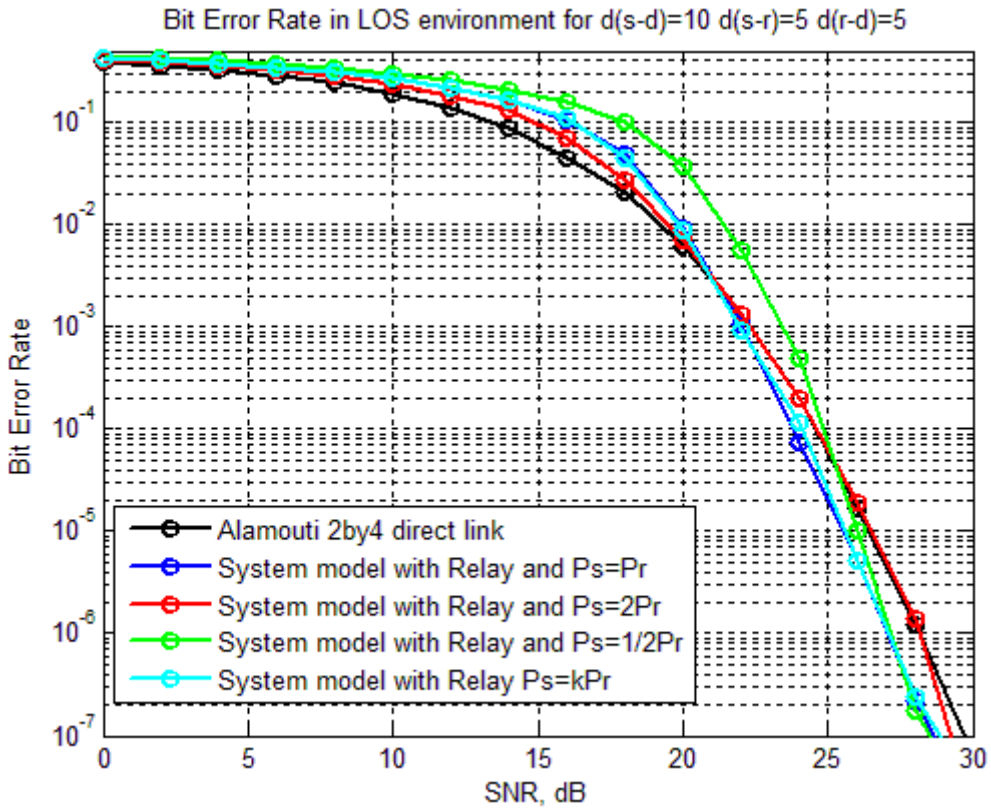

Figure 3.9 System bit error rate in LOS environment

We observe that for low SNRs the direct link transmission is slightly better than the three node relaying model. However, for $SNR > 20$ dBs the space-time coded cooperation becomes better. The best bit error rate is for the case where $P_s = P_r = P_{tot}/2$. For $SNR = 25$ dBs the probability of error is approximately 1.1×10^{-5}.

3.3.1.2 NLOS Environment

Assuming that the relay is at equal distance from both the source and destination, in the case of non line-of-sight, we consider the following parameters:

$$
\begin{aligned}
d_{sd} &= 10 \\
d_{sr} &= d_{rd} = d_{sd}/2 = 5 \\
\beta_{sd} &= \beta_{sr} = \beta_{rd} = 4
\end{aligned}
\tag{3.17}
$$

The relay cooperation depends on the power allocated during the first phase at the source. The relay cooperates more when it receives a signal with more power, as shown below. It is why we observe that for the case $P_s = 2P_r$ the relay has the highest cooperation rate.

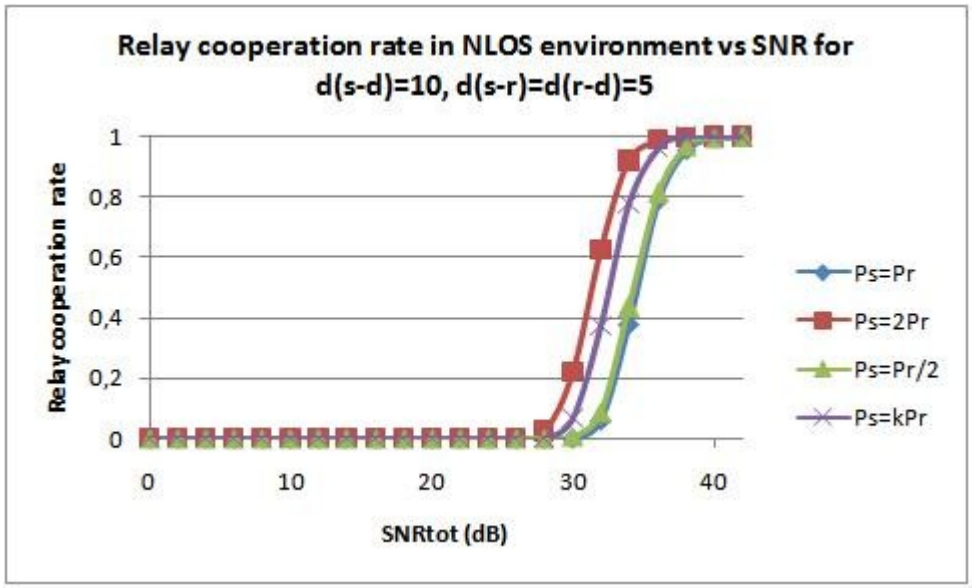

Figure 3.10 Relay cooperation vs total SNR in NLOS environment

Given the equal path loss factor and equal relay distance from both source and destination, $k = 1$ and the cases $P_s = k \times P_r = P_r$. For high SNR values, we observe that the best bit error rate performance is for $P_s = P_r$. The error rate of 10^{-5} is obtained for $SNR = 40 dBs$.

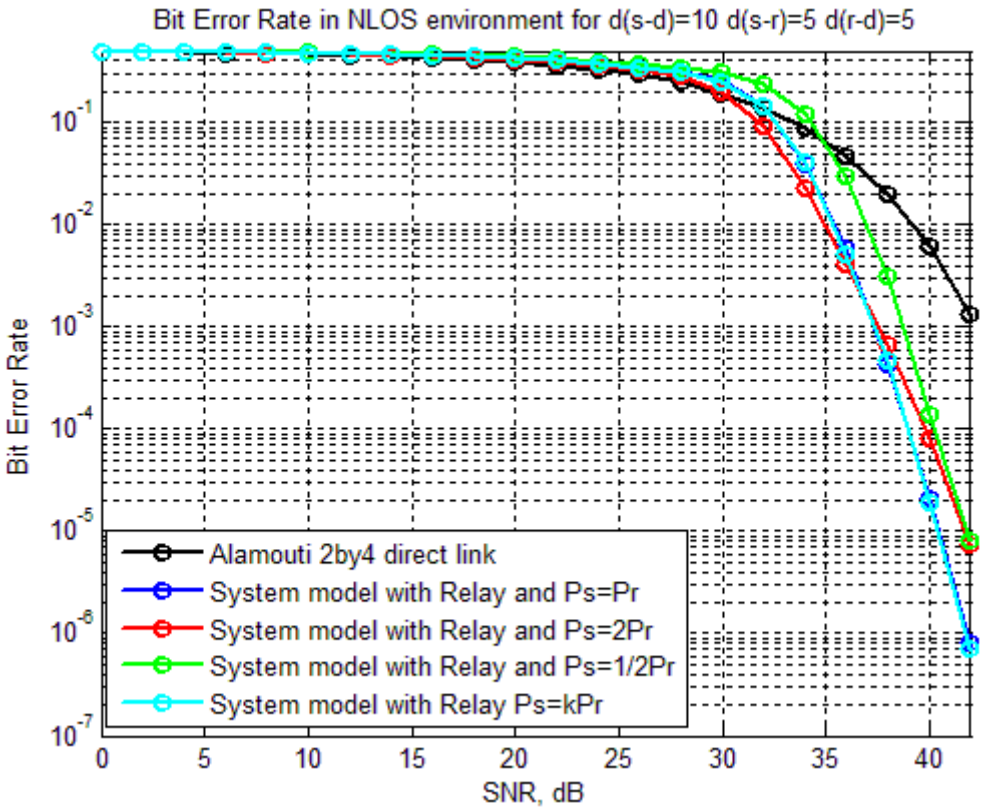

Figure 3.11 System bit error rate in NLOS environment

Also, we observe the space-time coded model presents an improvement of $5\,dBs$ compared to the direct link transmission for a bit error rate of 10^{-3}.

3.3.2 Case 2: Performance in function of the position of the relay

3.3.2.1 LOS Environment

In the next two sections, we have simulated the bit error rate in function of the distance for a given total system power. Assume $SNR = 25\,\text{dBs}$. We have moved the relay from position 1 to 9 with an increment of 1. Thus we observe the variation of the bit error rate according to different relay positions.

The Figure below shows the relay cooperation for different scenarios. For the static power allocations $P_s = \Pr$ $P_s = 2 \times P_r$ and $P_s = P_r / 2$, we see that the curve is decreasing as the position of the relay becomes closer to the destination. However, in the case of $P_s = \mu \times P_{tot}$ the coefficient $\mu = \frac{d_{sr}^{\beta_{sr}}}{(d_{sd} - d_{sr})^{\beta_{rd}}}$ is symmetric in $d_{sr} = 5$.

In three of the cases, the power is allocated statically and in one case the power allocation at the source and relay changes according to the position of the relay. In the case where all the links follow a line-of-sight environment, the power is allocated as shown below:

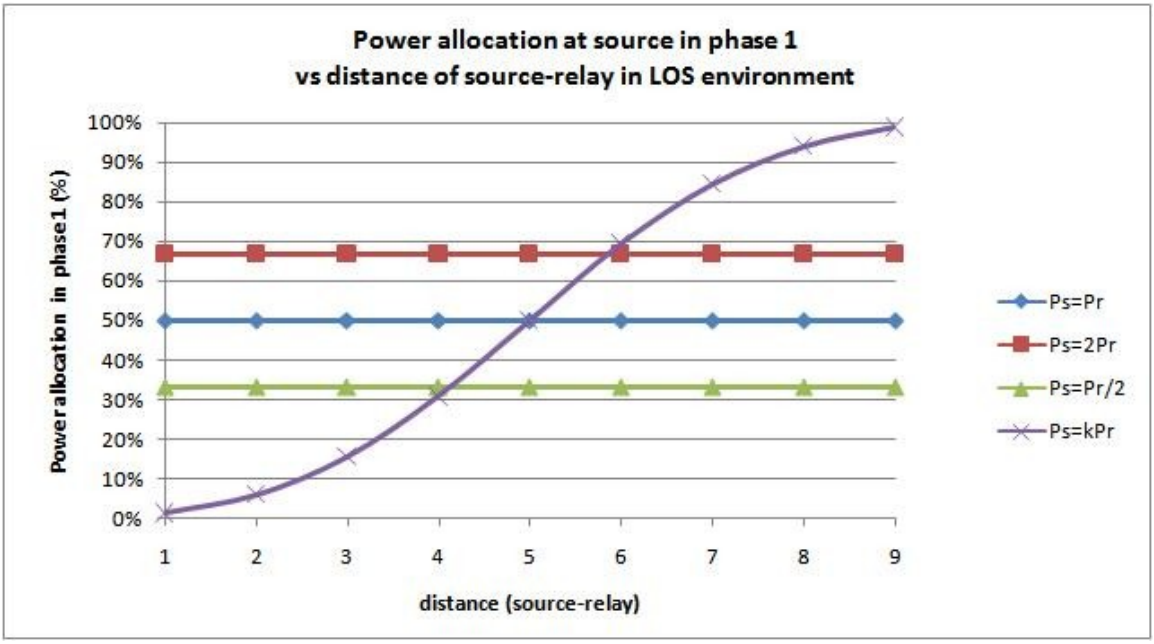

Figure 3.12 Power allocations vs relay position in LOS environment

Obviously, by comparing the above and below Figures, we observe that the highest collaboration rate corresponds to the most power allocated for a given position of the relay at a distance d_{sr}

For the position of the relay ranging from $d_{sr}=1$ to $d_{sr}=5$ the relay collaborates approximately all the time. However, as the distance grows and the path loss increases, the relay cooperates less. The highest collaboration rate corresponds to the most power allocated, which are for the cases $P_s=kP_r$, $P_s=2P_r$, $P_s=P_r$ and $P_s=P_r/2$ respectively.

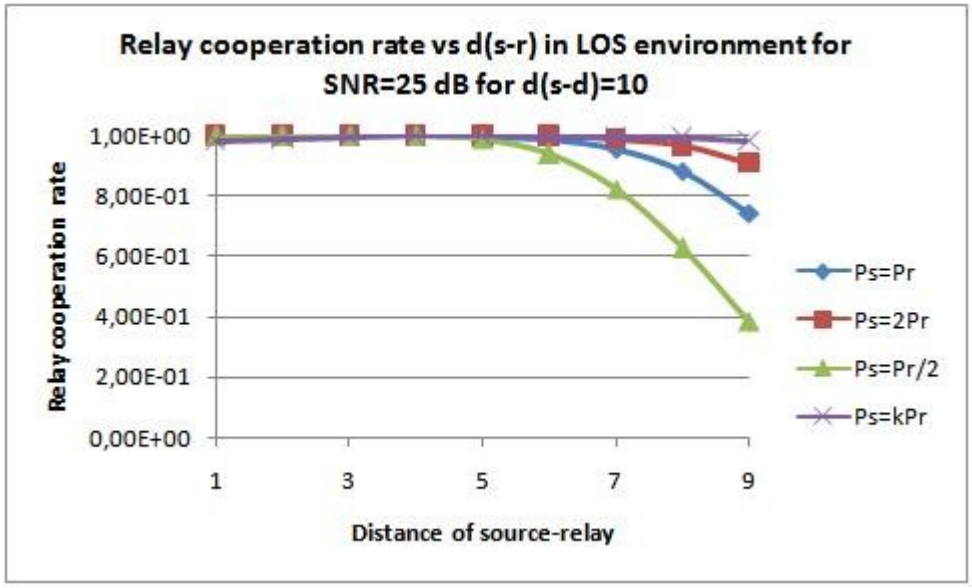

Figure 3.13 Relay cooperation vs relay position in LOS environment

For the different power allocations considered, the end-to-end bit error rate is not better than the direct link transmission for $d_{sr}\le 3.7$. The power allocation of $P_s=P_r/2$ reaches its best performance for $d_{sr}=4$ while $P_s=P_r$ has its lowest bit error rate for $d_{sr}=5$. For $P_s=2\times P_r$ and $P_s=k\times P_r$ the optimal performance of bit error rate is obtained for $d_{sr}=7$ and $d_{sr}=6$ respectively.

If we consider more precisely the case $P_s=2\times P_r$ and $d_{sr}=7$, we can determine the average power received at destination.

$$\overline{P}_{system} = \frac{P_s}{d_{s-d}^2} + rate \times \frac{P_r}{d_{r-d}^2} = \frac{2}{3} \times \frac{10^{2.5}}{10^2} + 9.907 \times 10^{-1} \times \frac{1}{3} \times \frac{10^{2.5}}{3^2} = 13.71 \qquad (3.18)$$

While the power received in the case of direct transmission is defined by

$$\overline{P}_{direct} = \frac{P}{d_{s-d}^2} = \frac{10^{2.5}}{10^2} = 3.1627 \qquad (3.19)$$

In the case of the system model, the mean received power at the destination is more than 4 times stronger:

$$f = \frac{\overline{P}_{system}}{\overline{P}_{direct}} = \frac{13.711}{3.1627} = 4.333. \qquad (3.20)$$

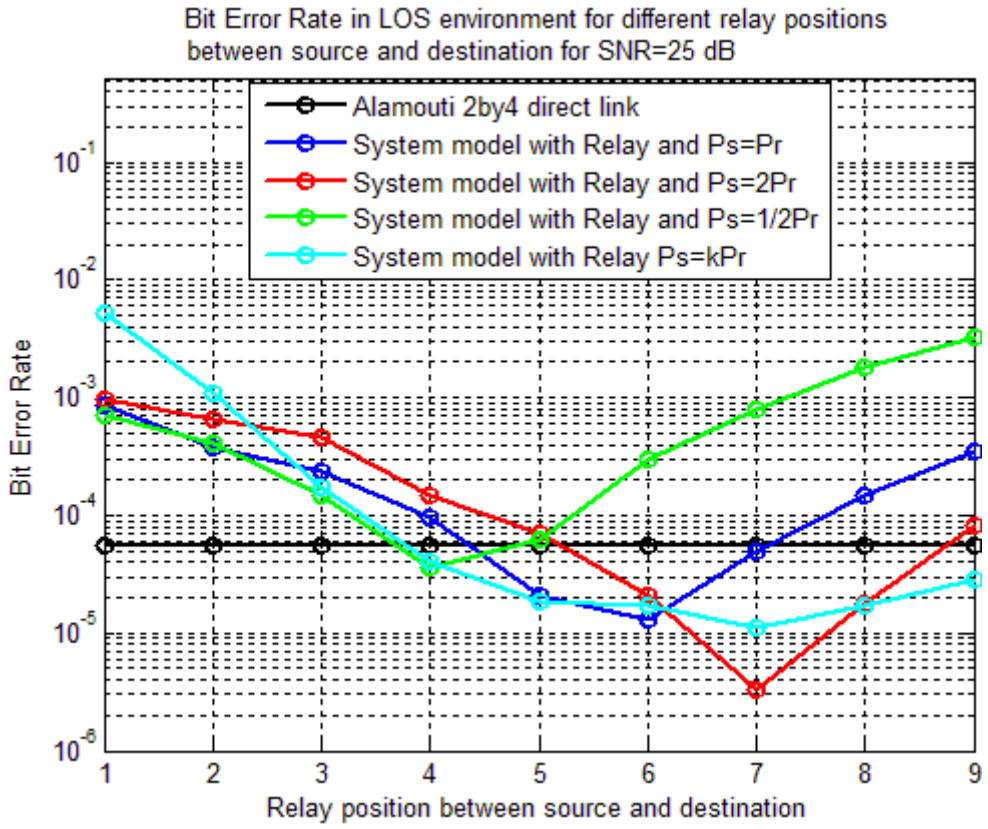

Figure 3.14 System bit error rate vs relay position in LOS environment

3.3.2.2 NLOS Environment

The power allocations considered in this case are the same as in the line-of-sight channel links. For the static power allocations, the power ratio allocated to the source and relay does not take into consideration of the relay position. However, the dynamic power allocation changes in function of the distance: the smaller the distance, the smaller power needed. Similarly, the bigger the distance, the more power is needed.

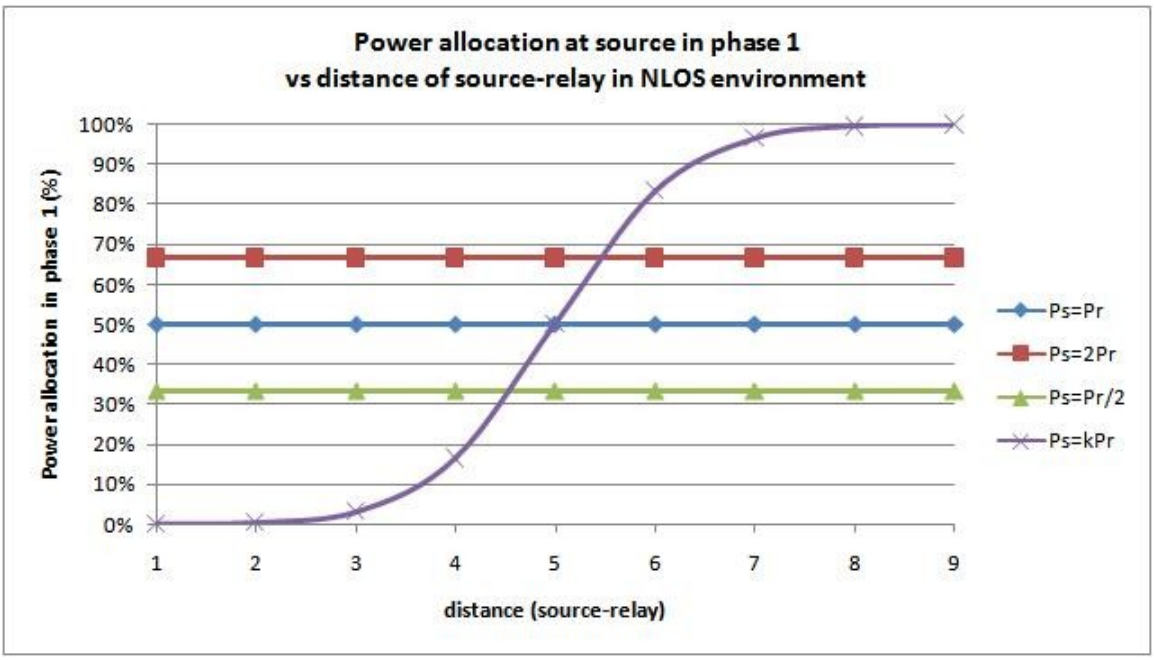

Figure 3.15 Power allocations vs relay position in NLOS environment

Just like for NLOS, the dynamic power allocation is symmetrical in $d_{sr} = 5$ and the cooperation rate as well; for the first half distance between the source and destination, less power is allocated to the relay in the case $P_s = k \times P_r$ and the relay cooperation is weaker. And for the second half distance, more power is allocated and the relay cooperation rate is better, as shown in Figures 3.15 and 3.16

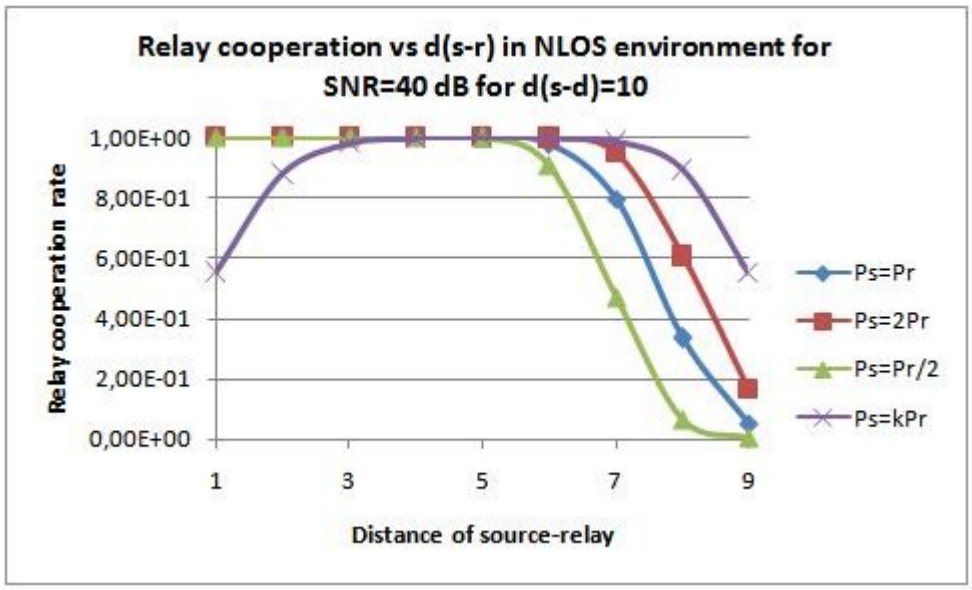

Figure 3.16 Relay cooperation vs relay position in NLOS environment

The improvement between the source-relay-destination model and the direct link transmission becomes more important in the case of NLOS due to the fact that the path loss coefficient is bigger ($4 > 2$). The direct transmission has a better result for d_{sr} ranging between 0 and 2 only.

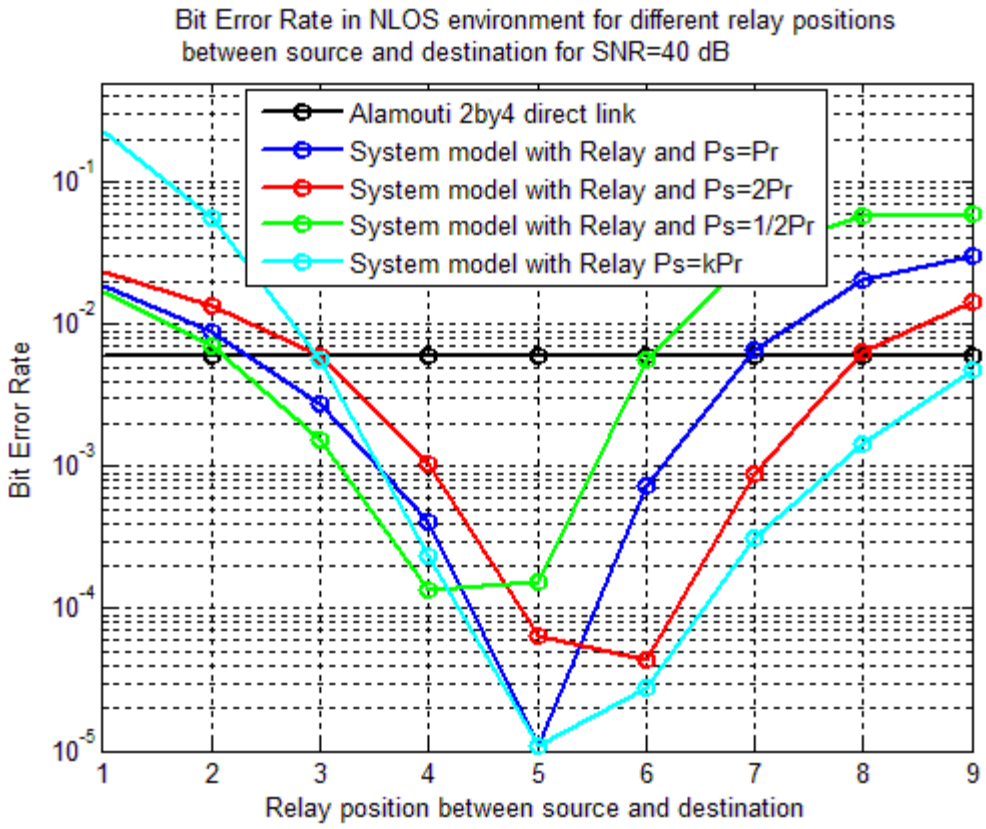

Figure 3.17 System bit error rate vs relay position in NLOS environment

If we consider more precisely the case $P_s = P_r$ and $d_{sr} = 5$, we can determine the average power received at destination.

$$\overline{P}_{system} = \frac{P_s}{d_{s-d}^2} + rate \times \frac{P_r}{d_{r-d}^2} = \frac{1}{2} \times \frac{10^4}{10^4} + 1 \times \frac{1}{2} \times \frac{10^4}{5^4} = 8.5 \qquad (3.21)$$

While the power received in the case of direct transmission is defined by

$$\overline{P}_{direct} = \frac{P}{d_{s-d}^2} = \frac{10^4}{10^4} = 1 \qquad (3.22)$$

In the case of the system model, the mean received power at the destination is 8.5 times stronger:

$$f = \frac{\overline{P}_{system}}{\overline{P}_{direct}} = \frac{8.5}{1} = 8.5 \tag{3.23}$$

This is why we observe a bit error rate of 10^{-5} for the space-time coded cooperation while it is 6.058×10^{-3} for a direct transmission.

3.3.3 Uplink Environment

For this subsection, we consider that the relay is close to the destination and that the source-relay link is LOS while the relay-destination link is NLOS as well as the source-destination link. The environment of this simulation can be resumed by the following equations

$$\begin{aligned} d_{sd} &= 10 \\ d_{sr} &= 3 \\ d_{rd} &= 7 \\ \beta_{sd} &= \beta_{rd} = 4 \\ \beta_{sr} &= 2 \end{aligned} \tag{3.24}$$

Figure 3.18 shows that the cooperation rate of the relay is approximately 1 for all the static power allocations considered: $P_s = 2\times P_r$, $P_s = P_r, P_s = P_r/2$, for $SNR > 20\,dBs$. However, for the case $P_1 = k\times P_2$ where $k = \frac{d_{sr}^{\beta_{sr}}}{(d_{sd}-d_{sr})^{\beta_{rd}}} = \frac{3^2}{7^4} = 3.748\times10^{-3}$, the cooperation rate of the relay Is virtually null for $SNR < 32\,dBs$ and gradually increases to become approximately 1 for $SNR > 40\,dBs$.

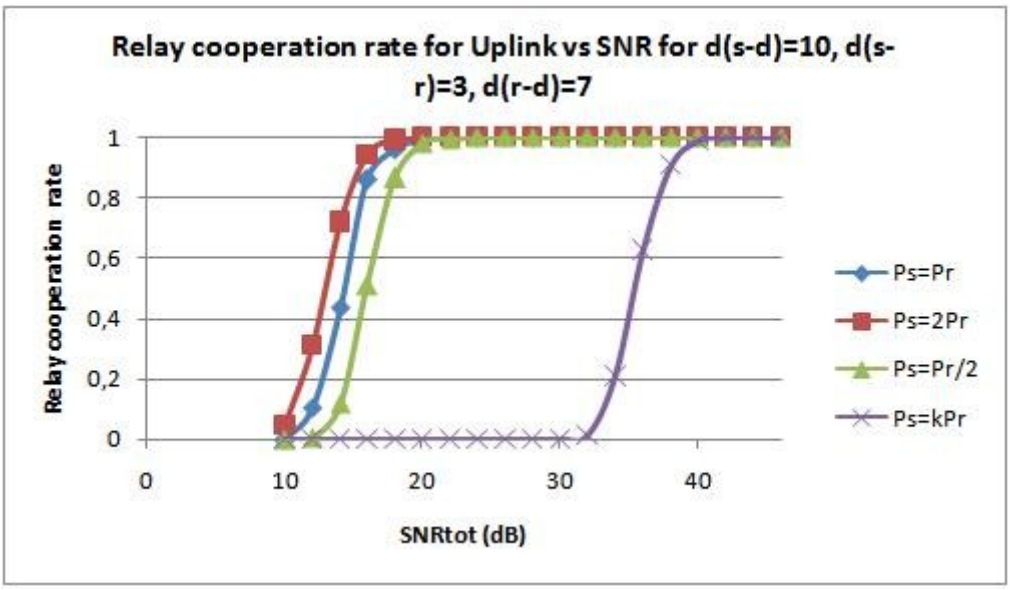

Figure 3.18 Relay cooperation vs total SNR in Uplink environment

For low SNR values, the static power allocations have the best bit error rate performance and the case of $P_s = k \times P_r$ present poor results due to the fact that the relay cooperation rate is almost null. However, for $SNR > 40\,dBs$ the relay cooperation rate becomes almost 1 in all the cases and the case $P_s = k \times P_r$ offers the best bit error rate performance at 4.51×10^{-7}.

Also, we observe the space-time coded model presents an improvement of $2\,dBs$ compared to the direct link transmission for a bit error rate of 10^{-4}.

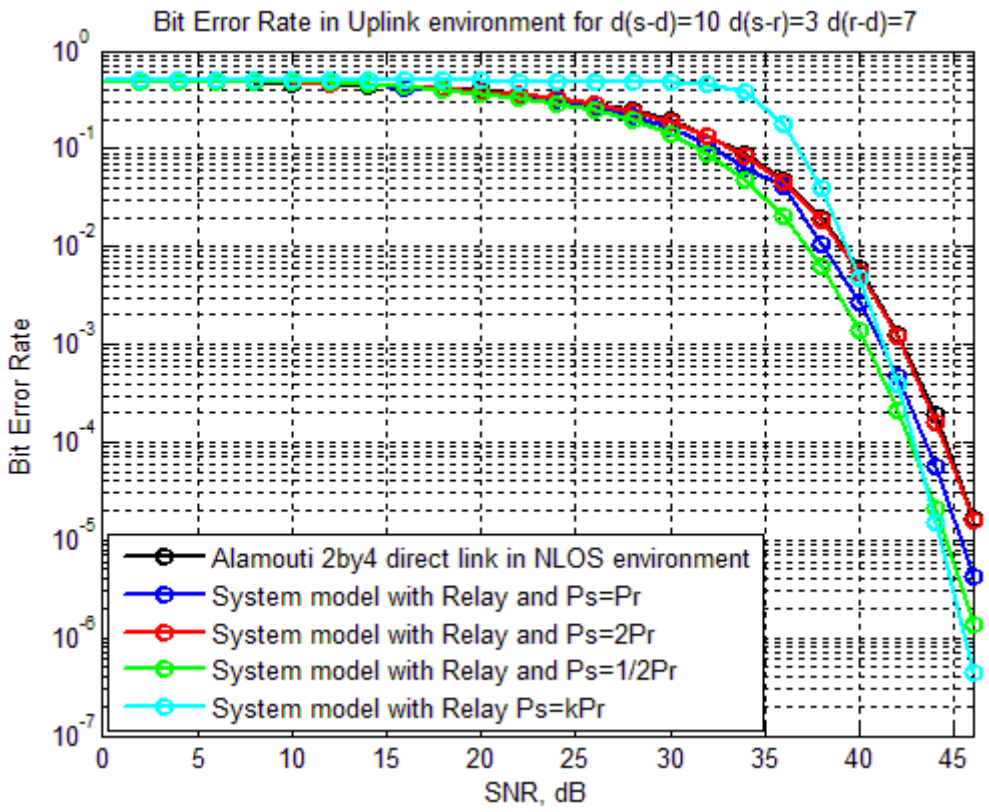

Figure 3.19 System bit error rate vs total SNR for Uplink environment

3.3.4 Downlink Environment

For this subsection, we consider that the relay is close to the destination and that the source-relay link is NLOS while the relay-destination link is LOS as well as the source-destination link. The environment of this simulation can be resumed by the following equations

$$
\begin{aligned}
d_{sd} &= 10 \\
d_{sr} &= 7 \\
d_{rd} &= 3 \\
\beta_{sd} &= \beta_{sr} = 4 \\
\beta_{rd} &= 2
\end{aligned}
\tag{3.25}
$$

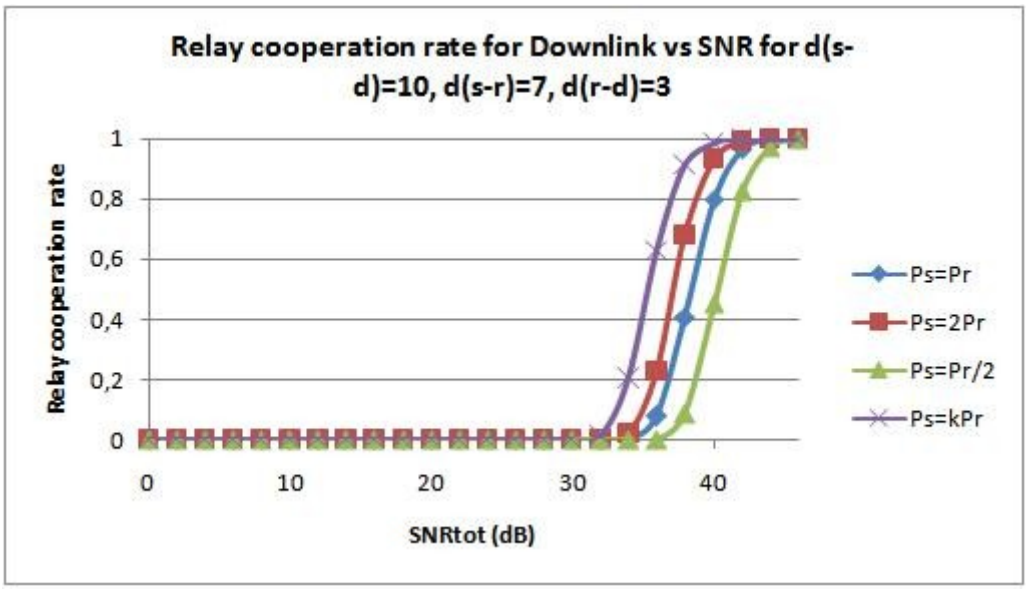

Figure 3.20 Relay cooperation vs total SNR in Downlink environment

The Figure above shows the cooperation rate of the relay for the defined downlink scenario and unlike the previous cases, the case of $P_s = k \times P_r$ has the highest cooperation rate for the relay.

Similarly, we observe that the case with the highest relay cooperation rate for the case of $P_1 = k \times P_2$ has the best end-to-end bit error rate. The bit error rate of 10^{-5} is obtained for $SNR = 42.5\,dBs$ while this error rate is obtained for $SNR = 46.5\,dBs$ for a direct transmission, which is an Improvement of $4\,dBs$.

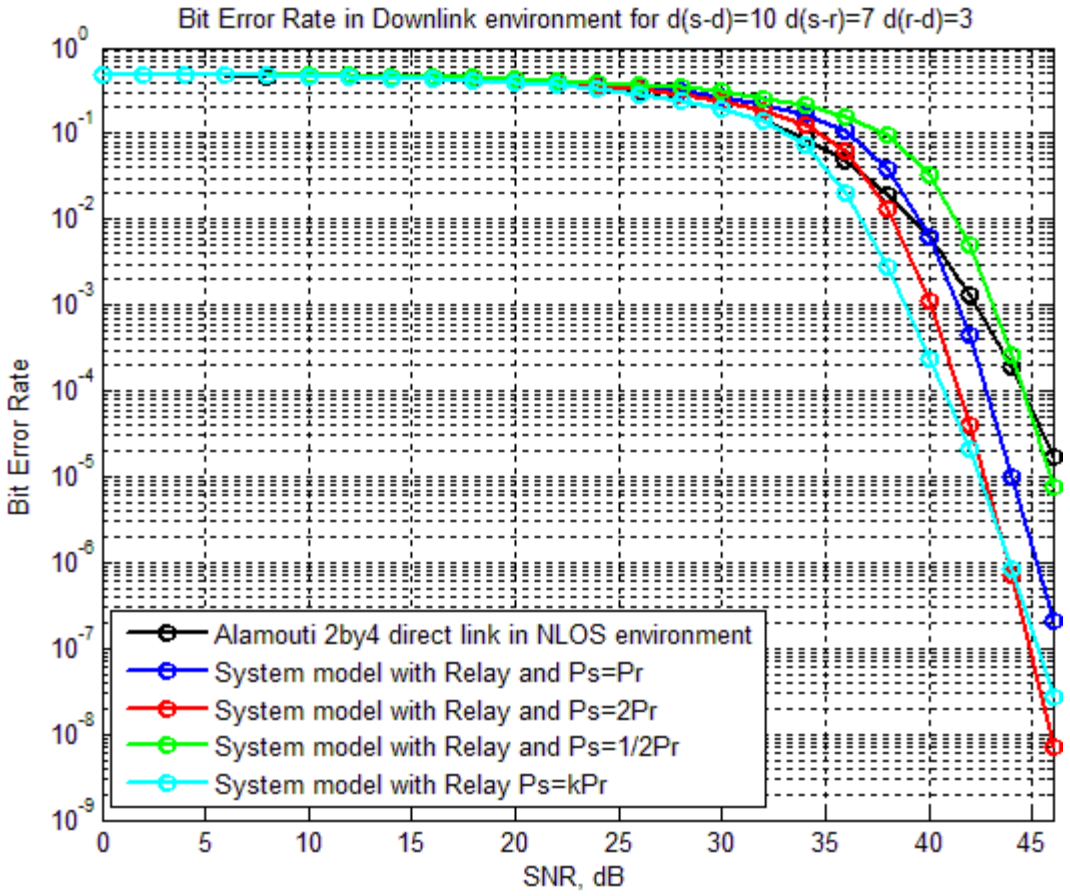

Figure 3.21 System bit error rate vs total SNR for Downlink environment

3.4 Summary

In this Chapter, we have studied the performance of a space-time coded cooperation model. In phase 1, the source broadcasts a first version of the message to both relay and destination. In the second phase, the relay cooperates by sending another version of the message if it successfully decodes, else, it remains idle. Different power allocations between the source and the relay were considered.

When the relay is at equal distance between the source and destination, the case of $P_s = P_r$ gives the best bit error rate performance ; 10^{-3} is obtained in NLOS for $SNR = 37\,dBs$, which is $5\,dBs$ better than Alamouti 2x4 code direct link transmission.

For the special case of uplink communication, the space-time coded model presents an improvement of $2\,dBs$ compared to the direct link transmission for a bit error rate of 10^{-4}.

For the downlink communication, the bit error rate of 10^{-5} is obtained for $SNR = 42.5\,dBs$ while this error rate is obtained for $SNR = 46.5\,dBs$ for a direct transmission, which is an Improvement of $4\,dBs$.

Chapter 4: Turbo coded space-time cooperation

In this Chapter, we consider a three terminals relay model similar to Chapter 3: a source, a relay and a destination in a slow Rayleigh fading channel. The main difference is the introduction of a Turbo encoder at the source and relay transmitters as well as an iterative turbo decoding process at the relay and destination. We analyze the system performance in various scenarios while focusing on some key factors, such as the cooperation rate and the bit error rate of the overall system.

We Assume a source mobile user that has two transmit antennas, a relay mobile user that has four receive antenna and two transmit antennas and finally a base station that has four receive antennas. Alamouti and space-time coding are applied and transmission is done over QPSK modulation, combined with Turbo code.

The system communication happens in two phases: in phase 1, the source broadcasts the message to both the relay and destination. If the message is received correctly at the relay, the relay transmits to the destination in phase 2; else the source sends the second part of the message in the second phase.

4.1 System model

In Chapter 4, the communication system is a Turbo coded space-time cooperative MIMO system composed of a source, relay and destination where the source has two transmitting antennas, the destination has four receiving antennas and the relay is a 2x4 terminal. The source and the relay are both composed of a Turbo-encoder and a space-

time encoder while the relay and the destination are composed of a Turbo-decoder and a space-time decoder as well.

4.1.1 Phase 1

The source is the only active terminal during phase 1. It is composed of a Turbo Encoder, followed by a space-time encoder. It also has 4 transmitting antennas. The structure of the Turbo Encoder is illustrated in Figure 4.1 and it is comprised of two recursive systematic convolutional codes in parallel with an interleaver in between. The constraint length of each RSC is $k = \upsilon + 1 = 3$ and the size of the interleaver corresponds to the frame length $l = 1440$.

The constraint length is the total number of bits involved in the encoding operation at each time step and $\upsilon = 2$ is the number of registers.

A Turbo-encoder is described by the generator vectors of each convolutional encoder. If we note GFi the feed-forward vector for encoder i and GRi the feed-backward vector for encoder, we use the notation PCCC(1,GF1/GR1,GF2/GR2) to illustrate the structure of the Turbo Encoder. In this section, we have used a PCCC(1,5/7,5/7) symmetric Turbo-encoder. The forward generator vectors are $GF_1 = GF_2 = [1\,0\,1] = 5_8$ and backward vectors are $GR_1 = GR_2 = [1\,1\,1] = 7_8$.

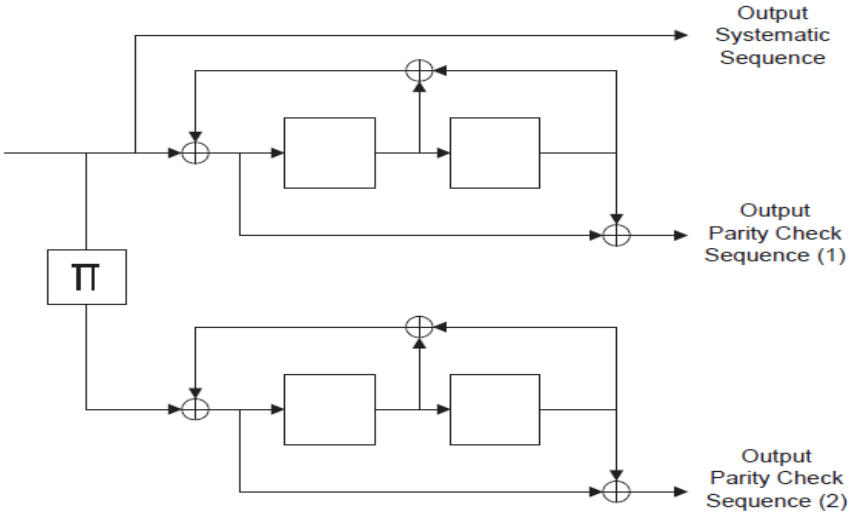

Figure 4.1 Turbo Encoder (1,5/7,5/7)

At the beginning, the encoder is at the state 0 '00' and the encoder state is forced to '00' in the end with tail bits which are appended at the end of the information sequence in order to force the encoders to the zero state. The trellis of each encoder is shown below:

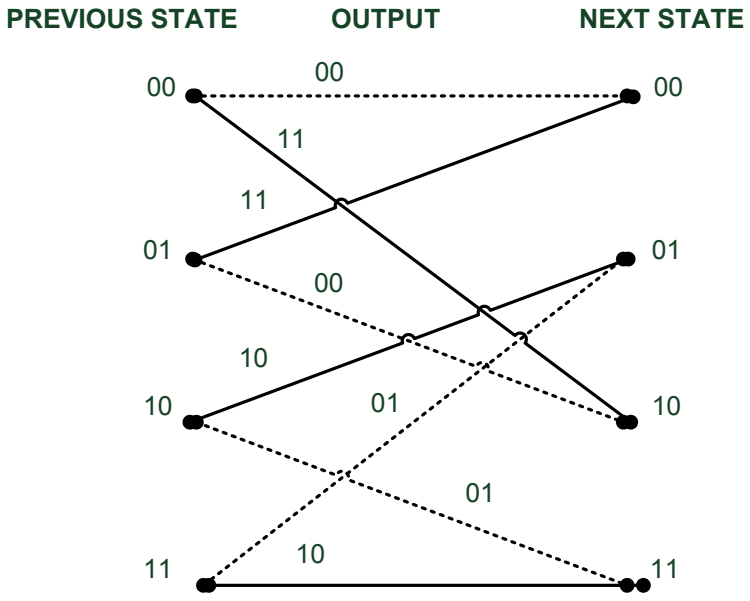

Figure 4.2 Trellis diagram of convolutional encoder (1,5/7)

The solid black lines represent the '0' input to the encoder while the dashed black lines mark a '1' as input. The output of each encoder is composed of 2 bits marked close to each line where the first bit is the systematic bit and the second bit is the encoded bit. If we assume D_1, D_2 the bits of the current state of the encoder, and I the input bit, we can resume the next states D_1^+, D_2^+ as well as the output bits S and U as:

$$D_1^+ = \text{mod}(D_1 + D_2 + I, 2) \tag{4.1}$$

$$D_2^+ = D_1 \tag{4.2}$$

$$S = I \tag{4.3}$$

$$U = \text{mod}(D_1 + I, 2) \tag{4.4}$$

Where S is the systematic bit and U the parity bit at the output of the encoder.

In the proposed model, we apply puncturing and only the odd bits of the systematic sequence and the parity 1 sequence are transmitted while the even bits are transmitted from parity 2. The removed bits are replaced by '0' in the sequence. By multiplexing the systematic and parity bits, the resulting vector becomes $\begin{bmatrix} 1 & 1 & 0 & 0 & 0 & 1 \end{bmatrix}$ where 1 means the bit is being sent and 0 means that this bit has been punctured.

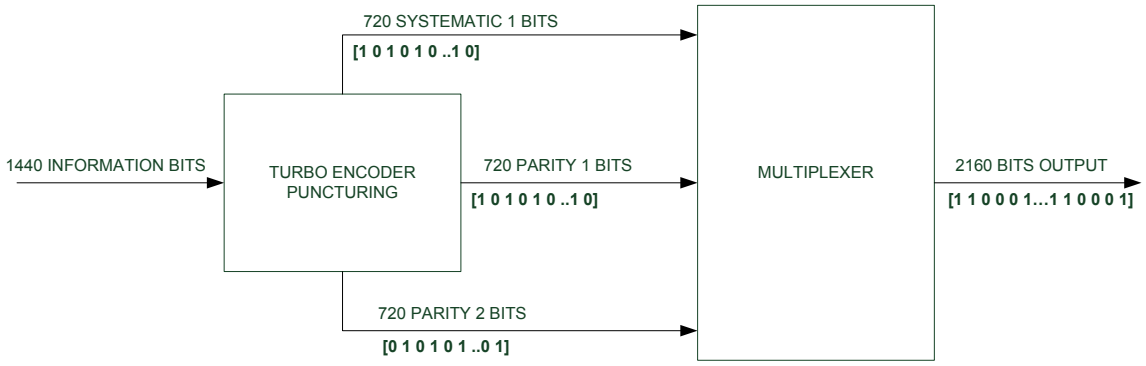

Figure 4.3 Puncturing and multiplexing at source in phase 1

This sequence will be of length $N = \frac{3}{2} \times l = \frac{3}{2} \times 1440 = 2160$ bits where systematic, parity 1 and parity 2 have each 720 bits. The code rate for this phase is $2/3$.

Thus, this sequence is encoded in a space-time encoder, exactly as presented in Chapter 3. It is a 2×4 Alamouti encoder. The channel links between the source and the relay and the source and destination are both slow Rayleigh fading channels. The amplitude and phase of the fading is constant during the entire use of the link for each frame.

Both the relay and the destination receive an Alamouti encoder version of the sequence output of the Turbo Encoder $[1 \quad 1 \quad 0 \quad 0 \quad 0 \quad 1]$. While the relay attempts to decode it, the destination waits for the second part of the frame, which is sent either by the source or the relay depending on the CRC check at the relay.

4.1.2 Phase 2

The frame received at the relay is encoded twice; space-time encoded and Turbo encoded. For the decoding, it first applies a space-time soft decoding, similar to Chapter 3, followed by a Turbo Decoder.

Assume the received signals at the relay are:

$$
\begin{aligned}
r_1 &= h_{11} \cdot x_1 + h_{21} \cdot x_2 + n_0 \\
r_2 &= -h_{11} \cdot x_2^* + h_{21} \cdot x_1^* + n_1 \\
r_3 &= h_{12} \cdot x_1 + h_{22} \cdot x_2 + n_2 \\
r_4 &= -h_{12} \cdot x_2^* + h_{22} \cdot x_1^* + n_3 \\
r_5 &= h_{13} \cdot x_1 + h_{23} \cdot x_2 + n_4 \\
r_6 &= -h_{13} \cdot x_2^* + h_{23} \cdot x_1^* + n_5 \\
r_7 &= h_{14} \cdot x_1 + h_{24} \cdot x_2 + n_6 \\
r_8 &= -h_{14} \cdot x_2^* + h_{24} \cdot x_1^* + n_7
\end{aligned}
\tag{4.5}
$$

Where h_{ij} is the Rayleigh fading channel on which antenna i is transmitting and antenna j is receiving.

They follow a soft space-time decoding:

$$
\begin{aligned}
\hat{x}_1 &= h_{11}^* \cdot r_1 + h_{21} \cdot r_2^* + h_{12}^* \cdot r_2 + h_{22} \cdot r_2^* + h_{13}^* \cdot r_1 + h_{23} \cdot r_2^* + h_{14}^* \cdot r_1 + h_{24} \cdot r_2^* \\
\hat{x}_2 &= h_{21}^* \cdot r_1 - h_{11} \cdot r_2^* + h_{22}^* \cdot r_1 - h_{12} \cdot r_2^* + h_{23}^* \cdot r_1 - h_{13} \cdot r_2^* + h_{24}^* \cdot r_1 - h_{14} \cdot r_2^*
\end{aligned}
\tag{4.6}
$$

Then $\hat{x}_1$ and $\hat{x}_2$ are demultiplexed to obtain the received log-likelihood ratio (LLR) of the systematic, parity 1, and parity 2 bits defined as y_{1s} y_{1p} and y_{2p}.

Similarly to the Turbo Encoder, the Turbo Decoder uses two SISO decoders that work together to estimate the transmitted information bits; both decoders are also separated by an interleaver which is identical to the one used at the encoder in phase 1 and the corresponding de-interleaver. The first decoder uses the parity 1 bits from the output of encoder 1, and the second decoder uses parity 2 bits which are obtained from encoder 2, and both decoders use the systematic bits. Iteratively, they both exchange estimations in form of likelihood or log-likelihood for suboptimal MAP algorithms.

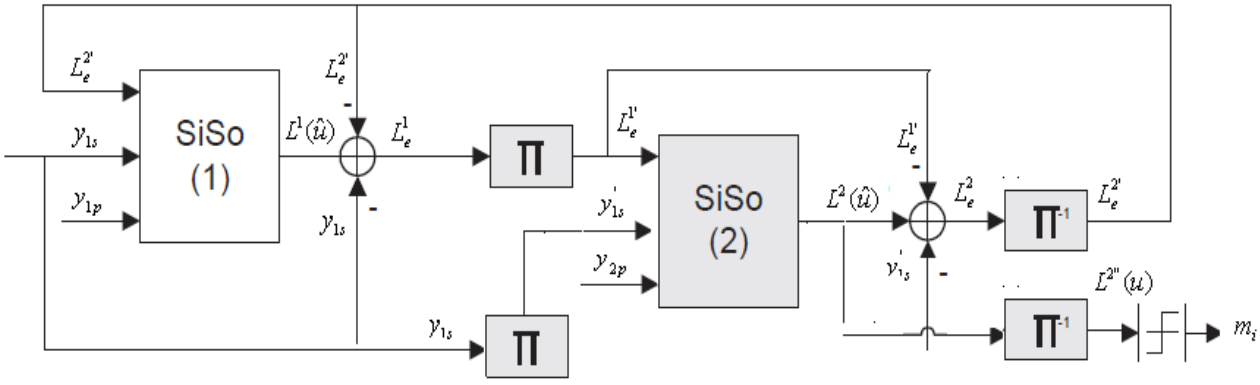

Figure 4.4 Turbo Decoder

Figure 4.4 contains all the factors used for the decoding process as defined by Valenti in [37]

First we note that $A^{'}$ is the interleaved version of A. We define $L^{i}(\hat{u})$ the a posteriori LLR at decoder i such that

$$L^{1}(\hat{u}) = \log \frac{P[m_i = 1 \mid y_{1s}, y_{1p,} L^{2}_{e'}]}{P[m_i = 0 \mid y_{1s}, y_{1p,} L^{2}_{e'}]} \tag{4.7}$$

$$L^{2}(\hat{u}) = \log \frac{P[m_i = 1 \mid y^{'}_{1s}, y_{2p,} L^{1}_{e'}]}{P[m_i = 0 \mid y^{'}_{1s}, y_{2p,} L^{1}_{e'}]} \tag{4.8}$$

Where L_e is the extrinsic value related to the LLR such that

$$L^{1}_{e} = L^{1}(\hat{u}) - L_c \times y_{1s} - L^{2}_{e'} \tag{4.9}$$

$$L^{2}_{e} = L^{2}(\hat{u}) - L^{'}_c \times y^{'}_{1s} - L^{1}_{e'} \tag{4.10}$$

The two decoders keep exchanging their soft extrinsic LLR L_e for a defined number of iterations and at the end, a hard decision is made according to

$$m_i = \begin{cases} 1 & if \quad L^{2"}(u) > 0 \\ 0 & else \end{cases} \tag{4.11}$$

Where $L^{2"}(u)$ is the de-interleaved version of $L^2(u)$.

At the beginning of the decoding process, the a posteriori LLR at decoder 1 is assumed to be 0 because both inputs (0 and 1) have equal probabilities.

In this Chapter, we apply the log-MAP algorithm is with a predefined number of 8 iterations.

The branch transition probabilities γ_k^{LM} and the forward α_k^{LM} and backward recursions β_k^{LM} are computed as shown in [48]:

$$\gamma_k^{LM}(s',s) = \frac{1}{2} \times L_c \times y_{k,1} \times u_k + \frac{1}{2} \sum_{v=2}^{n} L_c \times y_{k,v} \times x_{k,v} + \frac{1}{2} \times u_k \times L(u_k) \tag{4.12}$$

$$\alpha_k^{LM}(s) = \ln(\alpha_k(s)) = \ln(\sum_{s'} exp(\gamma_k^{LM}(s',s) + \alpha_{k-1}^{LM}(s))) \tag{4.13}$$

$$\beta_{k-1}^{LM}(s') = \ln(\beta_{k-1}(s')) = \ln(\sum_{s'} exp(\gamma_k^{LM}(s',s) + \beta_k^{LM}(s'))) \tag{4.14}$$

The resulting log-likelihood ratio is then computed as follows

$$\begin{aligned} L(\hat{u}_k) = & \ln(\sum_{u_k=+1}^{(s',s)} \exp(\gamma_k^{LM}(s',s) + \alpha_{k-1}^{LM}(s) + \beta_k^{LM}(s'))) \\ & - \ln(\sum_{u_k=-1}^{(s',s)} \exp(\gamma_k^{LM}(s',s) + \alpha_{k-1}^{LM}(s) + \beta_k^{LM}(s'))) \end{aligned} \tag{4.15}$$

L_c is defined as the channel reliability

$$L_c = 4 \times h_{i,j} \times \frac{E_s}{N_o} \tag{4.16}$$

After the 8 iterations, the information bits are decoded and pass a CRC check. If they are decoded correctly, the relay collaborates in phase 2; else, it remains idle and the source transmits in phase 2. The same Turbo Encoder and space-time encoder is applied in phase 2, whether at the source or relay.

In both cases, the information bits are Turbo-encoded and punctured such that the bits that were sent during phase 1 are replaced by zeros and the bits that were replaced by zeros in phase 1 are sent. By multiplexing the systematic and parity bits, the resulting vector becomes $\begin{bmatrix}0 & 0 & 1 & 1 & 1 & 0\end{bmatrix}$ where 1 means the bit is being sent and 0 means that this bit has been punctured.

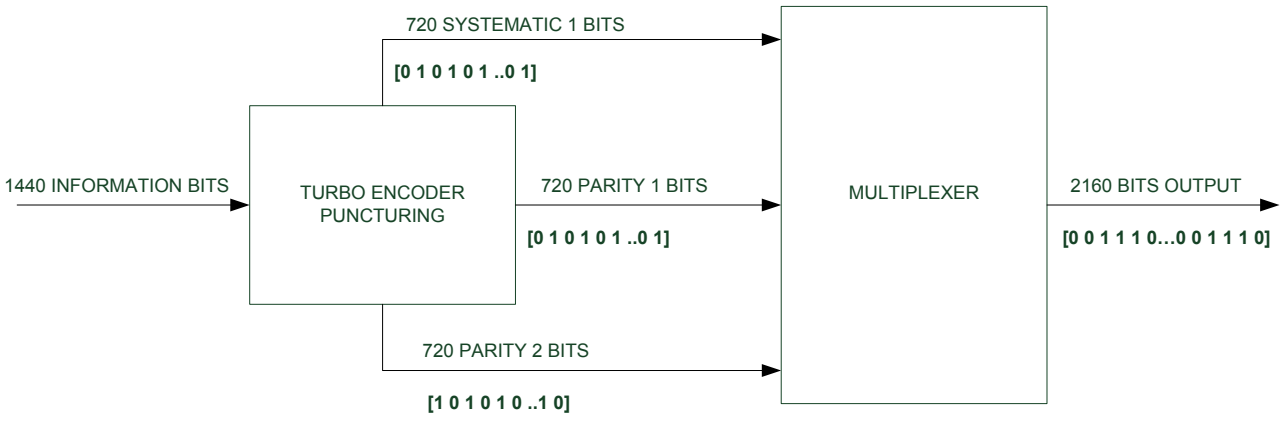

Figure 4.5 Puncturing and multiplexing at relay or source in phase 2

As in phase 1, this sequence will be of length $N = \frac{3}{2} \times l = \frac{3}{2} \times 1440 = 2160 \text{bits}$ where systematic, parity 1 and parity 2 have each 720 bits. The code rate for this phase is $2/3$.

If we consider the tail bits, the destination will then receive two sequences of 2162 bits each, while the information frame is composed of 1440 bits, which makes an overall code rate of $rate = \frac{1440}{2 \times 2162} = \frac{1440}{4324} = 0.3330 \approx \frac{1}{3}$

4.1.3 Decoding at destination

The destination receives all the systematic and parity bits in a two-phase transmission system. During phase 1, it receives the odd bits of systematic and parity 1, as well as the even bits of the parity 2 sequence sent from the source. And in phase 2, it receives the other half of systematic and parity bits from the relay in case of cooperation, or the source. The bits sent during phase 1 are defined as $y_{1s,odd}$, $y_{1p,odd}$, $y_{2p,even}$ and those sent during phase 2 are $y_{1s,even}$, $y_{1p,even}$, $y_{2p,odd}$ each of length 720 bits. The frames received are then de-multiplexed such that all the systematic bits are in a frame, all the parity 1 bits in a frame, and all the parity 2 bits in a frame such that

$$y_{1s,des} = [y_{1s,odd}(1) \quad y_{1s,even}(1) \quad y_{1s,odd}(2) \quad y_{1s,even}(2) \quad \ldots \quad y_{1s,odd}(720) \quad y_{1s,even}(720)] \quad (4.17)$$

$$y_{1p,des} = [y_{1p,odd}(1) \quad y_{1p,even}(1) \quad y_{1p,odd}(2) \quad y_{1p,even}(2) \quad \ldots \quad y_{1p,odd}(720) \quad y_{1p,even}(720)] \quad (4.18)$$

$$y_{2p,des} = [y_{2p,odd}(1) \quad y_{2p,even}(1) \quad y_{2p,odd}(2) \quad y_{2p,even}(2) \quad \ldots \quad y_{2p,odd}(720) \quad y_{2p,even}(720)] \quad (4.19)$$

In case the relay cannot decode correctly the information bits received from the source in phase 1, all the systematic and parity bits received in phase 2 at the destination will have the same channel state information. However, in case of cooperation, the bits received

during phase 2 will have a different channel state information and there will be more diversity.

The system model for Chapter 4 can be resumed in Figure 4.6

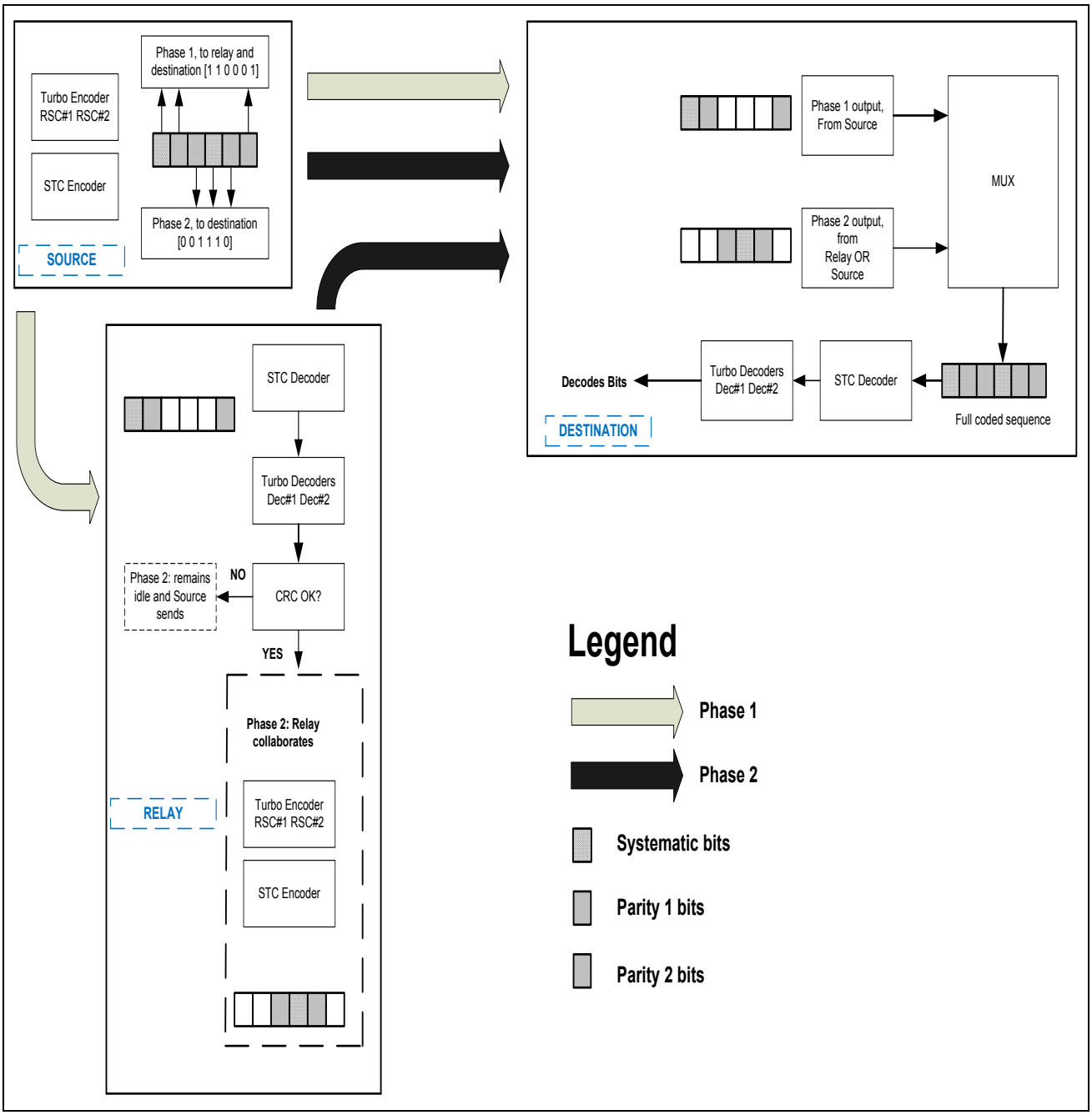

Figure 4.6 System model for Chapter 4

4.2 Power allocations

For Chapter 4, we have considered the same power allocations as in Chapter 3 with the sole difference that the source can send during phase 2. We identify P_i as the power allocated during phase i. The cases considered are the following

$$P_1 = P_2 \tag{4.20}$$

where transmitted power is shared equally during both phases

$$P_1 = 2 \times P_2 \tag{4.21}$$

where the transmitted power during phase 1 is twice stronger than phase 2

$$P_1 = P_2 / 2 \tag{4.22}$$

where the transmitted power during phase 1 is half the one of phase 2

$$P_1 = \mu \times P_{tot}, P_2 = (1-\mu) \times P_{tot} \qquad \mu \in [0 \quad 1] \tag{4.23}$$

where the transmitted power during each phase depends on the position of the relay such that

$$\mu = \frac{d_{sr}^{\alpha_{sr}}}{(d_{sd} - d_{sr})^{\alpha_{rd}}} \tag{4.24}$$

Combining (4.23) and (4.24) we obtain the relation between P_1 and P_2

$$\begin{aligned} P_1 &= kP_2 \\ k &= \frac{d_{sr}^{\alpha_{sr}}}{(d_{sd} - d_{sr})^{\alpha_{rd}}} \end{aligned} \tag{4.25}$$

Given that the source is composed of two antennas, we assume that the power in phase 1 is equally split between its antennas, such that

$$P_{s1,1} = P_{s1,2} = P_1 / 2 \tag{4.26}$$

Where $P_{s1,i}$ is the power at the source during phase 1 for antenna i.

During phase 2, if the relay cooperates, we can also write

$$P_{r2,1} = P_{r2,2} = P_2 / 2 \tag{4.27}$$

Else, the source transmits during phase 2 with equally split power between both antennas

$$P_{s2,1} = P_{s2,2} = P_2 / 2 \tag{4.28}$$

4.3 Space-time coded cooperation with Turbo-code

In this section, we present the results obtained with the model defined in 4.1 for many parameters: different path loss conditions (LOS, NLOS) are presented, relay position, and power allocations. We present both the relay cooperation as well as the end-to-end bit error rate.

Also, we have considered the distance between the source and destination is $d_{sd} = 10$ for this section.

4.3.1 Case 1: Relay at equal distance between source and destination

4.3.1.1 LOS Environment

In this case, we assume the following parameters

$$
\begin{aligned}
d_{sd} &= 10 \\
d_{sr} &= d_{rd} = d_{sd}/2 = 5 \\
\beta_{sd} &= \beta_{sr} = \beta_{rd} = 2
\end{aligned}
\tag{4.29}
$$

We observe that the relay cooperation is highest when the power during phase 1 is the highest, which is in the case $P_1 = 2 \times P_2$ and the lowest cooperation is for the case $P_1 = P_2/2$. Also, in this condition, given that $k = 1$ and $P_1 = P_2 = kP_2$ the purple curve shadows the blue one because they are the same.

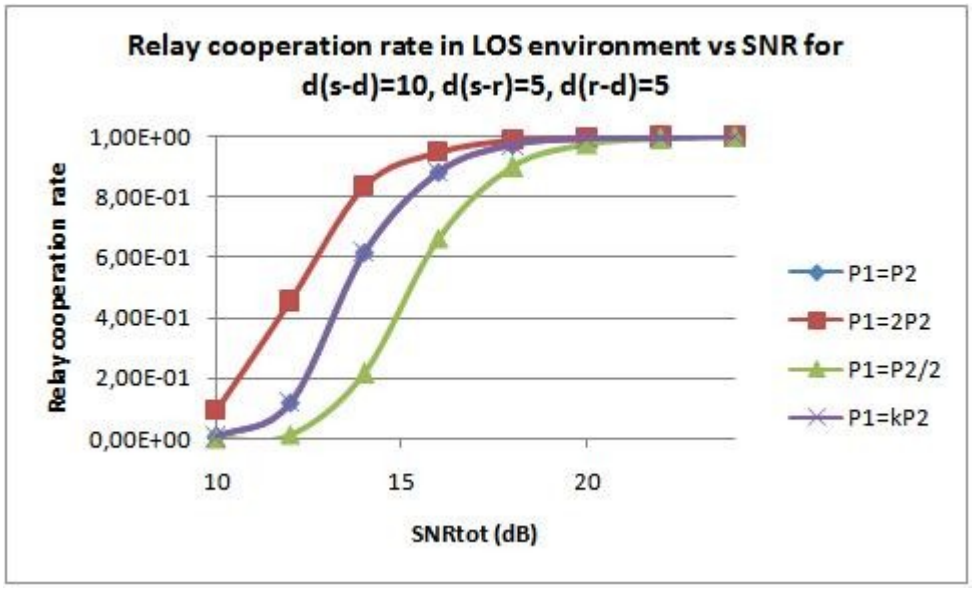

Figure 4.7 Relay cooperation vs total SNR in LOS environment

The case with the highest cooperation rate has the best bit error rate ratio vs SNR; when the relay collaborates, not only the destination receives a frame with another channel state information which adds more diversity, but the received frame has 4 times more power. If we note this factor f it can be defined as

$f = \frac{P_{r2}}{P_{s2}} = \frac{d_{s-d}^2}{d_{r-d}^2} = \frac{10^2}{5^2} = 4$ and its equivalent in dBs

$$F = 10 \times \log_{10}(f) = 6.02\, dBs$$

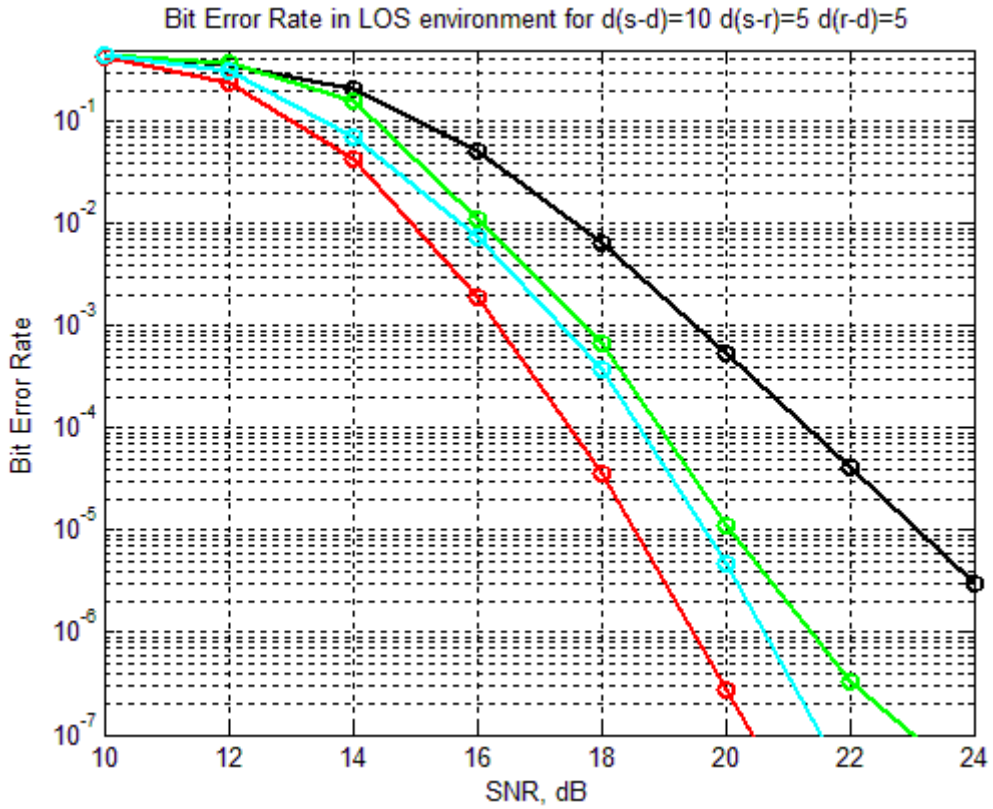

Figure 4.8 System bit error rate in LOS environment

For a bit error rate of 10^{-5} we observe a difference of more than $4.5\ \ dBs$ between the direct transmission and the system model with power allocation $P_1 = 2 \times P_2$. For the direct transmission, that threshold is obtained for $SNR = 23\, dBs$ while it is obtained for $SNR = 18.5\, dBs$ in the case of our system model.

4.3.1.2 NLOS Environment

We apply the same parameters as in the previous subsection but in a NLOS environment, where the path loss is more important:

$$
\begin{aligned}
&d_{sd} = 10 \\
&d_{sr} = d_{rd} = d_{sd}/2 = 5 \\
&\beta_{sd} = \beta_{sr} = \beta_{rd} = 4
\end{aligned}
\tag{4.30}
$$

Same as for LOS environment, when the frame is received with more power at the relay is correctly decoded more often, which is why the highest cooperation rate is for $P_1 = 2 \times P_2$ and the lowest cooperation is for the case $P_1 = P_2/2$.

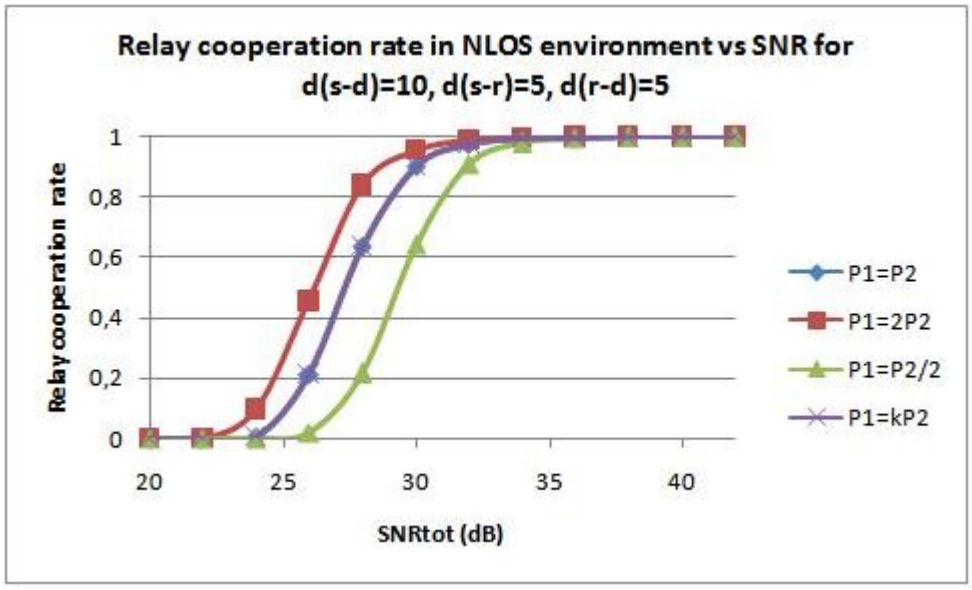

Figure 4.9 Relay cooperation vs total SNR in NLOS environment

The case with the highest cooperation rate has the best bit error rate ratio vs SNR; when the relay collaborates, the destination receives a frame that has 16 times more power compared to when the source transmits during the second phase. If we note this factor f it can be defined as

$$f = \frac{P_{r2}}{P_{s2}} = \frac{d_{s-d}^4}{d_{r-d}^4} = \frac{10^4}{5^4} = 16$$

and its equivalent in dBs

$$F = 10 \times \log_{10}(f) = 12.04\, dBs$$

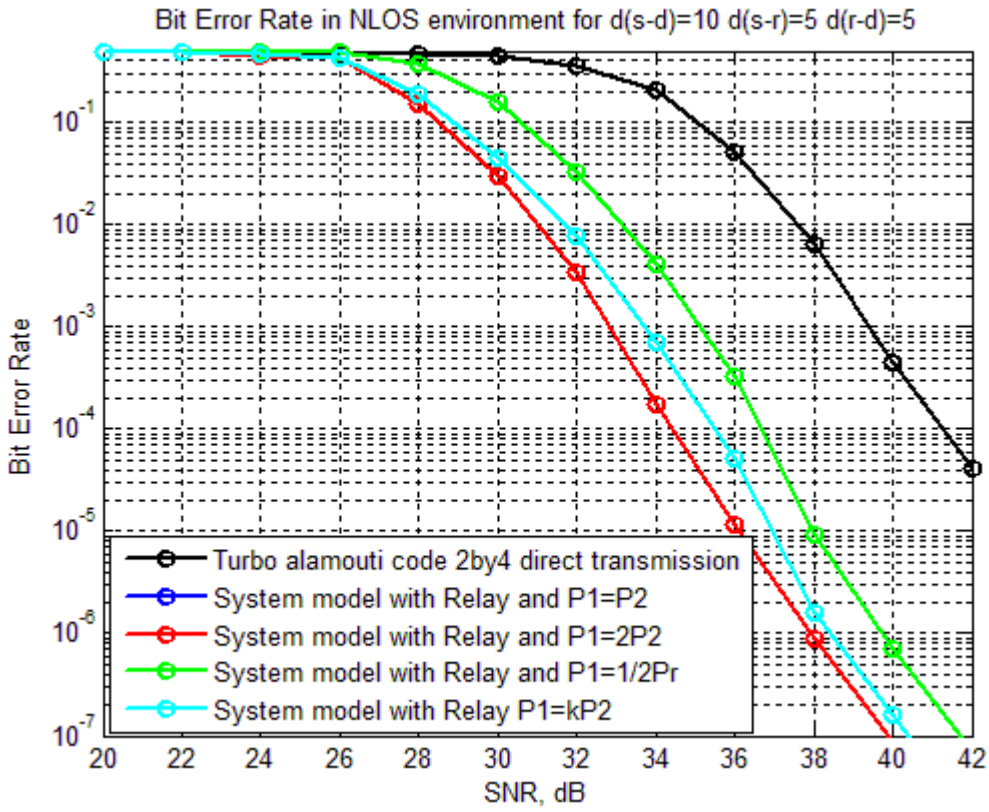

Figure 4.10 System bit error rate in NLOS environment

For a bit error rate of 10^{-4} we observe a difference of more than $7.5\ dBs$ between the direct transmission and the system model with power allocation $P_1 = 2 \times P_2$. For the direct transmission, that threshold is obtained for $SNR = 41.7\, dBs$ while it is obtained for $SNR = 34.2\, dBs$ in the case of our system model.

4.3.2 Case 2: Performance in function of the position of the relay

4.3.2.1 LOS Environment

In this section, we fix a constant system power and SNR and we change the position of the relay between the source and destination. We consider that $SNR = 16\,dBs$ and $d_{s-d} = 10$, we have $d_{s-r} \in [1 \quad 9]$ and $d_{r-d} = d_{s-d} - d_{s-r} = 10 - d_{s-r}$. The path loss coefficient is $\beta_{sd} = \beta_{sr} = \beta_{rd} = 2$ for all the links.

In the case of static power allocations, the cooperation rate of the relay decreases when the relay is closer to the destination as the frame received has a smaller power when the distance of the relay increases. However, in the case of $P_1 = kP_2$, the received power at the relay is equal to the received power at the destination from the relay in phase 2 when it collaborates. That explains why the purple curve is symmetric $d_{s-r} = 5$.

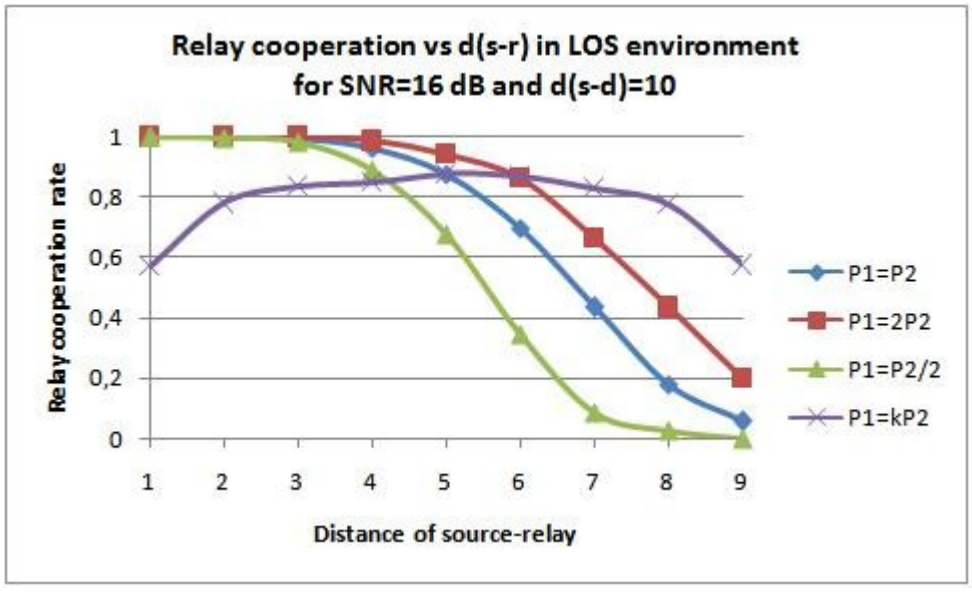

Figure 4.11 Relay cooperation vs relay position in LOS environment

The three static power allocations considered, $P_1 = 2 \times P_2$, $P_1 = P_2$ and $P_1 = P_2 / 2$ offer a better performance than the direct link transmission whatever the position of the relay.

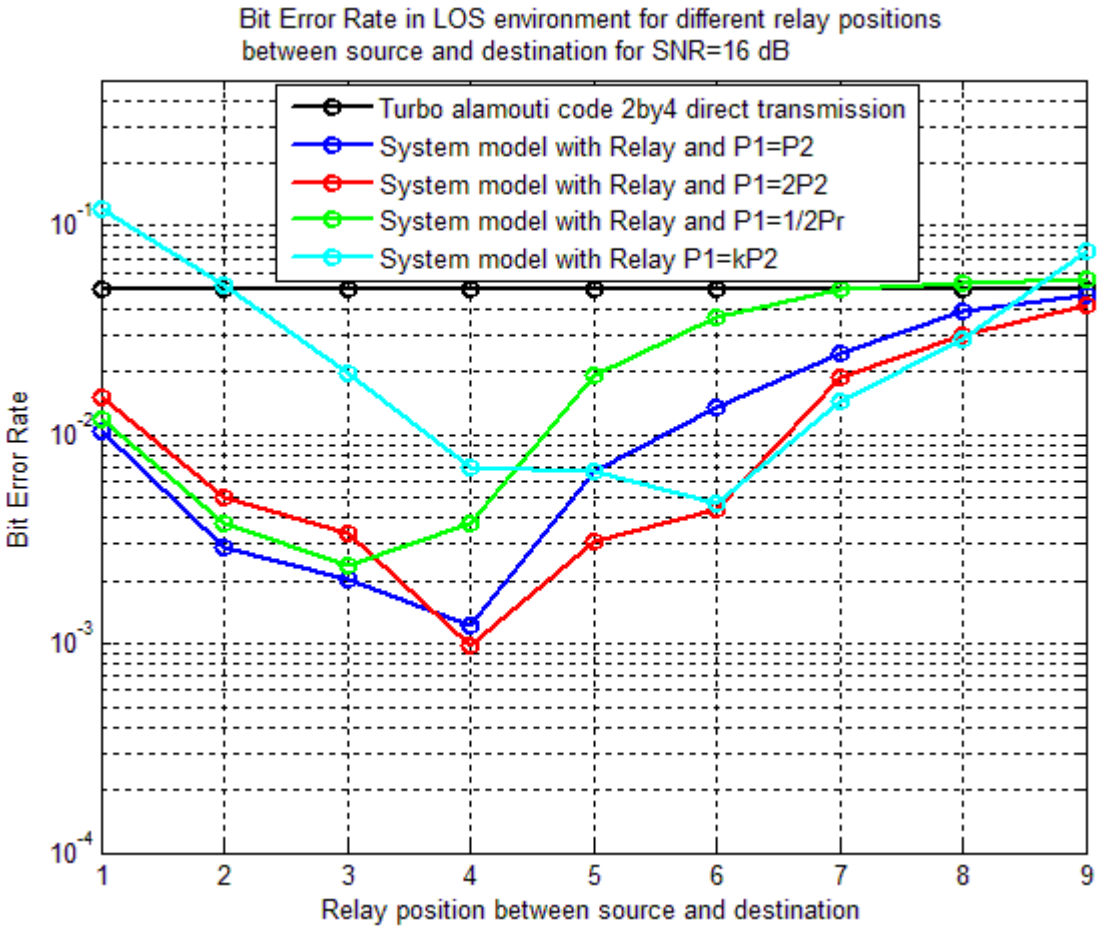

Figure 4.12 System bit error rate vs relay position in LOS environment

The best performance is obtained for the case $P_1 = 2 \times P_2$ for $d_{s-r} = 4$.

In the case of direct transmission, for $SNR = 16 dBs$ the received power is

$$P_{direct} = \frac{10^{1.6}}{10^2} = 3.9811 \times 10^{-1}$$

Considering the power allocation $P_1 = 2 \times P_2$ for $d_{s-r} = 4$, the received power at the destination is :

$$P=\begin{cases}\frac{2}{3}\times\frac{10^{1.6}}{10^{2}}+\frac{1}{3}\times\frac{10^{1.6}}{6^{2}}=6.340\times10^{-1}, & relay\quad collaborates\\ \frac{2}{3}\times\frac{10^{1.6}}{10^{2}}+\frac{1}{3}\times\frac{10^{1.6}}{10^{2}}=3.9811\times10^{-1}, & source\quad transmits\end{cases}$$

Given that the cooperation rate of the relay is $rate=9.88\times10^{-1}$ then the average received power is

$$\overline{P}_{system}=rate\times6.340\times10^{-1}+(1-rate)*3.9811\times10^{-1}=6.312\times10^{-1}$$

The received power at the destination in the proposed model is more than 1.5 times the power in direct transmission

$$f=\frac{\overline{P}_{system}}{\overline{P}_{direct}}=\frac{6.312\times10^{-1}}{3.981\times10^{-1}}=1.578$$

This explains why the bit error rate is 1×10^{-3} for $P_1=2\times P_2$ and $d_{s-r}=4$ while it is 1.4×10^{-2} for the direct transmission.

4.3.2.2 NLOS Environment

In this section, we fix a constant system power and SNR and we change the position of the relay between the source and destination. We consider that $SNR=32\,dBs$ and $d_{s-d}=10$, we have $d_{s-r}\in[1\quad 9]$ and $d_{r-d}=d_{s-d}-d_{s-r}=10-d_{s-r}$. The path loss coefficient is $\beta_{sd}=\beta_{sr}=\beta_{rd}=4$ for all the links.

In the case of static power allocations, the cooperation rate of the relay decreases when the relay is closer to the destination as the frame received has a smaller power when the distance of the relay increases. However, in the case of $P_1=kP_2$, the received power at

the relay is equal to the received power at the destination from the relay in phase 2 when it collaborates. That explains why the purple curve is symmetric $d_{s-r} = 5$.

The three static power allocations considered, $P_1 = 2 \times P_2$, $P_1 = P_2$ and $P_1 = P_2 / 2$ offer a better performance than the direct link transmission whatever the position of the relay.

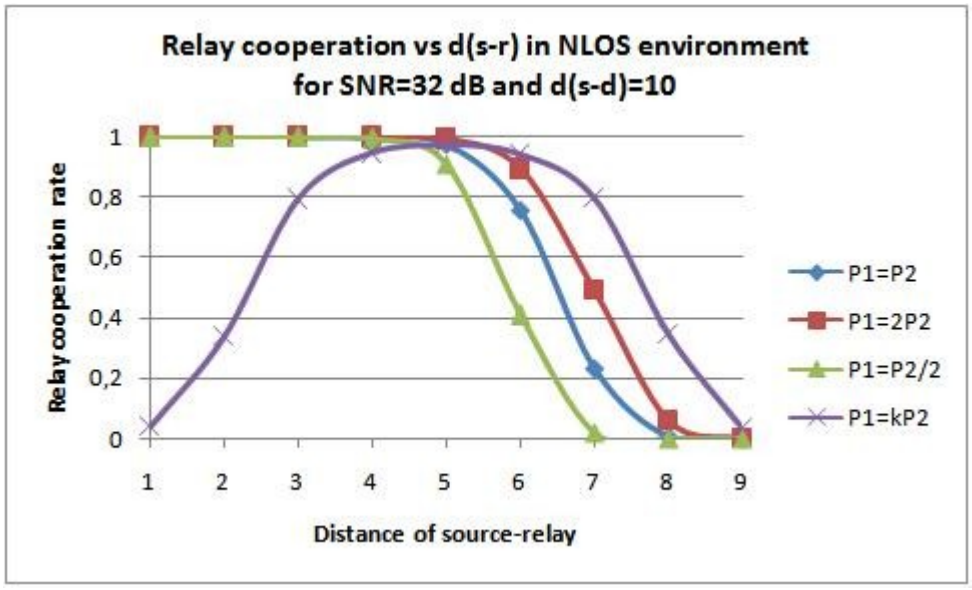

Figure 4.13 Relay cooperation vs relay position in NLOS environment

The best performance is obtained for the case $P_1 = P_2 / 2$ for $d_{s-r} = 4$.

In the case of direct transmission, for $SNR = 32\,dBs$ the received power is

$$P_{direct} = \frac{10^{3.2}}{10^4} = 1.5849 \times 10^{-1}$$

Considering the power allocation $P_1 = P_2 / 2$ for $d_{s-r} = 4$, the received power at the destination is :

$$P = \begin{cases} \frac{1}{3} \times \frac{10^{3.2}}{10^4} + \frac{2}{3} \times \frac{10^{3.2}}{6^4} = 8.681 \times 10^{-1}, & relay \quad collaborates \\ \\ \frac{1}{3} \times \frac{10^{3.2}}{10^4} + \frac{2}{3} \times \frac{10^{3.2}}{10^4} = 1.5849 \times 10^{-1}, & source \quad transmits \end{cases}$$

Given that the cooperation rate of the relay is $rate = 9.93 \times 10^{-1}$ then the average received power is

$$\overline{P}_{system} = rate \times 8.681 \times 10^{-1} + (1 - rate) * 1.5849 \times 10^{-1} = 8.6314 \times 10^{-1}$$

The received power at the destination in the proposed model is more than 1.5 times the power in direct transmission

$$f = \frac{\overline{P}_{system}}{\overline{P}_{direct}} = \frac{8.6314 \times 10^{-1}}{1.5849 \times 10^{-1}} = 5.446$$

This explains why the bit error rate is 2.92×10^{-3} for $P_1 = P_2 / 2$ and $d_{s-r} = 4$ while it is 3.8×10^{-1} for the direct transmission.

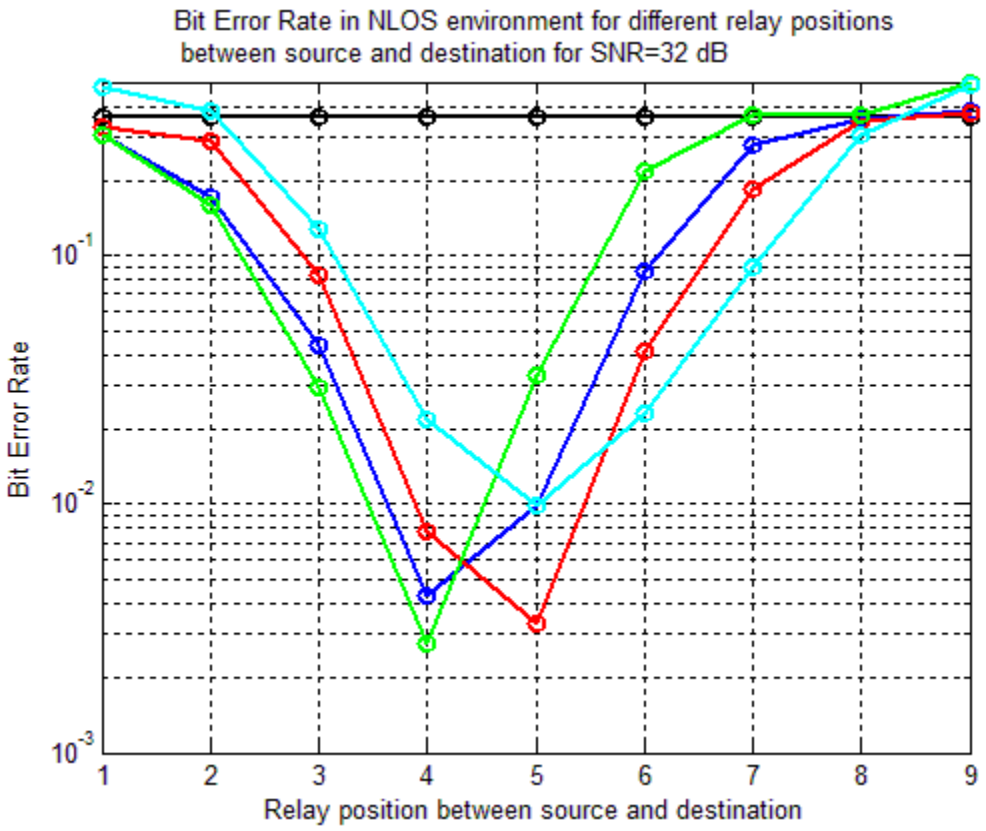

Figure 4.14 System bit error rate vs relay position in NLOS environment

4.3.3 Uplink Environment

For this subsection, we consider that the relay is close to the source and that the source-relay link is LOS while the relay-destination link is NLOS as well as the source-destination link. The environment of this simulation can be resumed by the following equations

$$
\begin{aligned}
d_{sd} &= 10 \\
d_{sr} &= 3 \\
d_{rd} &= 7 \\
\beta_{sd} &= \beta_{rd} = 4 \\
\beta_{sr} &= 2
\end{aligned}
\tag{4.30}
$$

Figure 4.14 shows that the cooperation rate of the relay is approximately 1 for all the static power allocations considered: $P_1 = 2 \times P_2$, $P_1 = P_2$, $P_1 = P_2 / 2$, for $SNR > 20\,dBs$. However, for the case $P_1 = k \times P_2$ where $k = \dfrac{d_{sr}^{\alpha_{sr}}}{(d_{sd} - d_{sr})^{\alpha_{rd}}} = \dfrac{3^2}{7^4} = 3.748 \times 10^{-3}$, the cooperation rate of the relay Is virtually null for $SNR = 20\,dBs$ and gradually increases to become approximately 1 for $SNR > 34\,dBs$.

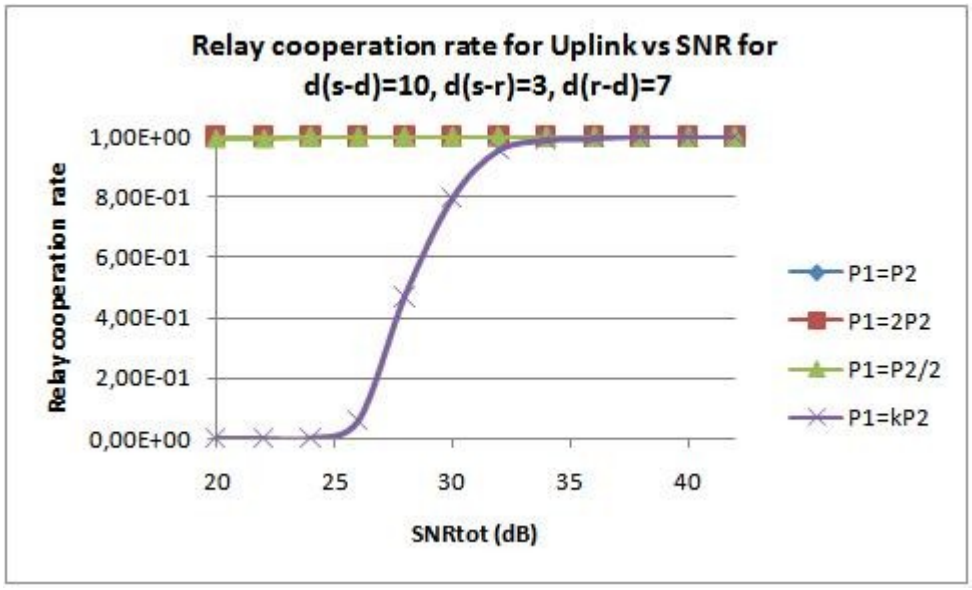

Figure 4.15 Relay cooperation vs total SNR in Uplink environment

The best bit error rate performance is obtained for the cases of $P_1 = P_2$ and $P_1 = P_2 / 2$; we observe an improvement of $6\,dBs$ compared to the direct link performance for a bit error

rate of 10^{-4}. We obtain this value for $SNR = 41 dBs$ for a direct transmission while it is obtained for $SNR = 35 dBs$ for the system model.

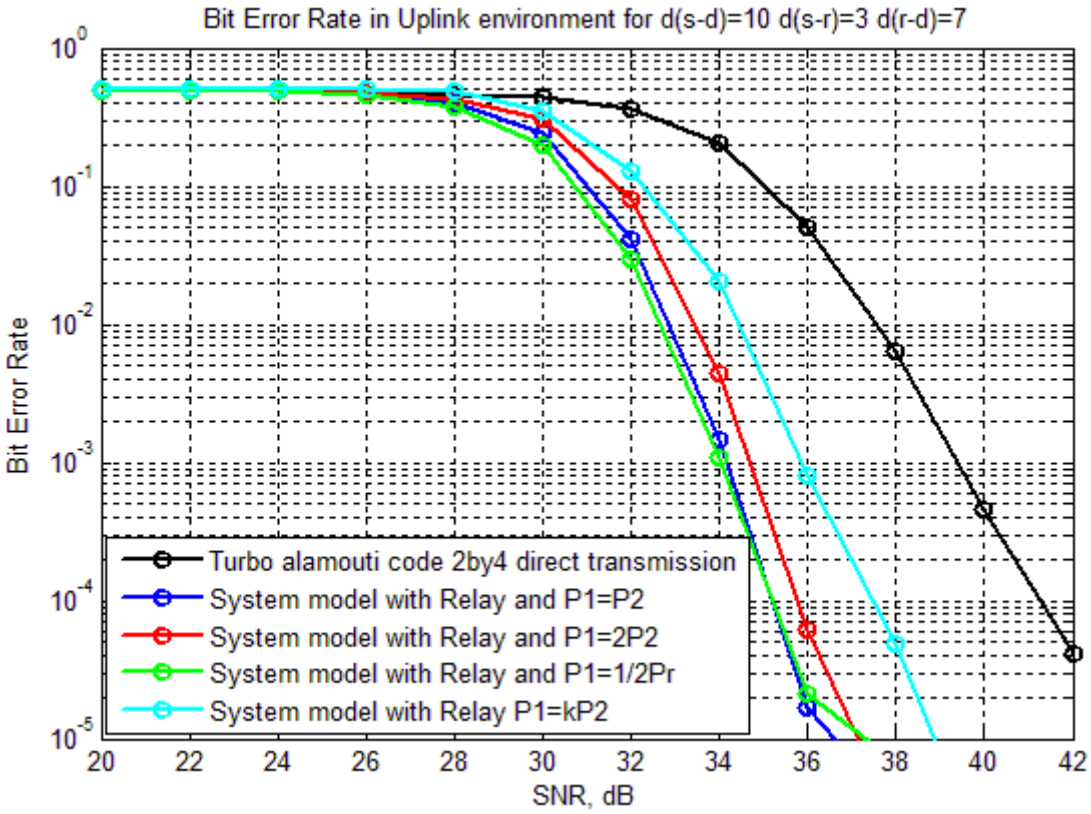

Figure 4.16 System bit error rate vs total SNR for Uplink environment

4.3.4 Downlink Environment

For this subsection, we consider that the relay is close to the destination and that the source-relay link is NLOS while the relay-destination link is LOS as well as the source-destination link. The environment of this simulation can be resumed by the following equations

$$
\begin{aligned}
d_{sd} &= 10 \\
d_{sr} &= 7 \\
d_{rd} &= 3 \\
\beta_{sd} &= \beta_{sr} = 4 \\
\beta_{rd} &= 2
\end{aligned}
\tag{4.31}
$$

For $SNR < 30\,dBs$ the relay does not cooperate very much because of the attenuated power received at the relay. The relay cooperation is almost null for all the cases except for $P_s = 2 \times P_r$ where the cooperate rate is 9.72×10^{-2}. For $SNR > 30\,dBs$ the cooperation rate is the highest for the case of dynamic power allocation; assume $SNR = 32\,dBs$, $k = \dfrac{d_{sr}^{\alpha_{sr}}}{(d_{sd} - d_{sr})^{\alpha_{rd}}} = \dfrac{7^4}{3^2} = 2.668 \times 10^2$ and $P_1 = k \times P_2$.

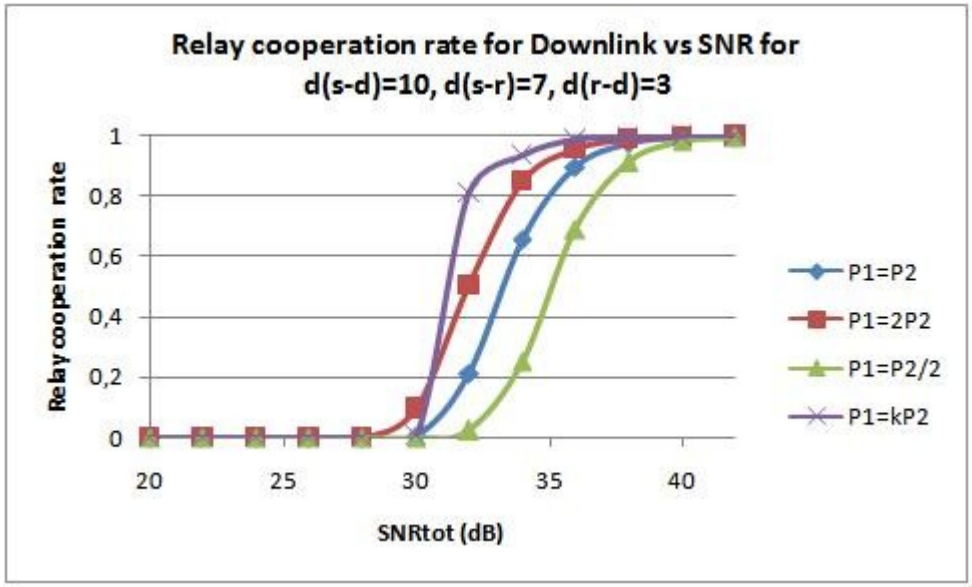

Figure 4.17 Relay cooperation vs total SNR in Downlink environment

Similarly, we observe that the case with the highest relay cooperation rate for the case of $P_1 = k \times P_2$ has the best end-to-end bit error rate. For $SNR = 37.5\,dBs$ the bit error rate is

10^{-4} while this error rate is obtained for $SNR = 41.5\,dBs$ for a direct transmission, which is an Improvement of $4\,dBs$.

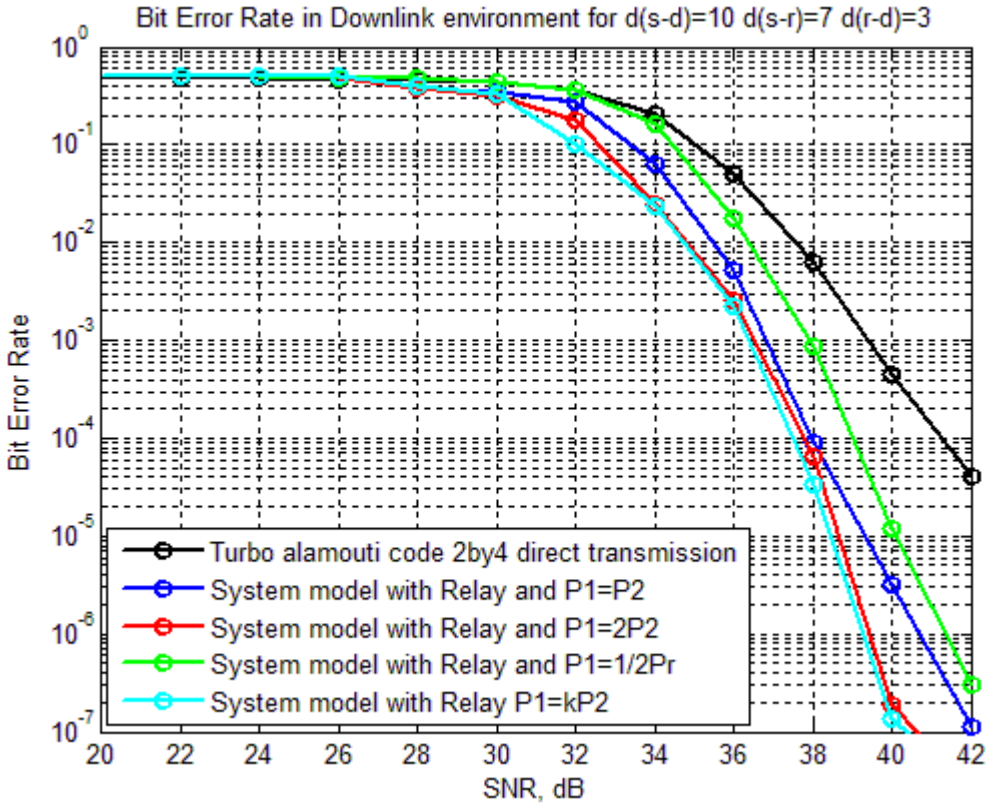

Figure 4.18 System bit error rate vs total SNR for Downlink environment

4.4 Comparison of space-time code and Turbo coded space-time cooperation

4.4.1 Case 1: Relay at equal distance between source and destination

4.4.1.1 LOS Environment

In this subsection, we compare the performances of the model presented in Chapter 3 and the one in Chapter 4 for a relay at equal position between the source and the destination in a LOS environment. Below are the parameters used for the simulation:

$$
\begin{aligned}
d_{sd} &= 10 \\
d_{sr} &= d_{rd} = d_{sd}/2 = 5 \\
\beta_{sd} &= \beta_{sr} = \beta_{rd} = 2
\end{aligned}
\tag{4.32}
$$

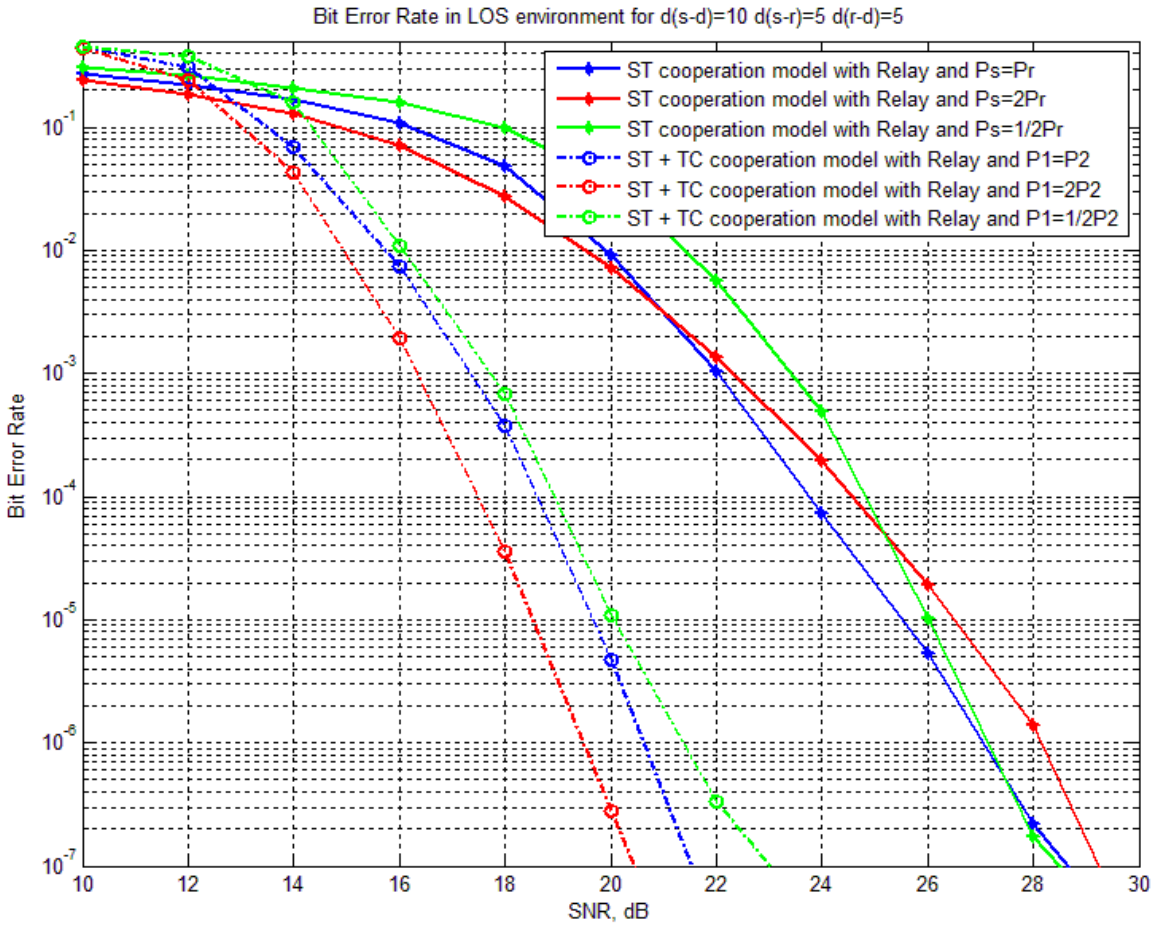

Figure 4.19 Comparison of models in LOS environment

The Turbo coded space-time cooperation model has a much better performance; the bit error rate threshold of 10^{-5} is met for $SNR = 18.5\,dBs$ while it is obtained for $SNR = 25.5\,dBs$ for space-time cooperation, which is a difference of $7\,dBs$.

4.4.1.2 NLOS Environment

We compare the performances of the model presented in Chapter 3 and the one in Chapter 4 for a relay at equal position between the source and the destination in a NLOS environment. Below are the parameters used for the simulation:

$$\begin{aligned} d_{sd} &= 10 \\ d_{sr} &= d_{rd} = d_{sd}/2 = 5 \\ \beta_{sd} &= \beta_{sr} = \beta_{rd} = 4 \end{aligned} \tag{4.33}$$

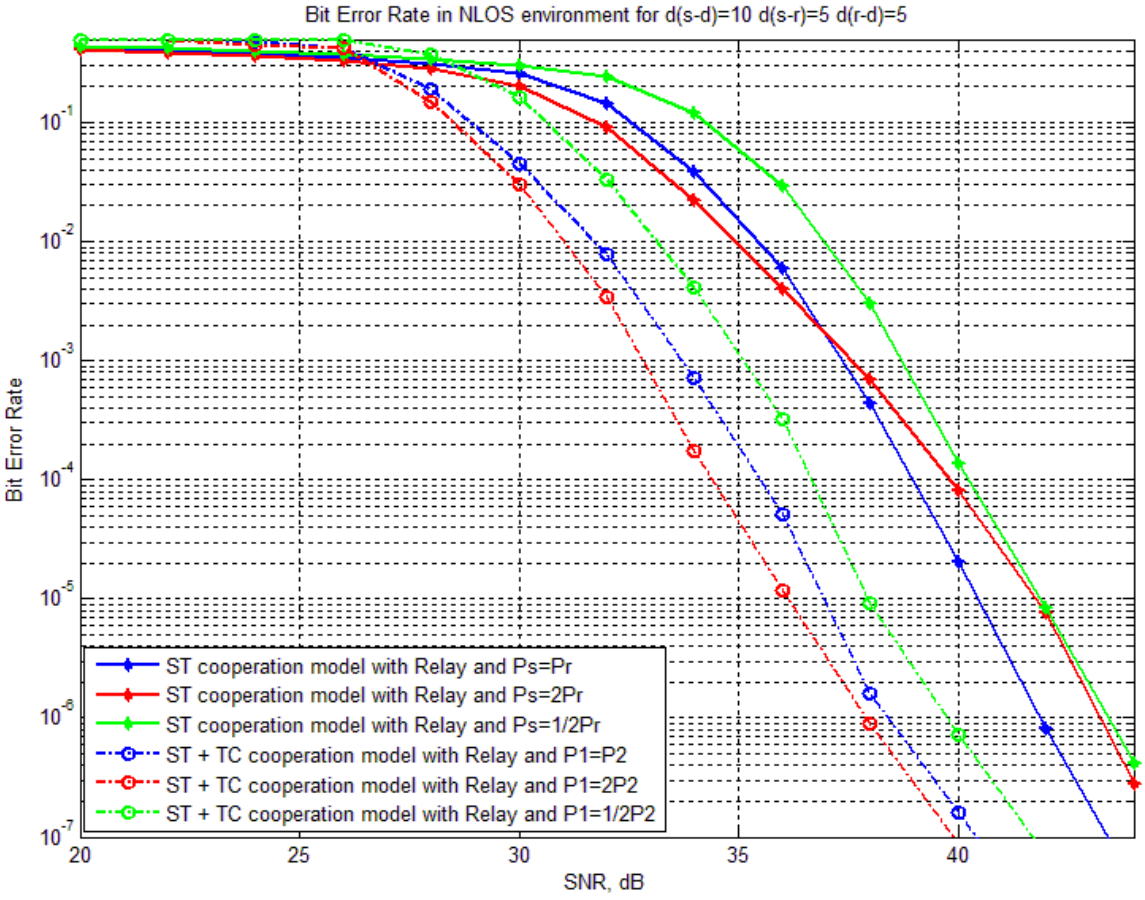

Figure 4.20 Comparison of models in NLOS environment

The Turbo coded space-time cooperation model has a much better performance; the bit error rate threshold of 10^{-5} is met for $SNR = 36 dBs$ while it is obtained for $SNR = 40.5 dBs$ for space-time cooperation, which is a difference of $4.5 dBs$.

4.4.2 Uplink Environment

In this subsection, we compare the performances of the model presented in Chapter 3 and the one in Chapter 4 for a relay at equal position between the source and the destination in an uplink communication. Below are the parameters used for the simulation:

$$\begin{aligned} d_{sd} &= 10 \\ d_{sr} &= 3 \\ d_{rd} &= 7 \\ \beta_{sd} &= \beta_{rd} = 4 \\ \beta_{sr} &= 2 \end{aligned} \tag{4.34}$$

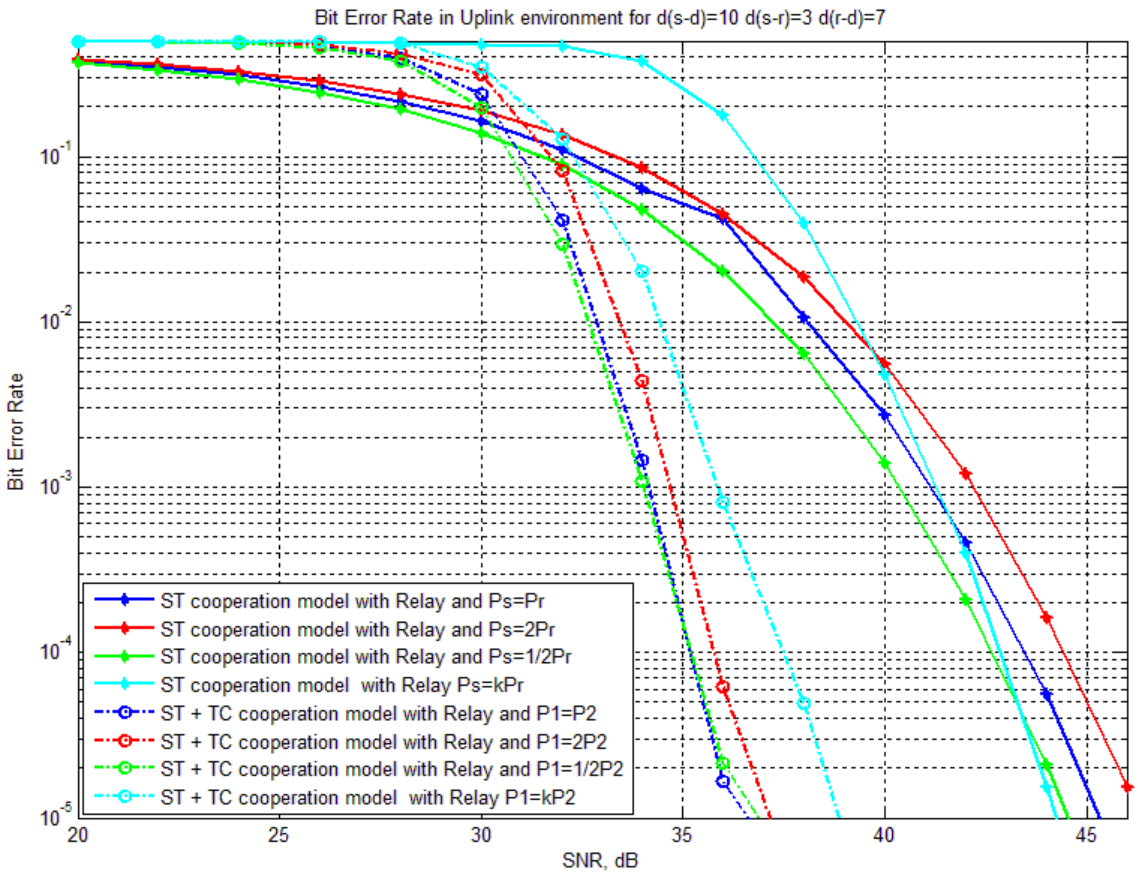

Figure 4.21 Comparison of models in uplink environment

The Turbo coded space-time cooperation model has a much better performance; the bit error rate threshold of 10^{-4} is met for $SNR = 35.2\,dBs$ while it is obtained for $SNR = 43\,dBs$ for space-time cooperation, which is a difference of $7.8\,dBs$.

4.4.3 Downlink Environment

In this subsection, we compare the performances of the model presented in Chapter 3 and the one in Chapter 4 for a relay at equal position between the source and

the destination in an uplink communication. Below are the parameters used for the simulation:

$$
\begin{aligned}
d_{sd} &= 10 \\
d_{sr} &= 7 \\
d_{rd} &= 3 \\
\beta_{sd} &= \beta_{sr} = 4 \\
\beta_{rd} &= 2
\end{aligned}
\tag{4.35}
$$

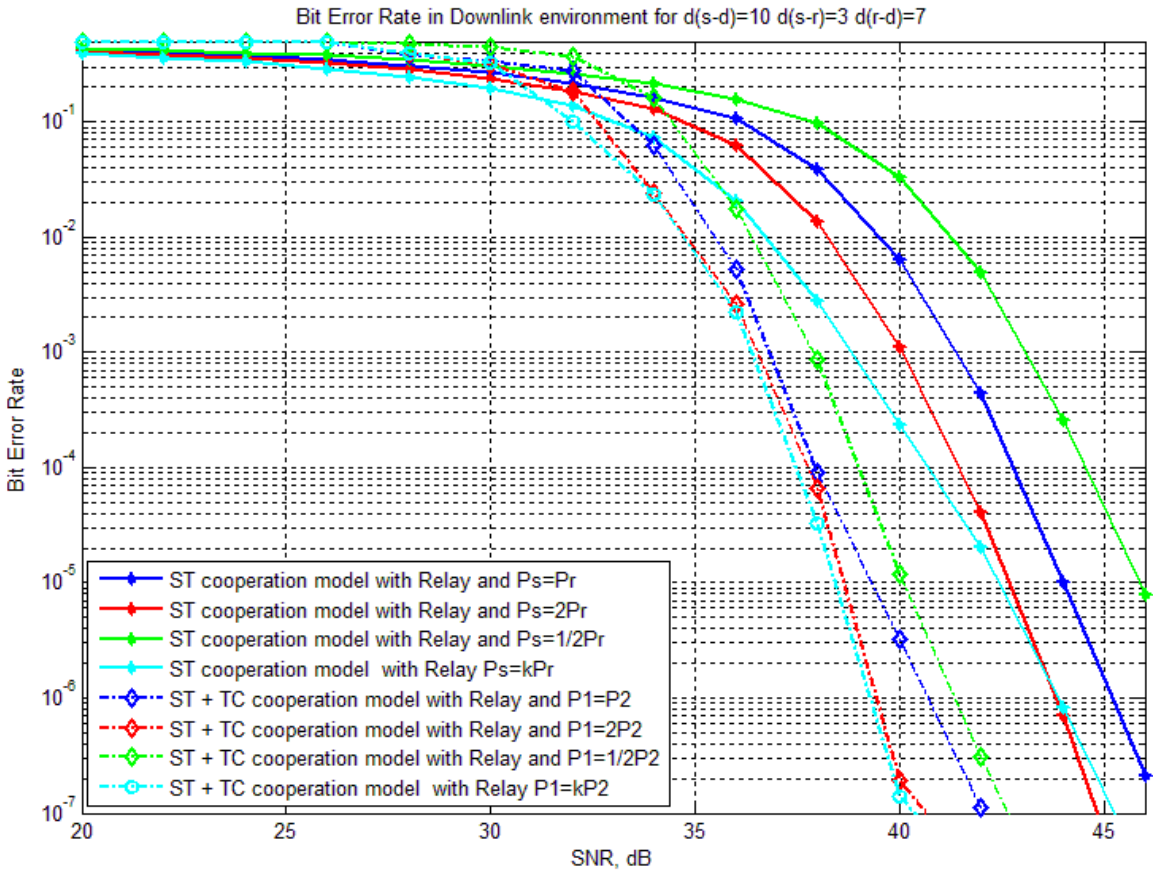

Figure 4.22 Comparison of models in downlink environment

The Turbo coded space-time cooperation model has a much better performance; the bit error rate threshold of 10^{-5} is met for $SNR = 38.3\,dBs$ while it is obtained for $SNR = 42.5\,dBs$ for space-time cooperation, which is a difference of $4.2\,dBs$.

4.5 Summary

In this chapter we proposed a turbo coded space-time cooperation composed of three terminals, a source, relay and a destination. The relay only cooperates if CRC check is successful, and both transmitters (source and relay) are composed of two antennas while both receivers (relay and destination) are composed of four antennas.

By comparing this model to the space-time coded cooperation model proposed in chapter 3, simulations show a coding gain in all the proposed scenarios: LOS, NLOS, downlink and uplink communications. For instance, in the case of LOS where the relay is at equal distance between the source and destination, the bit error rate of 10^{-5} is achieved for $SNR = 18.5\,dBs$ while it is obtained for $SNR = 25.5\,dBs$ for space-time cooperation, which is a difference of $7\,dBs$

Chapter 5: Conclusion and future work

In this section we summarize the work that was done during the thesis and more specifically in Chapters 3 and 4; in the first part we present the simulation results and we recommend future research work in the second part.

5.1 Conclusion

A space-time coded cooperation model was proposed in chapter 3; the source and relay both use a 2x4 Alamouti encoder and transmit in a two phase transmission system. During the first one, the source broadcasts to both the relay and destination. If the relay is able successfully decode, it will send another version of the message during the second phase and the source remains silent. Else, both source and relay remain silent. We apply the decode and forward protocol and we assume that only the destination has full knowledge of the channel state information and the fading coefficients. Also, we consider four different power allocations scenarios: three static allocations and one that adjusts depending on the path loss coefficient and the relay's position. Bit error rate performances were simulated for LOS and NLOS in which the path loss exponent is $\beta = 2$ or $\beta = 4$ respectively when the relay is at equal position between the source and destination. The proposed model in Chapter 3 offers a 5 dBs improvement for a bit error rate of 10^{-3} in NLOS. Uplink and downlink transmissions were also presented, as well as for a mobile relay between the source and the destination. As part of our analysis, we also present the relay cooperation rate for each scenario. For a downlink transmission, the bit error rate of 10^{-5} is obtained for $SNR = 42.5\,dBs$ while this error rate is obtained for

$SNR = 46.5\,dBs$ for a direct transmission, which is an Improvement of $4\,dBs$.

In Chapter 4, we extend this analysis to Turbo-coded space-time cooperation; during phase one, the odd bits of the systematic and parity 1 sequences as well as the even bits of the parity 2 sequence are encoded in a 2x4 Alamouti code then broadcasted to both the relay and the destination. A CRC check is applied at the relay and if it is successful, the relay Turbo-encodes the information message, then encodes it in a 2x4 Alamouti format and sends the other half of systematic and parity bits to the destination. Else, it is the source that sends the frame to the destination. We have shown that the turbo coded space-time cooperation provides a $7\ \ dBs$ improvement compared to a space-time coded cooperation for a bit error-rate of 10^{-5} when the relay is at equal distance between source and destination in a LOS environment. In an uplink transmission, the model proposed in chapter 4 provides a gain of $7.8\ \ dBs$ for a bit error rate of 10^{-4}.

5.2 Future work

The work through this thesis was based on two aspects: Alamouti code as well as turbo codes. There are many ways to extend the results to enhanced and more developed models:

- Further research can be done to have more transmitting and receiving antennas and extend the model to a 4x4 space-time or a generalized $n \times m$ model instead of Alamouti 2x4.

- The work on the 3-user cooperation scheme can also be extended to a 4-user or generalized N-user model by having at least 2 relay terminals between the source and the destination.

- The model can also enhanced by changing the protocol at the relay; hybrid DF/AF can be considered as well as log likelihood ratio threshold-based relaying. That way, the relay cooperation rate would be improved.

- One can also consider to analytically evaluate the performance of both above described models in chapter 3 and 4.

All of the above are suggestions and recommendations on future research regarding the models presented in chapters 3 and 4.

References

[1] G.J. Foschini, "Layered space-time architecture for wireless communication in a fading environment when using multi-element antennas." Bell Labs Tech. J., 1996, Issue 2, Vol. 1, pp. 41-59.

[2] J. N. Laneman, D. N. C. Tse, G. W. Wornell., "Cooperative diversity in wireless networks: efficient protocols and outage behavior." in IEEE Transactions on information Theory, December 2004, Issue 12, Vol. 50, pp. 3062-3080.

[3] J. N. Laneman, G. W. Wornell., "Distributed space-time coded protocols for exploiting cooperative diversity in wireless networks." in IEEE Transactions on information Theory, October 2003, Issue 10, Vol. 49, pp. 2415-2525.

[4] T. E. Hunter, A. Nosratinia., "Performance analysis of coded cooperation diversity." 2003. International Conference on Communications ICC03. Vol. 4, pp. 2688-2692.

[5] W.C. Jakes, "New Techniques for Mobile Radio." Bell Laboratory Record, December 1970, pp. 326-330.

[6] T.M. Duman, A. Ghrayeb., Coding for MIMO communication Systems, UK : John Wiley & Sons, 2007

[7] T. Zhou, H. Sharif, M. Hempel, P. Mahasukhon, W. Wang, T. Ma, "A Deterministic Approach to Evaluate Path Loss Exponents in Large-Scale Outdoor 802.11 WLANs", IEEE Conference on Local Computer Networks (LCN 2009) Zürich, Switzerland; 20-23 October 2009

[8] T.S. Rappaport, "Wireless Communications Principles and practice", Prentice Hall, 2002.

[9] Hai-ying Shang, Yu Han, Ji-hua Lu., “Statistical analysis of Rician and Nakagami-m fading channel using Multipath Shape Factors”, 2nd International Conference on Computational Intelligence and Natural Computing Proceedings (CINC), Beijing, China, vol.1, pp.398-401, 2010

[10] C. E. Shannon, "A mathematical theory of communication", Bell System Technical Journal, vol. 27, pp. 379-423 and 623-656, July and October, 1948.

[11] M. K. Simon and M.-S. Alouini, Digital communication over fading channels, 2nd ed., New York: John Wiley & Sons, 2005.

[12] A. F. Naguib and R. Calderbank, “Space-time coding and signal processing for high data rate wireless communications”, IEEE Signal Processing Magazine, vol. 17, no. 3, pp. 76–92, Mar. 2000.

[13] Z. Liu, G. B. Giannakis, S. Zhuo and B. Muquet, “Space-time coding for broadband wireless communications”, Wireless Communications and Mobile Computing, vol. 1,no. 1, pp. 35–53, Jan. 2001.

[14] G. J. Foschini and M. J. Gans, "On Limits of Wireless Communications in a Fading Environment when Using Multiple Antennas" Wireless Personal Communications, vol. 6, pp. 311-335, 1998.

[15] E. Telatar, "Capacity of multi-antenna Gaussian Channels." European Transaction on Telecommunications, Issue 6, Vol. 10, pp. 585-595, December 1999.

[16] D. Tse and P. Viswanath, "Fundamentals of Wireless Communications", Cambridge, 2006

[17] L. Zheng, D.N.C. Tse., "Diversity and multiplexing: a fundamental tradeoff in multiple-antenna channels.", in IEEE Transactions on information Theory, May 2003, Issue 5, Vol. 49, pp. 1073-1096.

[18] V. Tarokh, N. Seshadri, and A. R. Calderbank, “Space-time codes for high data rate wireless communication: performance analysis and code construction,”, in IEEE Transactions on information Theory, pp. 744-765, Mar. 1998.

[19] S. M. Alamouti, "A Simple Transmit Diversity Technique for Wireless Communications." IEEE Journal on Selected Areas in Communications, October 1998, Issue 8, Vol. 16, pp. 1451-1458.

[20] V. Tarokh, H. Jafarkhani, and A. R. Calderbank, “Space-time block codes for high data rate wireless communications: performance results,”, in IEEE Journal on Selected Areas Communications, vol. 17, pp. 451-460, Mar. 1999.

[21] J.N. Laneman, Cooperative diversity in wireless networks: algorithms and architectures, Ph.D. Thesis, Massachusetts Institute of Technology, Cambridge, MA, 2002

[22] S. Mallick, P.Kaligineedi, M.M.Rashid, and V.K.Bhargava, “Radio resource optimization in cooperative wireless communication networks,” in Cooperative Cellular Wireless Networks. Cambridge University Press, 2001

[23] L.B. Le, S.A. Vorobyov, K. Phan, and T.L. Ngoc, “Resource allocation and QoS provisioning for wireless relay networks,” in Quality-of-Service Architectures for Wireless Networks: Performance Metrics and Management. IGI Global, 2009

[24] E.C. Van der Meulen, “Three-terminal communication channels,” Advances in Applied Probability, vol. 3, pp. 120-154, 1971

[25] T. M. Cover and A. A. El Gamal, “Capacity theorems for the relay channel,” in IEEE Transactions on information Theory, vol. 25, no. 5, pp. 572 - 584, Sept. 1979.

[26] T. Cover and J.A. Thomas, Elements of Information Theory, UK:John Wiley&Sons, 2006

[27] A. Sendonaris, E. Erkip, and B. Aazhang, "User Cooperation Diversity Part I and Part II” IEEE Transactions on Communications, vol. 51, no. 11, pp. 1927–48, November 2003.

[28] M. Dohler, Virtual antenna arrays, Ph.D. dissertation, King’s College London, London, UK

[29] A. Host-Madsen and J. Zhang, “Capacity bounds and power allocation for wireless relay channels,” IEEE Transactions on information Theory, vol. 51, no. 6, pp. 2020–2040, Jun, 2006.

[30] R. Nabar, H. Bölcskei, and F. Kneubuhler, “Fading relay channels: Performance limits and space-time signal design,” in IEEE Journal on Selected Areas in Communications, vol. 22, no. 6, pp. 1099-1109, Aug. 2004

[31] H. Ochiai, P. Mitran, and V. Tarokh, “Variable-rate two-phase collaborative communications protocols for wireless networks," IEEE Transactions on information Theory, vol. 52, no. 9, pp. 4299-4312, Sept. 2006.

[32] C. Berrou, A. Glavieux and P. Thitimajshima, "Near Shanon limit error correcting coding and decoding: Turbo codes," in IEEE Proceedings of the International Conference on Communications, Geneva, 1993.

[33] C. Berrou and A. Glavieux, "Near optimum error correcting coding and decoding: Turbo codes," IEEE Transactions on Communications, vol. 44, no. 10, pp. 1261-1271, October 1996.

[34] R. Pyndiah, P. Combelles and P. Adde, "A very low complexity block turbo decoder for product codes," in IEEE Global Telecommunications Conf., 1996. GLOBECOM '96., 1996.

[35] P. Ferry, c. Adde and G. Graton, "Turbo decoder synchronization procedure: application to the CAS5093 integrated circuit," in Proceedings of the Third IEEE Int. Conf. on Electronics, Circuits and Systems, 1996. ICECS '96., 1996.

[36] C. Berrou, Practical considerations on turbo-codes, KPN Research, La haye, 1996.

[37] M. Valenti, "Turbo codes and iterative processing," in IEEE New Zealand Wireless Communications Symposium, Auckland, 1998.

[38] C. Berrou, S. Evano and G. Battail, "Turbo block codes," in Turbo coding seminar, Sweden, 1996.

[39] P. Adde, R. Pyndiah and O. Raoul, "Performance and complexity of block turbo decoder circuit," in 3rd Int. Conf. on Electronics, Circuits and System, 1996. ICECS '96., Rodos, 1996.

[40] M. Jezequel, C. Berrou, C. Douillard and P. Penard, "Characteristics of a sixteen-state turbo encoder/decoder (turbo4)," in Int. Symp. on Turbo codes and Related Topics, Brest, 1997.

[41] C. Berrou, M. Jezequel and C. Douillard, "Multidimensional Turbo codes," in Information Theory and Networking Workshop, Metsovo, 1999.

[42] C. Berrou and M. Jezequel, "Non-binary convolutional codes for turbo coding," Electronics letters, vol. 35, no. 1, pp. 39-40, January 1999.

[43] K. Sripimanwat, Turbo code applications, a journey from a paper to realization, Dordrecht: Springer, 2005.

[44] S. Benedetto and G. Montorsi, “Unveiling turbo codes: Some results on parallel concatenated coding schemes," IEEE Transactions on information Theory, vol. 42, no. 2, pp.409-429, Mar. 1996.

[45] S. Benedetto and G. Montorsi, “Design of parallel concatenated convolutional codes," IEEE Transactions on Communications, vol. 44, no. 5, pp. 591-600, May 1996.

[46] G. D. Forney, "The Viterbi algorithm," Proceedings of the IEEE, vol. 61, no. 3, pp. 268-278, March 1973.

[47] L. R. Bahl, J. Cocke, F. Jelinek and J. Raviv, "Optimal decoding of linear codes for minimizing symbol error rate," IEEE Trans. Inf. Theory, vol. 20, no. 2, pp. 284-287, March 1974.

[48] M. R. Soleymani, Y. Gao and U. Vilaipornsawai, Turbo coding for satellite and wireless communications, MA: Kluwer Academic Publishers, 2002.

[49] P. Robertson, P. Hoeher and E. Villebrun, "Optimal and Sub-Optimal Maximum A Posteriori Algorithms Suitable for Turbo Decoding," European Transactions on Telecommunications, vol. 8, pp. 119-125, April 1997.

[50] G. Ganesan and P. Stoica (May 2001). "Space–time block codes: A maximum SNR approach". IEEE Transactions on Information Theory, vol.47 pp. 1650–1656, May 2001

[51] L.L. Hanzo, T. H. Liew, B. L. Yeap, R. Y. S. Tee, S.X Ng, Turbo Coding, Turbo Equalisation and Space-Time Coding: EXIT-Chart-Aided Near-Capacity Designs for Wireless Channels, UK: Wiley-IEEE Press, 2002

[52] A. Abdaoui, S. S. Ikki, M. H. Ahmed, and E. Chatelet, "On the performance analysis of a MIMO-relaying scheme with space-time block codes," IEEE Transactions Vehicular Technology, vol. 59, no. 7, pp. 3604–3609, Sep. 2010.

[53] B. Vucetic, J. Yuan, Space-Time Coding, UK : John Wiley & Sons, 2003